SANDIA REPORT

SAND2018-3229
Unlimited Release
Printed March 28, 2018

Sierra/SolidMechanics 4.48 Capabilities in Development

SIERRA Solid Mechanics Team
Computational Solid Mechanics and Structural Dynamics Department
Engineering Sciences Center

Prepared by
Sandia National Laboratories
Albuquerque, New Mexico 87185 and Livermore, California 94550

Sandia National Laboratories is a multimission laboratory managed and operated by National Technology and Engineering Solutions of Sandia, LLC., a wholly owned subsidiary of Honeywell International, Inc., for the U.S. Department of Energy's National Nuclear Security Administration under contract DE-NA0003525.

Issued by Sandia National Laboratories, operated for the United States Department of Energy by National Technology and Engineering Solutions of Sandia, LLC.

Available to DOE and DOE contractors from
U.S. Department of Energy
Office of Scientific and Technical Information
P.O. Box 62
Oak Ridge, TN 37831

Telephone: (865) 576-8401
Facsimile: (865) 576-5728
E-Mail: reports@adonis.osti.gov
Online ordering: http://www.osti.gov/bridge

Available to the public from
U.S. Department of Commerce
National Technical Information Service
5285 Port Royal Rd
Springfield, VA 22161

Telephone: (800) 553-6847
Facsimile: (703) 605-6900
E-Mail: orders@ntis.fedworld.gov
Online ordering: http://www.ntis.gov/help/ordermethods.asp?loc=7-4-0#online

SAND2018-3229
Unlimited Release
Printed: March 28, 2018

Sierra/SolidMechanics 4.48 Capabilities in Development

SIERRA Solid Mechanics Team
Computational Solid Mechanics and Structural Dynamics Department
Engineering Sciences Center
Sandia National Laboratories
Box 5800
Albuquerque, NM 87185-0380

Acknowledgments

This document is the result of the collective effort of many individuals. The current core development team responsible for the Sierra/SM codes includes Nathan K. Crane, Gabriel J. de Frias, San Le, David J. Littlewood, Mark T. Merewether, Matthew D. Mosby, Kendall H. Pierson, Julia A. Plews, Vicki L. Porter, Timothy R. Shelton, Jesse D. Thomas, Michael R. Tupek, Michael G. Veilleux, and Patrick G. Xavier. This document is written and maintained by this team.

Outside the core development team, there are many other individuals who have contributed to this manual. Nicole L. Breivik, J. Franklin Dempsey, Jeffery D. Gruda, Kevin N. Long, Kyran D. (Kim) Mish, and Chi S. (David) Lo have provided valuable input from the user community as Product Managers.

Many others have contributed to this document, either directly or indirectly. These include, but are not limited to Manoj K. Bhardwaj, Arthur Brown, James V. Cox, David M. Day, James W. Foulk III, Jason D. Hales, Brian D. Giffin, Steven P. Gomez, Arne S. Gullerud, Daniel C. Hammerand, Martin W. Heinstein, David M. Hensinger, Michael C. Hillman, Jason T. Ivey, Timothy D. Kostka, J. Richard Koteras, Alex J. Lindblad, Edward Love, Jakob T. Ostien, Rhonda K. Reinert, Nathaniel S. Roehrig, William M. Scherzinger, Gregory D. Sjaardema, Benjamin W. Spencer, Brian L. Stevens, Julia R. Walker, Gerald W. Wellman, and Edouard Yreux.

Contents

List of Figures

List of Tables

Chapter 1

Introduction

This document is a user's guide for capabilities that are not considered mature but are available in Sierra/SolidMechanics (Sierra/SM) for early adopters. The determination of maturity of a capability is determined by many aspects: having regression and verification level testing, documentation of functionality and syntax, and usability are such considerations. Capabilities in this document are lacking in one or many of these aspects.

Chapter 2

Representative Volume Elements

This chapter describes the Representative Volume Element (RVE) capability, which is a multi-scale technique that uses a separate finite element model to represent the material response at a point.

The use of representative volume elements (RVEs) is a multi-scale technique in which the material response at element integration points in a reference mesh is computed using an RVE that is itself discretized with finite elements. RVEs are typically used to represent local, periodic material inhomogeneities such as fibers or random micro structures to avoid the requirement of a global mesh with elements small enough to capture local material phenomena.

In the current implementation of RVEs, periodic boundary conditions are applied to each RVE representing the deformation of a parent element and the stresses are computed in the elements of the RVE. These stresses are then volume-averaged over the RVE and the resulting homogenized stresses are passed back to the parent element.

This chapter explains how to use the RVE capability. Section 2.1 gives a detailed description of how RVEs are incorporated into an analysis. Details of the mesh requirements are delineated in Section 2.2 and the commands needed in an input file are described in Section 2.3.

Known Issue: The capability to use RVEs with reference mesh multi integration point elements is still under development and should be used with caution.

2.1 RVE Processing

The use of the RVE capability requires two regions, each with its own mesh file. One region processes the reference mesh and the other processes all the RVEs. The commands used in the input file for the reference mesh region are the same as any other Sierra/SM region with the exception that a special RVE material model is used for every element block that uses an RVE. The RVE region is similar to an ordinary region. The only differences are that an RVE region has a line command for defining the RVEs' relationship to parent elements in the reference region and has restrictions on the use of boundary conditions.

The processing of an RVE essentially replaces the constitutive model of the parent element in the reference mesh. The steps followed at each iteration/time step of the reference mesh during an analysis using RVEs are as follows:

1. Internal force algorithm is called in the reference region to compute rate of deformation.
2. Each RVE gets the rate of deformation from its integration point on its parent element in the reference region.
3. The rate of deformation is applied to each RVE as a periodic boundary condition using prescribed velocity.
4. The RVE region is solved to obtain the stress in each element of each RVE.
5. The stresses in the elements of an RVE are volume-averaged over the RVE.
6. Each RVE passes its homogenized or volume-averaged stress tensor back to its integration point of its parent element in the reference mesh.
7. The reference region computes internal force again. Element blocks whose elements have associated RVEs do not compute a stress; they simply use the stress passed to them from their RVE.

2.2 Mesh Requirements

Two mesh files, one for the reference region and one for the RVE region, are required for an RVE analysis. Figure 2.1 shows an example of the two meshes. The reference mesh of a bar with six single integration point elements is shown on the upper left. On the lower right is the mesh for the RVE region containing six RVEs, one for each element (since the elements have only one integration point) of the reference region. In this case, the first five RVEs each consist of two element blocks and the last RVE has four.

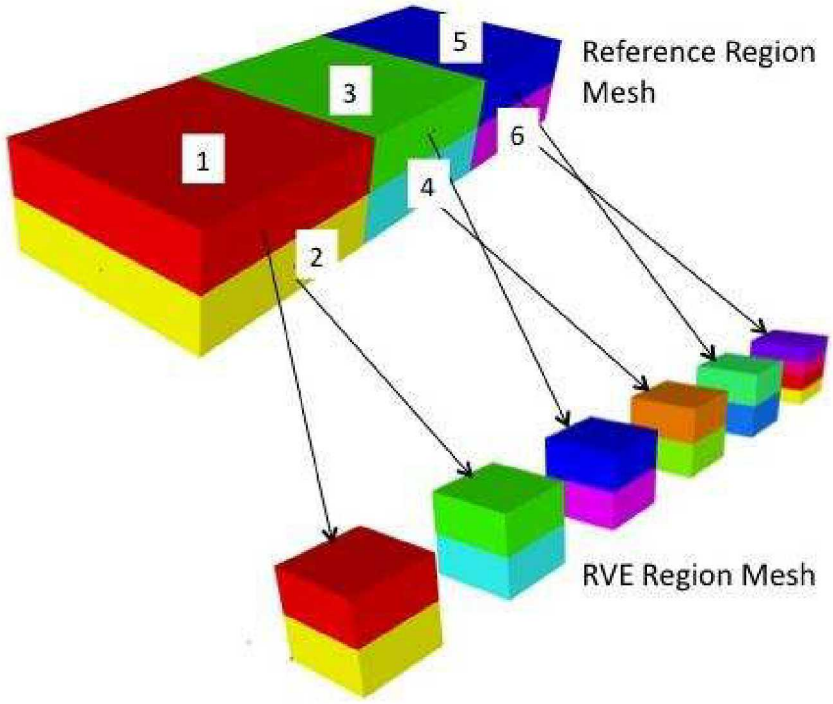

Figure 2.1: Example of meshes for RVE analysis

In general, each RVE should be a cube with any discretization the user desires. All RVEs must be aligned with the global x, y, and z axes. For stress computations, these axes are rotated into a local coordinate system, which can be specified on the reference mesh elements if these reference elements are uniform gradient hexahedra. In other words, if a local coordinate system is specified on a reference mesh uniform gradient element, the RVE global axes will be rotated internally in Sierra/SM to align with the local system on the associated parent element. So the global X axis for an RVE is actually the local X' axis in the parent element.

Additional mesh requirements apply if the mesh does not match across opposing surfaces of the RVE. In this case, the RVE must include a block of membrane elements on the exterior surfaces with matching discretization on opposing surfaces (+x/-x, +y/-y, +z/-z). In order to minimize the effects of this membrane layer on the RVE response, it should be made as thin as possible. This membrane layer then must be tied to the underlying non matching RVE surfaces.

The RVE mesh must contain sidesets or node sets on each surface of every RVE. The RVE may be enclosed with one sideset that spans all six surfaces of the curb, or the user may specify individual

sidesets or node sets on each face. These sidesets/node sets are used to apply the periodic boundary conditions on the RVE. Sierra/SM generates the boundary conditions internally so the user does not have to include them in the input file. However, this assumes that the sidesets/node sets exist in the mesh file numbered in a specified order. If individual sidesets/node sets are used on each face of the RVE, the six sidesets/node sets must be numbered consecutively, starting with the positive-x face, followed by the negative-x face, positive-y face, negative-y face, positive-z face, and ending with the negative-z face. The beginning sideset id (for the positive-x face) is set by the user in the input file.

2.3 Input Commands

There are several input commands that are relevant to RVEs. In the reference region, these commands include a special RVE material model and commands to define and use a local coordinate system along which an associated RVE will be aligned. In addition to the reference region, an RVE region is needed using the `BEGIN RVE REGION` command block. The RVE region command block uses the same nested commands as any other Sierra/SM region (with some restrictions as explained in this section) and an additional line command that relates the RVEs to their parent elements in the reference region.

2.3.1 RVE Material Model

In an RVE analysis, any elements of the reference mesh that use an RVE must use the RVE material model. This model is defined similar to other material models as described in the User's Guide but uses the RVE keyword on the `BEGIN PARAMETERS FOR MODEL` command line as follows:

```
BEGIN MATERIAL <string>mat_name
  #
  DENSITY = <real>density_value
  #
  BEGIN PARAMETERS FOR MODEL RVE
    YOUNGS MODULUS = <real>youngs_modulus
    POISSONS RATIO = <real>poissons_ratio
  END PARAMETERS FOR MODEL RVE
  #
END [MATERIAL <string>mat_name]
```

Currently, the RVE material model tells the reference element not to perform a constitutive evaluation but to instead accept the stress tensor obtained from computation on an RVE. However, the use of an RVE material model still requires the input of Young's modulus and Poissons ratio. These values may be used for time step estimation and hourglass computations, even though they are not used in a constitutive evaluation.

Element blocks in the RVE region can use any material model that is supported in Sierra/SM other than RVE.

2.3.2 Embedded Coordinate System

The finite element model of an element block in the reference mesh that uses RVEs can use an embedded coordinate system to orient the RVE relative to the reference element, if the reference elements are uniform gradient hexes. A coordinate system is defined in the sierra scope as described in the User's Guide. A local coordinate system is then associated with an element block through the use of a `COORDINATE SYSTEM` command line within a `BEGIN SOLID SECTION` command block.

```
BEGIN SOLID SECTION <string>section_name
  #
```

```
    COORDINATE SYSTEM = <string>coord_sys_name
    #
  END [SOLID SECTION <string>section_name]
```

The string `coord_sys_name` must be a name associated in the input file with a `BEGIN COORDINATE SYSTEM` command block in the sierra scope. This coordinate system will then be used on all elements of a block associated with a `BEGIN PARAMETERS FOR BLOCK` command block that includes the command line specifying this solid section.

Known Issue: Currently, the rotation of RVEs to a local element block coordinate system only works with uniform gradient hexes in the reference mesh.

2.3.3 RVE Region

A representative volume element (RVE) region must be a quasistatic region specified with the RVE keyword in the `BEGIN RVE REGION` command line. The RVE region uses the same block commands and line commands as any other quasistatic region with the addition of line commands that define which element blocks of the reference region are associated with RVEs. There are also some restrictions on boundary conditions as described in Section 2.3.6.

```
BEGIN RVE REGION <string>rve_region_name
   #
   # Definition of RVEs
   ELEMENTS <integer>elem_i:<integer>elem_j
     <integer>num_intg_pts_per_elem
     BLOCKS <integer>blk_i:<integer>blk_j
     SURFACE|NODESET <integer> start_id INCREMENT
               <integer> k
   #
   # Boundary Conditions
   #
   # Results Output Definition
   #
   # Solver Definition
   #
END [RVE REGION <string>rve_region_name]
```

2.3.4 Definition of RVEs

One or more `ELEMENTS` command lines are used to associate elements of the reference region mesh with RVEs in the RVE region. In the

```
ELEMENTS <integer>elem_i:<integer>elem_j
  <integer>num_intg_pts_per_elem
```

```
BLOCKS <integer>blk_i:<integer>blk_j
SURFACE|NODESET <integer>start_id INCREMENT
                <integer>incr
```

command line, elements numbered `elem_i` through `elem_j` of the reference mesh and their `num_intg_pts_per_elem` integration points will be associated with RVEs (for a total number of RVEs equal to (`elem_j` - `elem_i` + 1) * `num_intg_pts_per_elem`), and each RVE will consist of `blk_i` - `blk_j` + 1 element blocks. Each integration point will be associated with a separate RVE. The block IDs of the first RVE must be `blk_i` through `blk_j` and subsequent RVEs (if `elem_j` is greater than `elem_i` or `num_intg_pts_per_elem` is greater than 1) must have consecutively increasing numbers for their block IDs.

Similarly `start_id` gives the `surface_id` of the first RVE if a single, encompassing surface is used, or the first `surface_id` or `nodelist_id` of the first RVE (the positive x surface as explained in Section 2.2) if six individual sidesets/nodeset are used. The remaining surfaces (nodesets) of the first RVE and all the surfaces of the following RVEs must be consecutively numbered following `start_id` in the mesh file as explained in Section 2.2.

The increment value `incr` indicates the number of sidesets present on the exterior of the RVEs. This is used to determine how to increment the IDs of the sidesets from one RVE to the next and to determine how to prescribe periodic boundary conditions on the RVE. The increment can have a value of either one or six. A value of one indicates that each RVE has one sideset that encompasses all six faces, while a value of six specifies that six sidesets or nodesets are present, one on each face. Nodesets are not allowed for the case where `incr` is one.

The following example shows the use of the `ELEMENTS` command line:

```
elements 1:5 1 blocks 1:2 surface 7 increment 6
elements 6:6 1 blocks 11:14 nodeset 15 increment 6
```

These commands generate the RVEs shown in Figure 2.1.

The first `ELEMENTS` command line specifies that elements with element IDs 1 through 5 in the parent region mesh each have one integration point and that each integration point has an RVE with two element blocks. The RVE associated with the integration point of element 1 of the parent region will have two element blocks starting with `block_id` of 1 and ending with a `block_id` of 2. Subsequent RVEs will have consecutively numbered element blocks. For example: the integration point of parent element 2 will be associated with an RVE that consists of element blocks 3 and 4 in the RVE region, the integration point of parent element 3 will be associated with the RVE that has element blocks 5 and 6, etc. Again, this is the case for the first five elements of the parent region mesh. The keyword `SURFACE` specifies that all the periodic boundary conditions generated by the code for the RVEs for elements 1 to 5 will use sidesets in the RVE region mesh. These sidesets will start with id 7 for the positive-x face of the RVE associated with parent element 1 and continue consecutively for the other faces of the RVE and the RVEs associated with the integration points of parent elements 2 through 5 (in the order specified in Section 2.2). In other words, the positive-x face of the RVE for parent element 1 is sideset 7, negative-x is sideset 8, positive-y is sideset 9, negative-y is sideset 10, positive-z is sideset 11, and negative-z is sideset

12. The sidesets for the RVE for parent element 2 will start with id 13 and continue consecutively in the same face order. The process continues for all five RVEs specified in this command line.

The second `ELEMENTS` line specifies that the integration point of element 6 of the parent region mesh will be associated with the RVE that consists of element blocks 11, 12, 13, and 14. The `NODESET` keyword says this RVE has a nodeset associated with each face of the RVE, starting with nodeset id 15 on the positive-x face, with id's increasing consecutively for the other five faces in the same order described in the paragraph above.

The six elements specified in these command lines must be in element blocks of the reference region mesh that use the RVE material model.

2.3.5 Multi-Point Constraints

In the case in which the RVE has non matching surfaces, and therefore includes a block of membrane elements on the exterior surfaces, the user must specify a set of multi-point constraints (MPCs) to tie the membranes to the surface. This is done in the input file through use of an `MPC` command block:

```
RESOLVE MULTIPLE MPCS = ERROR
BEGIN MPC
  MASTER SURFACE = <string>membrane_surface_id
  SLAVE SURFACE  = <string>RVE_surface_id
  SEARCH TOLERANCE = <real>tolerance
END
```

In this case, the `membrane_surface_id` corresponds to the single sideset that encompasses the membrane block is the master and the single sideset that encompasses the exterior surfaces of the RVE is the slave. While the underlying RVE may have non matching exterior surfaces, the opposing surfaces of the membrane block must have matching discretizations. More detailed information on the use of MPCs, is discussed in the User's Guide.

2.3.6 RVE Boundary Conditions

Strain rates computed by elements in the reference region are applied through periodic prescribed velocity boundary conditions on the faces of the associated RVEs. These are generated internally by Sierra/SM so the periodic boundary conditions do not need to be in the user's input file. However, because the RVE region is quasistatic, each of the RVEs must be fixed against rigid body motion. This must be done in the input file through use of the prescribed velocity boundary conditions:

```
BEGIN PRESCRIBED VELOCITY pres_vel_name
  NODE SET = <string>nodelist_name
  FUNCTION = <string>function_name
  SCALE FACTOR = <real>scale_factor
  COMPONENT = <string>X|Y|Z
END [PRESCRIBED VELOCITY pres_vel_name]
```

This type of boundary condition is described in detail in the User's Guide but the use for RVEs is restricted- Either the function must always evaluate to 0.0 or the `scale_factor` must have a value of 0. This is essentially a way of using the prescribed velocity boundary condition to fix the nodes in `nodelist_name`. However, in order for these conditions to work with the periodic boundary conditions used to apply the strain rate, `PRESCRIBED VELOCITY` must be used rather than `FIXED DISPLACEMENT` or `PRESCRIBED DISPLACEMENT` boundary conditions.

Generally, three `BEGIN PRESCRIBED VELOCITY` command blocks will be needed, one each for X, Y, and Z components. In order to eliminate rigid body motion without over constraining the motion, each `BEGIN PRESCRIBED VELOCITY` block should constrain exactly one node of an RVE in one component direction. (However, `nodelist_name` may contain nodes from multiple RVEs. Separate boundary condition blocks are not required for each RVE.). To prevent rigid body rotations, the three constrained nodes on each RVE should not be collinear.

Chapter 3

Explicit Subcycling

This chapter describes how to setup an analysis to use explicit subcycling. Subcycling can be used to run different parts of the mesh at different time step sizes to improve speed.

Warning: Explicit subcycling is a capability still in the development stages. This capability is not yet recommended for general use.

Explicit subcycling can be used in an explicit transient dynamics analysis to run one part of the mesh at a small time step while running another connected part of the mesh at a large time step. Explicit subcycling can provide a substantial model speedup only if two properties hold. First, some region of the mesh must have a substantially smaller element critical time step than another region of the mesh. Second, the portion of the mesh with the small critical time step must contain a small fraction of the total number of elements used by the analysis.

Explicit subcycling divides the analysis domain into two regions: A coarse region iterating with a large time step and a fine region iterating at a smaller time step that is some integer fraction of the coarse time step. At the coarse mesh time step, both regions sync up to the same analysis time and exchange information. Using the standard analysis technique, every element must run at the same small time step. Testing has shown that an analysis run using subcycling can give equally accurate results as an analysis run without subcycling. The accuracy of the simulation is subject to several restrictions on cross region communication and compatible capabilities.

3.1 Specifying Subcycling in Input

The recommended method to turn on subcycling is to use a feature to automatically generate the coarse and fine regions in the input deck. This is done by adding the following command to the presto region.

```
SUBCYCLE BLOCKS = <string list>block_names
```

If this command is present, Sierra/SMwill automatically generate and run a new input deck that can be used for the subcycling. If the original input deck is named 'input.i' the automatically generated subcycling input deck will be named 'input.subcycle.i'. The block_names specified are the names of the blocks that are targeted for inclusion in the fine region (run with the small time step).

The algorithm to split the regions is done as follows.

- 1. Define the trial coarse region based off of everything not in the fine region.
- 2. Compute the critical time step of the coarse region as the smallest element time step in that region.
- 3. Compute the maximum time step each node can be integrated at as the smallest time step of any element near the node.
- 4. For every element in the mesh, if the element is attached to only nodes with time steps greater than or equal to the coarse region time step, place the element in the coarse region.
- 5. For every element in the mesh, if the element is attached to any node with time steps less than the coarse region time step, place the element in the fine region.
- 6. Split all boundary conditions defined on the coarse and fine region appropriately and write to appropriate results files. Each region will generate independent output files.

The mathematical foundations of the subcycling algorithm used in Sierra/SM can be found in Reference [1]. The portions of this paper specifically used in Sierra/SM are: Explicit-Explicit, Central Difference, and Linear Interpolation method.

3.2 Limitations of Subcycling

Subcycling is currently incompatible either in whole or in part with many other capabilities. The capabilities that have incompatibility with subcycling include but may not be limited to the following:

- Subcycling is incompatible with most capabilities that require an auxiliary region. This include representative volume elements (RVE), Gemini coupling, and multi-procedure analysis coupled via hand-offs or solution control.
- Subcycling currently does not work with implicit dynamics, implicit statics, or modal analysis.
- Subcycling is currently not compatible with rigid bodies.
- Subcycling is incompatible with any critical time step computation method other than the default element based time step calculation. This includes nodal based and Lanczos algorithm based time step computation methods.

Additionally several capabilities will not function correctly if that capability is operating at or near the boundary between the coarse and fine region. If such a capability is included in the subcycling analysis and that capability happens to cross the coarse/fine boundary, accuracy and stability problems may result. The capabilities that are known to be have restrictions when used with subcycling include but may not be limited to:

- Element death near the subcycling boundary may not be able to correctly determine when a node shared between the two regions goes inactive (leading to accuracy and stability issues).
- Contact between any surface in the fine region and any surface in the coarse region cannot be evaluated.
- Methods that define a force from an external load (such as CTH) can only be coupled to the deformation of the coarse.
- No non-local element or boundary condition can span the coarse to the fine boundary. This includes nodal based tetrahedra, MPCs, Spot Welds, Super Elements, Peridynamic bonds, Cylindrical Joints, and the J-Integral computation.
- Nodal output quantities at the coarse to fine boundary may not be displayed properly in plot files. Contributions to quantities such as nodal force may exist in both the fine and coarse region and the outputs would need to be summed from both.

3.3 Other Subcycling Issues

In parallel, subcycling will perform best if a mesh rebalance is performed to ensure both the fine and coarse regions are divided evenly among the processor sets. A mesh rebalance command similar to the one below can be used to automatically performance such a mesh rebalance. See the User's Guide for more information on mesh rebalancing.

```
BEGIN REBALANCE
     PERIODIC REBALANCE = AUTO
     DELETE DEACTIVATED ELEMENTS AFTER REBALANCE = ON
END
```

References

[1] Willem E.M. Bruijs. *Subcyling in Transient Finite Element Analysi*. PhD thesis, Technical University of Eindhoven, 1234.

Chapter 4

Automatic Time Step Selector

For performance reasons, it is sometimes desired to run at the highest possible time step in explicit dynamics. The `NODE BASED TIME STEP` and the `LANCZOS TIME STEP` have proven to yield a higher time step than the default element time step for most problems. However, because these routines take significantly more time to calculate, sometimes the performance benefits are unseen. The automatic time step selector attempts to weigh the performance benefits of each time step calculation. The time steps are compared every hundred steps, and the one proving most beneficial is used for the proceeding hundred steps.

Currently, only the node based time step and the element time step are compared. Because the node based time step takes longer to calculate than the element based time step (as noted above), a scale factor is used when comparing the two. To run with the automatic time step selector, the following must be included in the input file:

In the `BEGIN PARAMETERS FOR PRESTO REGION` block, the following line must be included:

```
BEGIN PARAMETERS FOR PRESTO REGION <string>presto_region
  TIME STEP SELECTOR = AUTO
END PARAMETERS FOR PRESTO REGION <string>presto_region
```

Additionally, the node based time step syntax must also be included in the input file:

```
BEGIN NODE BASED TIME STEP PARAMETERS <string>name
END NODE BASED TIME STEP PARAMETERS <string>name
```

Chapter 5

Modal Analysis

This chapter describes a simple modal analysis capability. This capability will compute the lowest few vibration eigenmodes and values at the end of each model load step. This capability only works with solid uniform gradient hex elements and augmented Lagrange tied contact.

5.1 Modal Analysis

Warning: Modal analysis is still a capability in the early development stages. This capability is not recommended for general use, nor will any use of this capability currently be supported by the Sierra/SMdevelopment.

```
BEGIN LANCZOS EIGEN SOLVER
  MASS MATRIX = IDENTITY|LUMPED(LUMPED)
  NUMBER OF EIGENPAIRS = <integer>N
  DEBUG = OFF|ON(OFF)
END
```

The command `NUMBER OF EIGENPAIRS` defines the number of eigenvalues and modes to compute. The lowest `N` modes will be computed. Significant expense is required to compute and store each mode, thus `N` should be kept relatively small (no more than 25 or so).

The `DEBUG` command turns on or off additional debugging outputs from the eigensolver.

The `MASS MATRIX` allows the user to selectively compute the eigenvalues of the tangent stiffness matrix when `IDENTITY` is set. Otherwise, the standard eigenvalue problem is computed with both the tangent stiffness matrix and the lumped mass matrix. A consistent mass matrix is not available at this time.

Chapter 6

Solvers and Solver Options

6.1 Newton Solver

```
BEGIN SOLVER
  BEGIN NEWTON
     #
     # convergence criteria commands
     #
     TARGET RESIDUAL = <real>target_resid
       [DURING <string list>period_names]
     TARGET RELATIVE RESIDUAL = <real>target_rel_resid(1.0e-4)
       [DURING <string list>period_names]
     ACCEPTABLE RESIDUAL = <real>accept_resid
       [DURING <string list>period_names]
     ACCEPTABLE RELATIVE RESIDUAL = <real>accept_rel_resid
       [DURING <string list>period_names]
     REFERENCE = EXTERNAL|INTERNAL|BELYTSCHKO|RESIDUAL|ENERGY
       (EXTERNAL) [DURING <string list>period_names]
     RESIDUAL NORM TYPE = ALL|TRANSLATION|SCALE_RB_ROTATIONS
       (ALL) [DURING <string list>period_names]
     #
     # iteration control
     #
     MINIMUM ITERATIONS = <integer>min_iter(0)
       [DURING <string list>period_names]
     MAXIMUM ITERATIONS = <integer>max_iter
       [DURING <string list>period_names]
     #
     # Selection of the linear solver for use in solving
     # linearized Newton iterations
     #
     LINEAR SOLVER = <string>linear_solver_name
  END
END
```

The Newton solver is an nonlinear equation solver that is an alternative to the default conjugate gradient (CG) solver. Each iteration of the Newton solver consists of reforming current tangent stiffness matrix and re-solving the equation set with that current tangent. The Newton solver is typically significantly more expensive than the CG solver but may be more robust if there is substantial nonlinearity occurring over a time step. The Newton solver may also potentially prevent overshooting of yielding or other material nonlinearity. If a model has very nonlinear materials and is failing to converge with the CG solver the Newton solver may be worth trying.

The convergence criteria and iteration control commands in the Newton solver behave identically to the equivalent commands in the CG solver. The `LINEAR SOLVER` specifies the solver to use during the linearized equation solution step each Newton iteration. the `FETI` solver is recommended but any available linear may work.

6.2 Control Contact : Control Subset

```
BEGIN CONTROL CONTACT
  CONTROL SUBSET = ADAGIO|ALL|ARS|JAS|SST
END
```

By default all implicit contact constraints are enforced simultaneously. The `CONTROL SUBSET` option to the control contact solver block is an experimental option for enforcing different types of constraints at different levels of the multilevel solver. . For example the following input will control the node face (ADAGIO) contact constraints at level one and the analytic rigid surface contact constraints (ARS) at level two. This means that ARS constraints are found held constant while ADAGIO constraints are iteratively solved. Then the ARS constraints are updated and again held constant while the ADAGIO constraints are iteratively solved again.

```
begin control contact control_al
  level = 1
  target relative residual = 5.e-04
  control subset = ADAGIO
end control contact

begin control contact control_ars
  level = 2
  target relative residual = 1.e-3
  control subset = ARS
end control contact
```

Use of the `CONTROL SUBSET` will substantially increase analysis cost, but may lead to more robust convergence if the model contains potentially conflicting contact constraint types acting on the same nodes.

Chapter 7

eXtended Finite Element Method (XFEM)

Warning: This capability is in development, and its behavior may change considerably due to its status as an active research topic.

The `XFEM` command block may be used to introduce discontinuities in a finite element mesh via the eXtended Finite Element Method (XFEM). Use cases for XFEM include modeling stationary or propagating cracks in a finite element mesh, fast mesh generation via XFEM "carving," and adding or removing material layers to simulate, e.g., material wear or additive manufacturing processes. At its simplest, the XFEM provides a framework supporting duplication of mesh elements and subsequent partitioning and assignation of material on each side of the cut surface to each duplicate. This duplication procedure is illustrated in Figure 7.1. Piecewise planar element cuts through both two-dimensional shell and three-dimensional mesh topologies are supported in the current XFEM implementation. When an element is cut, the necessary quantities on the duplicated elements are scaled by the volume fraction of the original cut element. The mass, volume, and the internal force contribution are all scaled by the volume fraction. All other element quantities are calculated as usual.

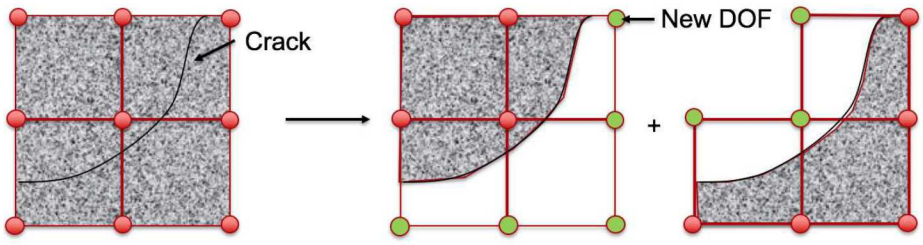

Figure 7.1: Example of XFEM element cutting and duplication.

The effective or cut volume of the domain is represented by the XFEM "submesh," a sub-element geometry which captures the discontinuity surface within each cut element duplicate. Submesh topologies for various element types are illustrated in Figure 7.2. The submesh output block, named `<block_name>_submesh`, will be created and output along with results for visualization purposes. Visualization with the submesh block is recommended as it offers an accurate repre-

sentation of crack surface and fragment geometries, as well as relevant element and nodal fields, whereas the XFEM computational elements themselves overlap and are therefore difficult to visualize.

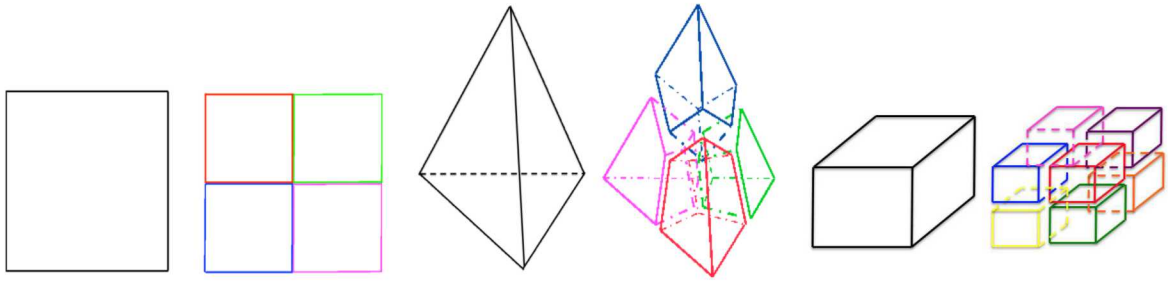

(a) Four-node quadrilateral **(b)** Four-node tetrahedral **(c)** Eight-node hexahedral

Figure 7.2: Illustration of XFEM submesh topology for various mesh element topologies.

7.1 General XFEM Commands

```
BEGIN XFEM <string>xfem_name
  BLOCK = <string list>block_name
  INCLUDE ALL BLOCKS
  ADD INFINITE PLANE = <real>px <real>py <real>pz
           <real>nx <real>ny <real>nz
  ADD DISC = <real>px <real>py <real>pz
           <real>nx <real>ny <real>nz
           <string>radius_function
  MECHANICS GROWTH START TIME = <real>time(0.0)
  MECHANICS GROWTH METHOD = <string>NOTHING|
           MECHANICS FAILURE(NOTHING)
  CRITERION = <string>{AVG NODAL|MAX NODAL|
           MIN NODAL|ELEMENT|GLOBAL}
           VALUE OF <string>variable
           {>=|>|=|<|<=} <real>threshold
  FAILURE SURFACE EVOLUTION = <string>PLANAR|PIECEWISE LINEAR|
           SINGLE CRACK(PLANAR)
  ANGLE CHANGE = <string>NONE|STRESS EIGENVECTOR|
           ONE RING|LENGTH SCALE(NONE)
  CREATE FACES = <string>ON|OFF(ON)
  GENERATION BY NUCLEATION = <string>NO|ELEMENT-BASED(NO)
  NUCLEATION CRITERION = <string>
           {AVG NODAL|MAX NODAL| MIN NODAL|ELEMENT|
           GLOBAL} VALUE OF <string>variable
           {>=|>|=|<|<=} <real>threshold
  CRACK BRANCHING = <string> RESTRICTED|ALLOWED(RESTRICTED)
  BRANCHING CRITERION = <string>
           {AVG NODAL|MAX NODAL| MIN NODAL|ELEMENT|
           GLOBAL} VALUE OF <string>variable
           {>=|>|=|<|<=} <real>threshold
  PROPAGATION ANGLE LIMIT = <real> angle
  ANGLE CHANGE LENGTH SCALE OUTER RADIUS = <real>outer_radius
  ANGLE CHANGE LENGTH SCALE INNER RADIUS = <real>inner_radius
  START TIME = <real>start_time
  INITIAL SURFACE COHESIVE = <string>FALSE|TRUE(FALSE)
  COHESIVE SECTION = <string>cohesive_section_name
  COHESIVE MATERIAL = <string>cohesive_material_name
  COHESIVE MODEL = <string>cohesive_model_name
  SOLID GROWTH DIRECTION VARIABLE =
           <string>direction_field_name(stress)
  SHELL GROWTH DIRECTION VARIABLE =
           <string>direction_field_name(memb_stress)
  VOLUME FRACTION LOWER BOUND = <real>lower_bound(0.0) DELETE|
           RETAIN(DELETE)
  CALCULATE FRAGMENT IDS = OFF|ON(OFF)
  INITIAL CUT WITH {SIDESET|STL}
```

```
            <string>file_or_surface_name
            REMOVE {INTERIOR|EXTERIOR|NOTHING(NOTHING)}
  CUT WITH DAMAGE VARIABLE = <string>variable_name
END [XFEM <string>xfem_name]
```

7.2 XFEM for Fracture and Fragmentation

The most common application of XFEM is modeling of fracture, fragmentation, and failure in structures. Currently supported fracture capabilities are

- prescribed, static or stationary cracks,
- prescribed cracks with a specified direction and rate of growth,
- prescribed cracks which are allowed to propagate by mechanics-based growth criteria, and
- cracks which are nucleated and propagated via mechanics-based criteria.

These capabilities are detailed below.

7.2.1 Fixed and Prescribed XFEM Discontinuities

A "fixed" XFEM discontinuity is stationary in both time and space; the failure surface does not change after initialization. A fixed infinite plane discontinuity can be inserted via the `ADD INFINITE PLANE` command, while a disc-shaped cut with a fixed radius may be inserted via the `ADD DISC` command. Note that the specified surfaces are used to cut the mesh in the reference configuration.

A "prescribed" XFEM discontinuity is restricted to propagate along a specific path in time. In order to prescribe an XFEM discontinuity, a disc must be inserted via the `ADD DISC` command. The discontinuity may "grow" by adding a time-varying function at the end of the `ADD DISC` command or by mechanics growth, described in Section 7.2.2 below.

7.2.2 Spontaneous Crack Nucleation, Growth, and Branching

The current XFEM implementation enables the natural evolution of fractures in materials based on mechanics nucleation, growth, and branching criteria.

Crack growth Growth, or propagation, can be enabled via the following command lines:

```
MECHANICS GROWTH METHOD = MECHANICS FAILURE
CRITERION = <string>{AVG NODAL|MAX NODAL|
          MIN NODAL|ELEMENT|GLOBAL}
          VALUE OF <string>variable
          {>=|>|=|<|<=} <real>threshold
FAILURE SURFACE EVOLUTION = PLANAR|PIECEWISE LINEAR|
          SINGLE CRACK(PLANAR)
```

The `CRITERION` command line specifies the criterion for propagation or growth of the crack from element to element. This command is precisely analogous to element death; refer to the User's Guide [1] chapter on elements for additional details. `FAILURE SURFACE EVOLUTION` specifies any geometric restrictions on fracture growth:

- `PLANAR` is the default option, which restricts the crack to grow only in the plane in which it is initialized, preventing the crack from turning or twisting.
- `PIECEWISE LINEAR` allows a crack to change directions such that it is planar within a single element; however, this option may lead to a fracture surface which is discontinuous from element to element.

Mechanics growth can be delayed in the analysis by specifying a start time (≥ 0) in the `MECHANICS GROWTH START TIME` command.

The way in which the crack growth angle change is computed can be specified via the `ANGLE CHANGE` command line in order to smooth or regularize sharply varying stress fields in the neighborhood of crack fronts. Available angle change options are

- `STRESS EIGENVECTOR`, which calculates the growth angle of the crack from the maximum principal stress eigenvector in the element to be cut;
- `ONE RING`, which defines the new failure plane by the maximum principal stress eigenvector of the *average* stress in the node-connected neighboring elements (or one-ring) of the element to be cut; and
- `LENGTH SCALE`, which computes the crack failure plane as the maximum principal stress eigenvector of the average stress in elements within a specified radial distance of the element to be cut. This distance can be specified via the `ANGLE CHANGE LENGTH SCALE OUTER RADIUS` command. By specifying `ANGLE CHANGE LENGTH SCALE INNER RADIUS`, in addition to including elements inside a given outer length scale, the growth algorithm will *exclude* elements within a given inner radius of the crack front from the direction computation. Because the length scale entails a computation involving, in general, a number of elements surrounding the crack front, this option may incur significant additional simulation time within in each load step.

The variable used to calculate the angle change can be specified via

```
SOLID GROWTH DIRECTION VARIABLE = ...
SHELL GROWTH DIRECTION VARIABLE = ...
```

for solid and shell elements, respectively. The default variable used for solid elements is "stress," while the default variable used for shell elements is "membrane stress."

Crack nucleation Spontaneous nucleation, or initiation, of cracks may be controlled by the command lines

```
GENERATION BY NUCLEATION = <string>NO|ELEMENT-BASED(NO)
NUCLEATION CRITERION = ...
```

Currently, only element-based nucleation is supported, in which a single element is cut if it exceeds the user-defined nucleation criterion (which follows the same form as the growth criterion). Nucleated cracks then grow normally according to the specified mechanics growth criterion.

Crack branching Branching behavior may also be modeled via the commands

```
CRACK BRANCHING = ALLOWED
BRANCHING CRITERION = ...
```

Currently, cracks may only branch from a single point on an element edge (i.e., from a virtual node on the element edge created by the first cut). Examples of eligible and ineligible branching locations are illustrated in Figure 7.3. All presently cut elements are branching candidates. The user-defined failure condition is examined for each element, and if the value exceeds the failure criteria, the stress eigenvectors are calculated and used to determine the possible branching direction.

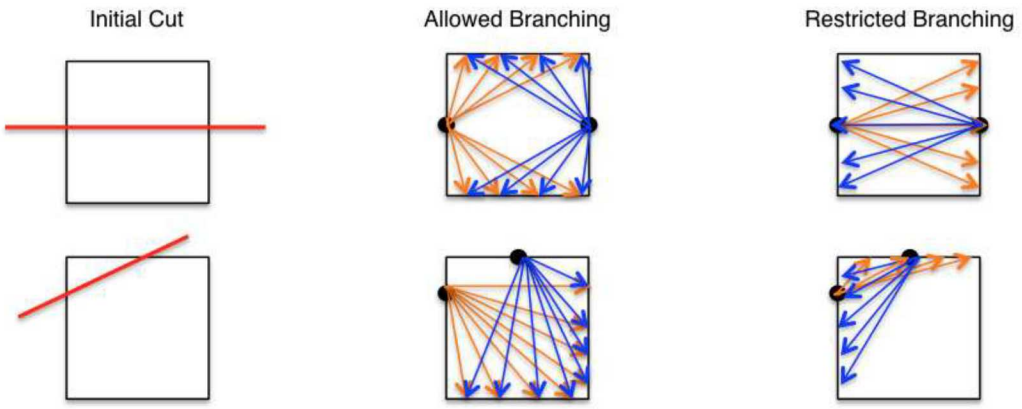

Figure 7.3: Example of allowed and restricted branching.

7.2.3 Cohesive Zone Insertion

Cohesive zones can be adaptively inserted between the XFEM discontinuities in order to better capture fracture patterns, convergence, and energy dissipation. To insert cohesive zones with XFEM,

- a cohesive section must be specified in the XFEM command block via the `COHESIVE SECTION` command line,
- a cohesive material must be specified via the `COHESIVE MATERIAL` command line, and
- a cohesive model must be specified via the `COHESIVE MODEL` command line.

In order for the cohesive zones to be inserted with the stress initialized to that of the failing element, the `INITIAL SURFACE COHESIVE = TRUE` option must be used.

Warning: Cohesive zone insertion for tetrahedral elements is not yet supported.

7.2.4 Other Options

Several miscellaneous or experimental XFEM capabilities are available for fracture and fragmentation analysis.

Volume Fraction Lower Bound By default, the XFEM implementation in Sierra does not "clip" or remove elements with arbitrarily small volume fractions. This can create issues with the conditioning of implicit solves.

The `VOLUME FRACTION LOWER BOUND` command allows the user to specify a threshold. By default, when a lower bound is provided with this command, elements whose volume fractions are

below the specified threshold will be removed from the calculation (DELETE). When the RETAIN option is specified, elements whose volume fractions are below this specified threshold will be retained, but have their volume fractions are reset to the lower bound specified by the threshold value. This insures that the smallest volume fraction of any partial element anywhere in the domain will not be smaller than the threshold.

Warning: The VOLUME FRACTION LOWER BOUND can result in the loss of mass conservation for an embedded object, whether in the default mode when these small volume fractions are removed or in the RETAIN mode when mass is added.

XFEM damage-based failure XFEM can also be used to cut the mesh along a specific field on the mesh (such as a phase field damage variable). The name of this variable is specified via the CUT WITH DAMAGE VARIABLE command.

Warning: The CUT WITH DAMAGE VARIABLE option is very much in-development and not a hardened capability.

Identification of separate XFEM fragments The CALCULATE FRAGMENT IDS command can be used to output both element and nodal fragment ID fields. Turning this option to ON will set both the element variable called element_fragment_id as well as the nodal variable called node_fragment_id at the end of the simulation. Each ID corresponds to a distinct fragment from the XFEM simulation. Elements and nodes within a fragment will all be assigned the same fragment ID. Labeling of the fragment IDs is arbitrary, but the numbering always begins with 1 and goes to the total number of fragments in the simulation. Post-processing scripts can be use in conjunction with these fields to compute quantities such as fragment mass and momentum distributions.

7.3 XFEM Carving

In addition to modeling fracture and fragmentation, XFEM can also be used for fast mesh generation or wearing of surfaces via "carving." The carving procedure is roughly equivalent to an immersed boundary approach; boundary and contact surfaces are represented by the XFEM cut surface, and the effective carved element response is computed via XFEM volume fraction scaling.

The initial mesh may be carved with the command line

```
INITIAL CUT WITH {SIDESET|STL} = <string>file_or_surface_name
  [REMOVE {INTERIOR|EXTERIOR|NOTHING(NOTHING)}]
```

where `STL` indicates to carve the mesh with a stereolithography (STL) file [2], while the `SIDESET` option indicates to carve with a specified sideset from the input mesh file.

Carved material may be removed after the cut is made via the option `REMOVE {INTERIOR|EXTERIOR}`, where the "exterior" consists of all material points lying outside of the region bounded by the carving surface in the direction of its outward normal vector; similarly, the "interior" is the region bounded by the carving surface in the direction opposite its outward normal. As an example, the XFEM command block to cut all blocks with a surface defined in an STL file `file.stl` and remove material interior to the surface is the following:

```
BEGIN XFEM
  INCLUDE ALL BLOCKS
  INITIAL CUT WITH STL file.stl REMOVE INTERIOR
END [XFEM]
```

7.4 Use of XFEM with Existing Capabilities

An XFEM command block may be used in conjunction with a number of other core code capabilities, as enumerated in [1]. A brief list of compatible capabilities and usage guidelines are given below.

7.4.1 Contact

```
BEGIN CONTACT DEFINITION <string>name
  ...
  CONTACT SURFACE <string>name CONTAINS
        <string_block_name>_CONTACT_SURFACE
  BEGIN INTERACTION DEFAULTS
    SELF CONTACT = ON
    GENERAL CONTACT = ON
  END
  ...
END [CONTACT DEFINITION <string> name]
```

Contact may be enforced on a block that has been cut using XFEM, including the cut surface itself. Contact can be defined using the `GENERAL CONTACT = ON` command within the `INTERACTION DEFAULTS` section of the contact definition. A contact surface called `<string_block_name>_CONTACT_SURFACE` is created for each XFEM block; thus, a contact surface may be defined on an XFEM block by using the `CONTACT SURFACE <string>name CONTAINS <string_block_name>_CONTACT_SURFACE` command line. The XFEM contact surface is also output to the results file *as a shell element block* for visualization purposes.

7.4.2 CONWEP Blast Pressure

```
BEGIN BLAST PRESSURE <string> name
  BLOCK = <string_block_name>_submesh
  ...
END [BLAST PRESSURE <string> name]
```

XFEM can also be used in conjunction with a CONWEP blast pressure. The pressures that are applied to the cut faces are scaled by the area fraction of that cut face. The pressures are applied to the face throughout the duration of the blast.

7.4.3 Implicit Dynamics

XFEM may be run in implicit dynamics. If an implicit simulation is run, it is highly recommended to include an adaptive time stepping block, as shown below. Adaptive time stepping helps to account for the increased complexity of the problem during crack growth.

For additional guidance and command syntax, consult the User's Guide [1] section on implicit time step control.

Warning: Convergence of XFEM simulations in implicit dynamics mode is currently tenuous; robustness issues may occur when using this analysis combination.

References

[1] Sierra/SolidMechanics Team. Sierra/SolidMechanics 4.46 User's Guide. Technical Report SAND2017-9759, Sandia National Laboratories, Albuquerque, NM, 2017.

[2] 3D Systems, Inc. SLC File Specification, 1994.

Chapter 8

Explicit Control Modes

8.1 Limitations and Requirements

In explicit dynamic calculations, the Explicit Control Modes method uses a coarse mesh overlaying the actual problem mesh (called the reference or fine mesh) to increase the critical time step. The name *control mode* comes from the implicit multigrid solution algorithm in Adagio. The Explicit Control Modes algorithm is discussed in [1] and [2].

Warning: Explicit Control Modes is an experimental analysis technique. It has been shown to be an extremely useful technique on specific problems. However, it does not interoperate with some features, such as rigid bodies. Contact the Sierra/SM development team for more information on the features that do cooperate with Explicit Control Modes.

Known Issue: When using Explicit Control Modes, the Lanczos and Power Method time step estimators cannot yet be used with problems that have contact, rigid bodies, blocks in the fine mesh that are not controlled by the coarse mesh, or coarse elements that contain no fine nodes.

In explicit dynamics, nodal accelerations are computed by dividing the residual (external minus internal) force by the nodal mass. In the Explicit Control Modes algorithm, the reference mesh residual is mapped to the coarse mesh, and accelerations are computed on the coarse mesh. These accelerations are then interpolated back to the reference mesh. The portion of the residual with higher frequency content (i.e., that which is not representable by the basis functions of the coarse mesh) determines a fine mesh acceleration that is added to the acceleration interpolated from the coarse mesh.

By computing the acceleration on the coarse mesh, the Explicit Control Modes algorithm allows for the critical time step to be computed based on the size of the coarse mesh rather than the size of the reference mesh. A critical time step is estimated based on the coarse mesh. Mass scaling is applied to the high frequency component of the acceleration (computed on the reference mesh to increase the time step to the coarse mesh critical time step). Mass scaling introduces error, but the error only occurs in the high frequency part of the response. In contrast, traditional mass scaling

affects the full spectrum of structural response. Explicit Control Modes is effective in problems in which the coarse grid represents the frequency range of interest and is significantly coarser than the reference mesh to maximize the critical time step.

The choice of the degree of refinement in the coarse and reference meshes has a large influence on the effectiveness of the Explicit Control Modes algorithm. The reference mesh should be created to give a discretization that is appropriate to capture the geometry of the problem with sufficient refinement to adequately represent gradients in the discretized solution. The coarse mesh should completely overlay the reference mesh, and it should be coarser than the reference mesh at every location in the model. All coarse elements need not contain elements in the reference mesh; it is possible to use a coarse mesh that extends significantly beyond the domain of the reference mesh.

The user has the freedom to create a coarse mesh that gives an acceptable critical time step without using an excessively crude discretization. Remember that the reference mesh controls the spatial discretization, while the coarse mesh controls the temporal discretization of the model.

To use Explicit Control Modes, the user should set up the reference mesh file and the input file as usual, except that the following additional items must be provided:

- A coarse mesh must be generated, as discussed above. The coarse mesh must be in a separate file from the reference mesh, which is the real model.
- A second `FINITE ELEMENT MODEL` command block must be provided in addition to the standard definition for the reference finite element model in the input file. This command block is set up exactly like the first `FINITE ELEMENT MODEL` command block [3] except that the mesh file referenced is the coarse mesh instead of the reference mesh. Even though the coarse mesh uses no material models, each block in the coarse mesh must be assigned a material model.
- A `CONTROL MODES REGION` command block must appear alongside the standard `PRESTO REGION` command block within the `PRESTO PROCEDURE` command block. The presence of the `CONTROL MODES REGION` command block instructs Presto to use the Explicit Control Modes algorithm. The `CONTROL MODES REGION` command block is documented in Section 8.2. It contains the same commands used within the standard `PRESTO REGION` command block, except that the commands in the `CONTROL MODES REGION` command block are used to control the control modes algorithm and the boundary conditions on the coarse mesh.

8.2 Control Modes Region

```
BEGIN CONTROL MODES REGION
   #
   # model setup
   USE FINITE ELEMENT MODEL <string>model_name
   CONTROL BLOCKS [WITH <string>coarse_block] =
                        <string list>control_blocks
   #
   # time step control
   TIME STEP RATIO SCALING = <real>cm_time_scale(1.0)
   TIME STEP RATIO FUNCTION = <string>cm_time_func
   LANCZOS TIME STEP INTERVAL =
                           <integer>lanczos_interval
   POWER METHOD TIME STEP INTERVAL =
                              <integer>pm_interval
   #
   # mass scaling
   HIGH FREQUENCY MASS SCALING =
                           <real>cm_mass_scale(1.0)

   #
   # stiffness damping
   HIGH FREQUENCY STIFFNESS DAMPING COEFFICIENT =
                            <real>cm_stiff_damp(0.0)
   #
   # kinematic boundary condition commands
   BEGIN FIXED DISPLACEMENT
                           # Parameters for
                           # fixed displacement
   END [FIXED DISPLACEMENT]
   #
   # output commands
   BEGIN RESULTS OUTPUT <string> results_name
                           # Parameters for
                           # results output
   END RESULTS OUTPUT <string> results_name
END [CONTROL MODES REGION]
```

The `CONTROL MODES REGION` command block controls the behavior of the control modes algorithm and is placed alongside a standard `PRESTO REGION` command block within the `PRESTO PROCEDURE` scope. With the exception of the `CONTROL BLOCKS` command line, all the commands that can be used in this block are standard commands that appear in the Presto region. These commands have the same meaning in either context- they simply apply to the coarse mesh or to the reference mesh, depending on the region block in which they appear. Sections 8.2.1 through 8.2.3 describe the components of the `CONTROL MODES REGION` command block.

8.2.1 Model Setup Commands

```
USE FINITE ELEMENT MODEL <string>model_name
CONTROL BLOCKS [WITH <string>coarse_block] =
       <string list>control_blocks
```

The command lines listed above must appear in the `CONTROL MODES REGION` command block if Explicit Control Modes is used. The `USE FINITE ELEMENT MODEL` command line should reference the finite element model for the coarse mesh. This command line is used in the same way that the command line is used for the reference mesh [3].

The `CONTROL BLOCKS` command line provides a list of blocks in the reference mesh controlled by the coarse mesh. The block names are listed using the standard format for referencing mesh entities [3]. For example, the block with an ID of 1 would be listed as `block_1` in this command. Multiple `CONTROL BLOCKS` command lines may be used.

The `CONTROL BLOCKS` command line does not require the coarse blocks used to control the fine blocks to be listed. In the following example, blocks 10 and 11 are controlled by the coarse mesh, but the element blocks in the coarse mesh that control those blocks are not listed:

```
CONTROL BLOCKS = block_10 block_11
```

If the `CONTROL BLOCKS` command line is used in this manner, the search for fine nodes contained within coarse elements will be conducted for all elements in the coarse mesh. The coarse block used to control a given set of fine blocks can optionally be specified by using the `CONTROL BLOCKS WITH coarse_block` variant of the command. For example, the command:

```
CONTROL BLOCKS WITH block_1 = block_10 block_11
```

would use block 1 on the coarse mesh to control blocks 10 and 11 on the fine mesh. This variant of the command is necessary when the coarse blocks overlap. It removes any ambiguity about which coarse elements control which fine nodes. This is particularly useful for contact problems where the fine block on one side of an interface should be controlled by one block, and the fine block on the other side of the interface should be controlled by a different block. Only one coarse block can be listed in a given instance of this command. If there are multiple coarse blocks, they must be listed in separate commands.

8.2.2 Time Step Control Commands

The time step control commands for Explicit Control Modes are based on the Presto time step control commands (see the Explicit Dynamic Time Step Control chapter of [3]).

```
TIME STEP RATIO SCALING = <real>cm_time_scale(1.0)
TIME STEP RATIO FUNCTION = <string>cm_time_func
LANCZOS TIME STEP INTERVAL =
                          <integer>lanczos_interval
POWER METHOD TIME STEP INTERVAL =
                          <integer>pm_interval
```

The control modes algorithm computes a node-based time step for the coarse mesh at each time step and uses this as the default time step. This time step is typically larger than the critical time step for the fine mesh.

The `TIME STEP RATIO SCALING` and `TIME STEP RATIO FUNCTION` command lines allow the user to control the time step used with explicit control modes. The `TIME STEP RATIO SCALING` command is used to specify a scale factor `cm_time_scale`, which has a default value of 1.0. The `TIME STEP RATIO FUNCTION` command is used to specify a function `cm_time_func` that is used to control the scale factor as a function of time. At any given time, a scale factor, f_{ts}, is computed by multiplying `cm_time_scale` by the current value of the function. Both of these commands are optional and one can be used without the other.

The time step Δt, is computed as a function of f_{ts}, as well as of the time step of the fine mesh, Δt_f and the time step of the coarse mesh, Δt_c.

$$\Delta t = \Delta t_f + f_{ts}(\Delta t_c - \Delta t_f) \tag{8.1}$$

Thus, if the scale factor is zero, the time step of the fine mesh is used, and if it is one, the time step of the coarse mesh is used.

The nodal time step estimator for the coarse mesh typically works well on problems where the fine mesh overlaid by the coarse mesh is essentially isotropic. In cases where it is not, such as when there are significant voids covered by the coarse mesh, the nodal time step can be non-conservative, resulting in stability problems. The time step control command lines described above can be used to manually scale down the time step in such scenarios.

Here is an example of stubs for controlling the time step.

```
# Coarse/Fine mesh scaling function.
begin function cm_time_ratio
  type is piecewise linear
  begin values
    0.0      1.0
    0.005    1.0
    0.01     1.0
  end values
end
begin control modes region beamCoarse
    use finite element model beamCoarse
    control blocks = block_1
    filter = mass
    time step ratio scaling = 1.0
    time step ratio function = cm_time_ratio
    high frequency mass scaling = 1.0
end
```

This particular example uses the default parameters. Non-default parameters may be accessed by changing the corresponding 1.0 values.

Alternatively, either the Lanczos or Power Method global time step estimators can be applied to the coarse mesh to give an improved estimate of the stability limit. These are invoked using the `LANCZOS TIME STEP INTERVAL` or `POWER METHOD TIME STEP INTERVAL` command lines, respectively. Only one of these command lines can be used at a time, and both commands specify an interval at which the global time step estimate is calculated. When the global time step estimate is calculated, a ratio of the global estimate to the nodal estimate is calculated, and this ratio is used to scale the nodal estimate in subsequent time steps in which the global estimate is not computed.

Experience has shown that the time step predicted by the global time step estimators is typically slightly higher than the actual stability limit. For this reason, it is recommended that a scale factor of 0.9 be used in conjunction with these estimators. This can be set using the `TIME STEP SCALE FACTOR` command line in the `TIME CONTROL` block as described in [3].

8.2.3 Mass Scaling Commands

```
HIGH FREQUENCY MASS SCALING =
                        <real>cm_mass_scale(1.0)
```

The `HIGH FREQUENCY MASS SCALING` command line allows the user to control the mass scaling applied to the high frequency component of the response. The mass scaling factor required to stably integrate the high frequency response at the time step being used is computed at every node on the fine mesh. The parameter `cm_mass_scale` that can optionally be supplied with this command line is applied as a multiplier to that mass scaling. If that mass scaling (multiplied by `cm_mass_scale`) is greater than 1.0, then the scaled mass is used at that node. If not, the original nodal mass is used.

It may be useful for some models to use this command line to set `cm_mass_scale` to a value greater than 1.0 to stabilize the high frequency response. Experience has shown, however, that this is rarely needed.

It is also possible to request a consistent coarse mass matrix, instead of the default lumped mass matrix. Here is an example illustrating the syntax.

```
begin control modes region beamCoarse
  use finite element model beamCoarse
  control blocks = block_1
  coarse mass linear solver = feti
  coarse mass matrix = consistent
  filter = consistent
  time step ratio scaling = 0.2
end
```

8.2.4 Damping Commands

```
HIGH FREQUENCY STIFFNESS DAMPING COEFFICIENT =
                            <real>cm_stiff_damp(0.0)
```

The `HIGH FREQUENCY STIFFNESS DAMPING COEFFICIENT` command is used to apply stiffness-proportional damping on the high frequency portion of the response in Explicit Control

Modes. This may help reduce high frequency noise in problems that have abrupt loading such as that caused by contact. The default value of `cm_stiff_damp` is 0.0. The value specified for `cm_stiff_damp` can be between 0 and 1. It is recommended that small values (around 0.001) be specified if this option is used.

8.2.5 Kinematic Boundary Condition Commands

```
BEGIN FIXED DISPLACEMENT
       #
       # Parameters for fixed displacement
       #
END FIXED DISPLACEMENT
```

All types of kinematic boundary conditions can be applied to the coarse mesh. This is done by inserting a kinematic boundary condition command block in the `CONTROL MODES REGION` command block. The mesh entity (node set, surface, or block) to which the boundary condition is applied must exist on the coarse mesh.

This capability is potentially useful to ensure better enforcement of kinematic boundary conditions on the fine mesh by applying the same type of boundary condition on the portion of the coarse mesh that overlays the portion of the fine mesh to which boundary conditions are applied. For example, if there is a node set on the fine mesh that has a fixed displacement boundary condition, a node set can be created on the coarse mesh that covers the same physical domain. The same fixed displacement boundary condition could then be applied to the coarse mesh.

Although the capability to enforce boundary conditions on the coarse mesh is provided, it is not necessary to do so. It is also often difficult to create a node set on the coarse mesh that matches the discretization of the node set on the fine mesh. Users are advised to initially prescribe kinematic boundary conditions only on the fine mesh and only prescribe boundary conditions on the coarse if the initial results appear questionable.

8.2.6 Output Commands

```
BEGIN RESULTS OUTPUT <string> results_name
       #
       # Parameters for results output
       #
END RESULTS OUTPUT <string> results_name
```

Variables can be output from the coarse mesh just as they can from the fine mesh with Explicit Control Modes. Because the actual results of interest for the model all reside on the fine mesh, it is typically not necessary to output results on the coarse mesh. However, this can be helpful for debugging purposes.

The syntax for the results output for the coarse mesh is identical to that used for output from the fine mesh [3]. The only thing that differentiates the `RESULTS OUTPUT` command block for the coarse mesh from that of the fine mesh is that the results output block for the coarse mesh is put in the `CONTROL MODES REGION` command block instead of in the `PRESTO REGION` command

block. The output files for the coarse and fine mesh must be different from each other, so different output file names must be used within the output blocks for the coarse and fine meshes.

One of the most useful variables to output from the coarse mesh is the nodal `timestep`. This variable is similar in nature to the element `timestep`, which exists on the fine mesh, but is a nodal variable rather than an element variable and exists on the coarse mesh. The nodal `timestep` reports the critical time step calculated for each node on the coarse mesh. If the coarse time step is higher than expected, the output from `nodal_time_step` can be examined to see which region of the coarse mesh is controlling the time step.

Central difference time integration is performed on the coarse mesh in addition to the fine mesh, so the `displacement`, `velocity`, and `acceleration` variables can be requested for visualization on the coarse mesh.

8.2.7 ECM with Lanczos

As the known issue suggests that Lanczos works with ECM. Here's an example.

```
begin control modes region beamCoarse
  use finite element model beamCoarse
  control blocks = block_1
  filter = mass
  time step ratio scaling = 0.9
  high frequency mass scaling = 1.0
  lanczos time step interval = 100
end
```

Assume for clarity that the Lanczos time step size is significantly larger than the element time step size. Initially the `Element time step in Lanczos` is used. At the following time steps, the time step size increases the time step size by a factor of 1.1, the default value of the `time step increase factor` mentioned in [3] section 3.2.1.5. When the time step size is near to time Time step from Lanczos method, Lanczos time step, a different time step is used. The maximal time step may depend on `time step increase factor` and other Lanczos parameters. To compare to Lanczos with no coarse grid, add to the presto region block

```
begin lanczos parameters set1
  number eigenvalues = 50
  eigenvalue convergence tolerance = 1.0e-4
  update step interval = 100
  vector scale = 1.e-8
  debug = on
end lanczos parameters set1
```

In the case at hand, the ECM increases the time step from $4e-7$ to $1.5e-6$.

8.3 ECM Theory

Explicit transient dynamics is a well-established capability for modeling large deformations of structures. It is common practice in explicit transient dynamics to seek a balance between computational efficiency and accuracy. Mass scaling [4] has traditionally been used as an approach to increase the critical time step limit associated with the central difference time integrator. Unfortunately, this has an undesirable side effect of mass damping dynamic modal response over the entire frequency spectrum. To mitigate this effect, methods have been developed in which the damping is proportional to the frequency [5]. In Adagio the Explicit Control Modes algorithm performs an efficient modal decomposition of the frequency spectrum, allowing mass damping only on the high frequency modes. Examples will be presented that demonstrate that this approach yields accurate low frequency response, while often using larger time steps due to the mass scaling the high frequency response.

8.3.1 Introduction

Finite element analysis of transient dynamic problems is a production capability in many application areas. In these analyses an important question to be addressed by the analyst is the choice of using an explicit or implicit time integrator. It is well understood that the central difference explicit time integrator is efficient per time step but is restricted to taking relatively small, critical (or stable) time steps [6, 7]. An implicit time integrator, specifically the Hilber–Hughes–Taylor (HHT) time integrator [8], with the proper choice of parameters has no such stability limit allowing larger time steps but produces a system of equations that need to be solved every time step. As noted in [8], a consequence of choosing a large time step for the implicit time integrator is that it produces numerical damping in all frequencies, but predominantly in the highest frequencies. Just how much damping and in what modes depends on the particular problem. Thus, the question of what time integrator to use is much more than simply one of efficiency. Certainly, one must know well the class of problems to be solved when making this choice.

Simulations requiring necessarily finer discretizations to accurately represent modal stiffness and resolve details in the stress field are amenable to Explicit Control Modes. For the explicit time integrator, this imposes a critical time step restriction that can be limiting. However for some—possibly many—analyses the structural response is in the lower frequency spectrum, i.e., the influence of the modal content inherent in fine mesh on the low-frequency dynamics is of interest and not necessarily the high-frequency dynamics themselves. More precisely, spatial resolution as opposed to temporal resolution is needed for many problems (this premise is one that we intend to support in the examples).

It seems appropriate, then, to consider an algorithmic approach that can improve the stability limit of the explicit time integrator. Most importantly, we recognize that this approach needs to be accurate for low-mode response and competitive with implicit dynamics.

8.3.2 Modal Decomposition Approach

The objective of this algorithm is to modally decompose the dynamics (in the context of an explicit transient dynamics time integrator) into low-frequency and high frequency response. Having this decomposition may provide options such as integrating the low-frequency modes with explicit time

integration and the high-frequency modes with an implicit time integrator.

The decomposition algorithm is based on applying multigrid concepts within an explicit central difference time integrator. We will limit the algorithm to consider only one addition level of coarsening. Thus, in addition to the fine mesh or reference mesh, we introduce a set of coarse basis functions that will describe the low-mode response.

The vector of external nodal forces on the fine mesh is f_{fm}^{ext}. Also the vector of internal nodal forces on the fine mesh f_{fm}^{int} is a obtained from the divergence of the stress. In this work we assume that there is no contact, in which case the nodal residual force is

$$r = f_{fm}^{ext} - f_{fm}^{int}.$$

Let M denote the diagonal, lumped [9], mass matrix for the fine mesh, and let x denote the vector of displacements on the fine mesh. Expressed in terms of the nodal displacements, the dynamic equilibrium equations is

$$M\ddot{x} = r. \tag{8.2}$$

Let Φ denote an interpolation (prolongation) matrix associated with a coarse space of functions. The number of rows in Φ equals the number of rows in x or r, while the number of columns in is typically smaller. The matrix can be obtained from either a coarse finite element mesh or by using an algebraic approach [10, 11]. Given Φ, the acceleration on the fine mesh can be written as

$$\ddot{x} = \Phi\ddot{q} + \ddot{x}_{hf} \tag{8.3}$$

where q is a vector of generalized displacements associated with the low frequency part of the response, and x_{hf} is a vector of displacements associated with the high frequency part of the response.

The task now is to derive the equation to accomplish this decomposition making use only of the residual vector, r, and mass matrix, M, on the fine mesh, recognizing that there are no properties on the coarse mesh in the usual finite element sense. As in the multigrid method, the modal stiffness of low-mode response and the corresponding mass matrix is obtained using a restriction operator of properties/quantities from the fine mesh.

The low and high frequencies are decoupled by imposing the M orthogonality,

$$\ddot{q}^T\Phi^T M\ddot{x}_{hf} = 0,$$

of the high and low frequency displacements. The orthogonality condition holds for all $\ddot{q}$ if and only if

$$\Phi^T M\ddot{x}_{hf} = 0. \tag{8.4}$$

Equation (8.4) implies that the high frequency part of the residual is orthogonal to the coarse space spanned by the columns of Φ. The coarse mesh mass matrix is given by

$$M_c = \Phi^T M\Phi.$$

Substitution of equation (8.3) into equation (8.2), pre-multiplying by Φ^T and making use of equation (8.4) leads to the low frequency equilibrium condition

$$M_c\ddot{q} = \Phi^T r. \tag{8.5}$$

This way of obtaining a coarse system from Φ is called *Galerkin coarsening* [11]. For reference, the coarse grid stiffness matrix K_c corresponding to the fine mesh tangent stiffness matrix K is given by

$$K_c = \Phi^T K \Phi.$$

Next the high frequency equilibrium equation is derived. Solving for $\ddot{q}$ in equation (8.5) gives

$$\ddot{q} = M_c^{-1} \Phi^T r. \tag{8.6}$$

From equation (8.2), equation (8.3), and equation (8.6) determine the high frequency equilibrium condition

$$M \ddot{x}_{hf} = r - M \Phi M_c^{-1} \Phi^T r. \tag{8.7}$$

At this point no approximations have been made. To sum up, substituting equation (8.6) and equation (8.7) into equation (8.3) leads to

$$\ddot{x} = \underbrace{\Phi M_c^{-1} \Phi^T r}_{\text{low frequency}} + \underbrace{M^{-1} \left(r - M \Phi M_c^{-1} \Phi^T r \right)}_{\text{high frequency}} \tag{8.8}$$

The lumped mass matrix is required to obtain the most accurate approximation properties for the explicit central difference time integrator [7, 12]. Thus, given that we are integrating the low-frequency response with central difference, a lumped representation is needed. It is unclear that the argument for finite elements and the fine mesh extend to the Galerkin coarse problem. The lumping is done simply by applying the restriction operator to the diagonal lumped fine mesh mass matrix,

$$M_c = \Phi^T M \Phi.$$

8.3.3 Explicit-Explicit Partitioning

First we consider explicit time integration for the low-frequency modes. The critical time step for integrating these modes is constructed, again via projection of nodal quantities on the fine mesh. If Δt_{cr}^{cm} denotes the critical time step for the coarse mesh, then a node-based estimate [6] is given by

$$\Delta t_{cr}^{cm} = \min_{\text{coarse nodes}} 2 \sqrt{\frac{\Phi^T M}{\Phi^T K^{max}}}$$

where K^{max} is a vector that contains the maximum modal stiffness for each node of the fine mesh. Details of the calculation of the maximum modal stiffness can be found in [6].

Next, we wish to make use of the assumption that the high-frequency dynamics are negligible. The accelerations represented by the second term in equation (8.8) correspond to those high-frequency modes. The idea is to replace M^{-1} in the second term of equation (8.8) by $\tilde{M}^{-1}$, where

$$\tilde{M} = M \alpha, \tag{8.9}$$

for a diagonal matrix α that contains a scale factor for each node of the fine mesh. These scale factors are greater than 1 wherever the nodal based time step at a fine mesh node is smaller than

the critical time step on the coarse mesh.

$$\alpha_i = \begin{cases} \frac{K_i^{max}}{4M_i}\left(\Delta t_{cr}^{cm}\right)^2 & \text{if } 2\sqrt{\frac{M_i}{K_i^{max}}} > \Delta t_{cr}^{cm} \\ 1 & \text{otherwise} \end{cases} \tag{8.10}$$

Consequently, the mass scaling produced by equation (8.10) is applied *only* to the high-frequency modes that could not otherwise be integrated stably with the central difference time integrator at the critical time step on the coarse mesh. The net result for the acceleration, $\ddot{x}$, on the reference mesh is of the form

$$\ddot{x} = \underbrace{\Phi M_c^{-1}\Phi^T r}_{\text{low frequency}} + \underbrace{\tilde{M}^{-1}\left(r - M\Phi M_c^{-1}\Phi^T r\right)}_{\text{mass-damped high frequency}} \tag{8.11}$$

8.3.4 Energy Ratio: a Measure of Approximation

Kinetic energy calculations can be performed for the low frequency and high frequency contributions separately. Using time integrated acceleration components in (16), the kinetic energy in the low frequencies is,

$$KE_{lf} = \frac{1}{2}M\|v_{lf} + \Delta t\Phi M_c^{-1}\Phi^T r\|^2 \tag{8.12}$$

Likewise, the kinetic energy in the high frequencies is,

$$KE_{hf} = \frac{1}{2}M\|v_{hf} + \Delta t\tilde{M}^{-1}\left(r - M\Phi M_c^{-1}\Phi^T r\right)\|^2 \tag{8.13}$$

With the kinetic energy quantities, an energy ratio is computed as follows,

$$\text{Energy Ratio} = \frac{KE_{lf}}{KE_{lf} + KE_{hf}}$$

Obviously, the time integrated estimates of the kinetic energies require additional memory yet they provide a useful measure for the approximations being made with the explicit-explicit modal filtering. When there is little or no approximation made using a mass-damped high frequency response the energy ratio is asymptotically approaching unity. In contrast, when the approximation error is significant, the energy ratio is well below one.

References

[1] Sierra/SolidMechanics Team. Sierra/SolidMechanics 4.46 Theory Manual. Technical Report SAND2017-9755, Sandia National Laboratories, Albuquerque, NM, 2017.

[2] B.W. Spencer, M.W. Heinstein, J.D. Hales, K.H. Pierson, and J.R. Overfelt. Multi-length scale algorithms for failure modeling in solid mechanics. Technical Report SAND2008-6499, Sandia National Laboratories, Albuquerque, NM, 2008.

[3] Sierra/SolidMechanics Team. Sierra/SolidMechanics 4.46 User's Guide. Technical Report SAND2017-9759, Sandia National Laboratories, Albuquerque, NM, 2017.

[4] T. Belytschko, W.K. Liu, and B. Moran. *Nonlinear Finite Elements for Continua and Structures*. John Wiley & Sons, 2000.

[5] L. Olovsson, K. Simonsson, and M. Unosson. Selective mass scaling for explicit finite element analyses. *International Journal for Numerical Methods in Engineering*, 63(10):1436–1445, 2005.

[6] M. Heinstein, F. Mello, and C. Dohrmann. A nodal-based stable time step predictor for transient dynamcis with explicit time integration. *Am Soc Mech Eng Press Vessels, Piping Division*, 343:225–229, 1996.

[7] T.J.R. Hughes. *The Finite Element Method: Linear static and dynamic finite element analysis*. Dover, 2000. Reprint of "The Finite Element Method", Prentice-Hall, 1987.

[8] H.M. Hilber, T.J.R. Hughes, and R.L. Talor. Improved numerical dissipation for time integration algorithms in structural dynamics. *Earthquake Engineering and Structural Dynamics*, 5: 283–292, 1977.

[9] E. Hinton, T. Rock, and O.C. Zienkiewicz. A note on mass lumped and related processes in the finite element method. *Earthquake Engineering and Structural Dynamics*, 4(3):245–249, 1976.

[10] A. Toselli and O. Widlund. *Domain Decomposition Methods – Algorithms and Theory*. Springer Series in Computational Mathematics. Springer, 2005.

[11] A. Brandt. General highly accurate algebraic coarsening. *Elect. Trans. Numer. Anal.*, 10: 1–20, 2000.

[12] R.D. Krieg and S.W. Key. Transient shell response by numerical time integration. *International Journal for Numerical Methods in Engineering*, 7:273–286, 1973.

Chapter 9

External Loadstep Predictor

Production-ready loadstep predictor types are available in Sierra/SM [1]. The `LOADSTEP PREDICTOR` command block controls the behavior of the predictor that is used to predict the solution at the beginning of a new load step. This command block is placed in the `SOLVER` scope.

The `EXTERNAL`, `EXTERNAL_FIRST` and `TANGENT` predictor types are special use capabilities currently under development.

```
BEGIN LOADSTEP PREDICTOR
       TYPE = <string>EXTERNAL|EXTERNAL_FIRST|TANGENT
END [LOADSTEP PREDICTOR]
```

The tangent predictor is selected with the `TANGENT` option, which is useful in combination with the tangent preconditioner. This type of predictor uses the tangent preconditioner to estimate the next load step's solution.

The other two predictor types use the solution from a file to predict the solution at new load steps. For instance, the external predictor file can come from the results output of a previous model run that included the command `OUTPUT EXTERNAL PREDICTOR VARIABLES` in the output block, i.e.:

```
BEGIN RESULTS OUTPUT
       OUTPUT EXTERNAL PREDICTOR VARIABLES
END [RESULTS OUTPUT]
```

If you would like to try the external predictor, please contact Sierra support for more information.

References

[1] Sierra/SolidMechanics Team. Sierra/SolidMechanics 4.46 User's Guide. Technical Report SAND2017-9759, Sandia National Laboratories, Albuquerque, NM, 2017.

Chapter 10

Total Lagrange

Total Lagrangian [1] formulations are written in terms of Lagrangian measures of stress and strain, where derivatives are taken with respect to the Lagrangian or material coordinates. This differs from the approach used in most other element formulations in the code including the uniform gradient hex, which computes derivatives with respect to the Eulerian or spatial coordinates. The currently implemented finite element topologies for the total Lagrange section are the 8-noded hexahedral, 20-noded hexahedral, 27-noded hexahedral, 13-noded pyramid, 4-noded tetrahedral, 10-noded tetrahedral, and 15-noded wedge elements.

```
BEGIN TOTAL LAGRANGE SECTION <string>section_name
    FORMULATION = <string>FULLY_INTEGRATED|
                            COMPOSITE_TET
                          (FULLY_INTEGRATED)
    STRAIN INCREMENTATION = <string>
                    STRONGLY_OBJECTIVE|
                    LOGARITHMIC_MAPPING
                   (LOGARITHMIC_MAPPING)
    CUBATURE DEGREE = <real>degree
    VOLUME AVERAGE J = <string>ON|OFF(OFF)
END [TOTAL LAGRANGE SECTION <string>section_name]
```

The defaults for the `FULLY_INTEGRATED` formulation are:

```
BEGIN TOTAL LAGRANGE SECTION <string>section_name
    FORMULATION = FULLY_INTEGRATED
    STRAIN INCREMENTATION = LOGARITHMIC_MAPPING
    CUBATURE DEGREE = 3
    VOLUME AVERAGE J = OFF
END [TOTAL LAGRANGE SECTION <string>section_name]
```

The defaults for the `COMPOSITE_TET` formulation are:

```
BEGIN TOTAL LAGRANGE SECTION <string>section_name
    FORMULATION = COMPOSITE_TET
```

```
    STRAIN INCREMENTATION = LOGARITHMIC_MAPPING
    CUBATURE DEGREE = 2
    VOLUME AVERAGE J = ON
END [TOTAL LAGRANGE SECTION <string>section_name]
```

10.1 Formulation

```
FORMULATION = <string>FULLY_INTEGRATED|
              COMPOSITE_TET(FULLY_INTEGRATED)
```

The FORMULATION command defaults to the FULLY_INTEGRATED formulation for the given finite element topology. For the 10-noded tetrahedral topology, the COMPOSITE_TET option exists, which uses a piecewise linear nodal basis instead of the standard quadratic nodal basis. For more information on the COMPOSITE_TET option please consult the Sierra/SM User's Manual chapter on Elements.

10.2 Strain Incrementation

```
STRAIN INCREMENTATION = <string>STRONGLY_OBJECTIVE|
    LOGARITHMIC_MAPPING(LOGARITHMIC_MAPPING)
```

In the total Lagrange formulation, the deformation gradient is always calculated as the derivative of the current configuration with respect to the reference configuration,

$$\boldsymbol{F}_{n+1} = \frac{\partial \boldsymbol{x}_{n+1}}{\partial \boldsymbol{X}}. \tag{10.1}$$

It follows that the incremental deformation gradient is defined as the deformation gradient between the configurations at times n and $n+1$ and can be written in terms of $\boldsymbol{F}_n$ and $\boldsymbol{F}_{n+1}$,

$$\boldsymbol{f}_{n+1} = \boldsymbol{F}_{n+1}\boldsymbol{F}_n^{-1}. \tag{10.2}$$

The `STRAIN INCREMENTATION` command is then specific to hypoelastic material models, that is, models that use the rate of deformation to increment the stress. Two approaches are available: the `STRONGLY_OBJECTIVE` option in the context of the total Lagrange formulation mirrors what is found in the `SOLID_SECTION` as described in [2],

$$\boldsymbol{d}_{n+1} = \frac{1}{2\Delta t}\log\left(\boldsymbol{f}_{n+1}\boldsymbol{f}_{n+1}^T\right); \tag{10.3}$$

the `LOGARITHMIC_MAPPING` option is comparatively more accurate in problems with large rotations,

$$\boldsymbol{d}_{n+1} = \text{sym}\,\frac{1}{\Delta t}\log\left(\boldsymbol{f}_{n+1}\right) \tag{10.4}$$

10.3 Volume Average J

```
VOLUME AVERAGE J = <string>ON|OFF
```

This command is used to construct a deformation gradient where the dilatational component is volume-averaged over the element domain. It is applicable for implicit and explicit problems employing nearly incompressible material response, such as metal plasticity, and may provide less stiff solutions in that case. In addition, if this command is `ON`, then the hydrostatic component of the stress is also volume averaged. The default setting is `OFF`.

10.4 Cubature Degree

```
CUBATURE DEGREE = <real>degree
```

This option effectively determines the number of integration points to be employed during numerical integration. For hexahedral elements, `CUBATURE DEGREE = 3` corresponds to 8 integration points, and for tetrahedral elements, `CUBATURE DEGREE = 3` corresponds to 5 integration points.

The following topology, formulation, and cubature combinations are available:

ELEMENT FAMILY	NUM. NODES	FORMULATION	CUBATURE DEGREE(S)
hexahedron	8	fully_integrated	3
	20	fully_integrated	3
	27	fully_integrated	3, 5
pyramid	13	fully_integrated	3
tetrahedron	4	fully_integrated	2, 3
	10	fully_integrated	2, 3, 4
tetrahedron	10	composite_tet	2, 3
wedge	15	fully_integrated	3

References

[1] K.-J. Bathe. Finite element formulations for large deformation dynamic analysis. *International Journal for Numerical Methods in Engineering*, 9:353–386, 1975.

[2] M.M. Rashid. Incremental kinematics for finite element applications. *International Journal for Numerical Methods in Engineering*, 36:3937–3956, 1993. doi.

Chapter 11

Bolt

Warning: The Bolt section is known to have limited functionality in implicit analyses.

```
BEGIN BOLT SECTION <string>section_name
  ATTACHMENT RADIUS = <real>radius
  SURFACE 1 = <string>surf1
  SURFACE 2 = <string>surf2
  NORMAL DISPLACEMENT FUNCTION = <string>normFunc
  SHEAR DISPLACEMENT FUNCTION = <string>shearFunc
END
```

The `BOLT` command block is used to define a two node beam or set of beams representing individual bolts or other fasteners. This capability is similar to the `SPOT WELD` capability. The beam elements should be meshed such that one beam end node is roughly on surface 1 and the other beam end node is roughly on surface 2. The beam element does not need to be meshed contiguous with the surface nodes.

The beam element is attached to all nodes and faces within a specified radius of the beam end nodes given by the `ATTACHMENT RADIUS` command. To be valid the bolt must find at least one face and three nodes within this radius on each surface.

The `NORMAL DISPLACEMENT FUNCTION` and `SHEAR DISPLACEMENT FUNCTION` define normal and shear force displacement functions for the bolt. The normal displacement function defines tensile response in positive x and compressive response in negative x. The shear displacement function is radially symmetric and only the positive x portion of the function will be used. The last point on the shear displacement function and the first and last points on the normal displacement function implicitly define the bolt failure criteria. Once a bolt fails the strength will ramp down over 10 steps and the bolt will provide zero force thereafter.

The bolt uses the same combined shear/normal mode failure as does the spot weld as defined in Equation 11.1. u_n is the bolt normal extension. The maximum value given for u_n in the normal displacement curve is $u_{n_{crit}}$, but is different for positive and negative displacements. u_t is the bolt

shear deformation. The maximum value given for u_t in the normal displacement curve is $u_{t_{crit}}$. The value p is a exponent that controls the shape of the failure surface, currently this exponent is defaulted to 2.

$$(u_n/u_{n_{crit}})^p + (u_t/u_{t_{crit}})^p < 1.0\,. \tag{11.1}$$

The original direction defining normal and shear displacement is defined by the bolt element orientation. This normal will rotate based on the rotation of attached faces, not rotation of the bolt element itself.

Table 11.1 describes the output variables available on the bolt elements.

Table 11.1: Bolt Element Output Variables

Name	**Description**
`displacement_normal`	Current normal displacement in bolt
`displacement_shear`	Current shear displacement in bolt
`force_normal`	Current normal force in bolt
`force_shear`	Current shear force in bolt
`bolt_death_status`	One for alive, zero for dead, some value between zero and one when fading out immediately after hitting the death criteria.

Chapter 12

Linear Beam

Warning: The Linear Beam section is known to have limited functionality in implicit analyses.

```
BEGIN LINEAR BEAM SECTION <string>section_name
    T AXIS = <real>tx <real>ty <real>tz
    AREA = <real>area
    I11 = <real>i11
    I22 = <real>i22
    I12 = <real>i12(0.0)
    J = <real>J
    SHEAR AREA 1 = <real>val(AREA)
    SHEAR AREA 2 = <real>val(AREA)
END
```

The `LINEAR BEAM SECTION` command block is used to specify the properties for a linear beam element. If this command block is referenced in an element block of three-dimensional, two-node elements, the elements in the block will be treated as beam elements. The name, `beam_section_name`, can be used by the `SECTION` command line in a `PARAMETERS FOR BLOCK` command block.

The beam geometry properties are defined via areas and moments of inertia for the beam section. The linear beam will behave as a linear elastic element. If a linear beam has a nonlinear material, only the elastic constants of that material, such as Young's modulus and Poisson's ratio, will affect the beam behavior.

The beam element is formulated in a local orthogonal RST coordinate system. The R axis of the beam lies along the beam element. The T axis direction is given in the input deck. If the provided T axis is not orthogonal to R, the closest vector to T that is orthogonal to R will be used define the T axis. The S axis is then constructed orthogonal to R and T based on the right hand rule (The actual method of forming these axes is slightly different from this description.). The `T AXIS` command in the linear beam behaves identically to the `T AXIS` command in the standard beam.

See the BEAM SECTION description in the Sierra/SolidMechanics User's Guide for more examples and discussion on use of the T AXIS command.

The following cross sectional properties are available for linear beams.

- AREA: Cross sectional area used to define axial and shear properties.
- I11: Bending moment of inertia in the T direction of the beam.
- I22: Bending moment of inertia in the S direction of the beam.
- I12: Product of inertial of the beam for asymmetric sections. This value is by default set to zero.
- J: Polar moment of inertia used to define beam torsional properties.
- SHEAR AREA 1: Area used for shear resistance in the T direction. If unspecified the cross sectional area AREA will be used.
- SHEAR AREA 2: Area used for shear resistance in the S direction. If unspecified the cross sectional area AREA will be used.

This linear beam is a Timoshenko (also called a Reissner-Mindlin) shear deformable thick beam. If the thickness is small relative to the length, it behaves like an Euler-Bernoulli beam. The pre-integrated element stiffness was taken directly from Reference [1].

Note, linear beam elements do not calculate element stress or stress based quantities. Linear beam elements generate nodal internal forces however no element specific output quantities are currently available on linear beam elements.

References

[1] J.S. Przemieniecki. *Theory of Matrix Structural Analysis*. Dover Publications Inc., New York, NY, 1985.

Chapter 13

Contact

This chapter describes contact features that are not fully tested or are still in development or have usability issues.

13.1 Analytic Contact Surfaces

This section describes the input syntax for defining analytic rigid contact surfaces in a Sierra/SM analysis.

A contact surface can be defined by an analytic surface. An analytic surface is defined by an algebraic expression, not by a collection of faces derived from elements. For example, an algebraic expression that defines the surface of a cylinder.

The contact node set can be used in a node to analytic surface interaction. Analytic surface can only interact with node-based or face-based surfaces, and cannot interact with each other.

Sierra/SM permits the definition of rigid analytic surfaces for use in contact. Contact evaluation between a deformable body and a rigid analytic surface can be faster than contact evaluation between two faceted bodies. Therefore, using a rigid analytic surface is more efficient than using a faceted body to try to approximate a geometric surface.

Several types of analytic surfaces definitions are available.

13.1.1 General Analytic Surfaces

Defining a general analytic body is somewhat involved. First the mathematical description of the body must be input at the sierra scope:

```
BEGIN ANALYTIC SURFACE <string>geomName
    ORIGIN = <real>Ox <real>Oy <real>Oz
    RAXIS  = <real>Rx <real>Ry <real>Rz
    SAXIS  = <real>Sx <real>Sy <real>Sz

    STARTING POINT = <real>start_r <real>start_s
    CIRCLE    =
        <real>p2r <real>p2s <real>p3r <real> p3s
    LINE      = <real>p2r <real>p1r
    REVOLVE   = <real>start_theta <real>end_theta
    TRANSLATE = <real>start_t <real> end_t
END
```

The analytic surface is created by defining a two dimensional set of lines and then extruding or revolving those lines to create a three dimensional surface.

The `ORIGIN` command defines the XYZ coordinates of the origin of the local two dimensional RS coordinate system. The `RAXIS` and `SAXIS` commands define the R and S axes for the two dimensional coordinate system. If R and S are not fully orthogonal as input `SAXIS` will be orthogonalized against `RAXIS`. A T axis is also defined that is orthogonal to both R and S and obeys the right hand rule.

Exactly one `STARTING POINT` command must be placed in the command block. The starting point command gives the coordinates for the first RS line segment point. Subsequent lines and curves are added by providing `LINE` and `CIRCLE` commands. The `LINE` command creates a new linear line segment from the end of the last line segment or the starting point to the provided

point. The CIRCLE command creates a new curved line segment. The CIRCLE command creates a circular arc going though the end of the last line segment or starting point and the two provided points. The circular arc will end at the last provided point p3.

Once all line segments are defined in RS coordinates, those line segments can be turned into a three dimensional body. The REVOLVE command revolves a set of lines about the R axis. The start angle and end angle for the revolve are specified in degrees with start_theta and end_theta. The zero degree line for theta is the S axis. The TRANSLATE commands extrudes the two dimensional line segments into a three dimensional surface. The extrusion is along the T axis starting from start_t and ending at end_t. Exactly one REVOLVE or one TRANSLATE command must be specified in the ANALYTIC SURFACE command block.

The geometry for the rigid body is defined at the BEGIN SIERRA scope. the rigid surface itself is input into the contact scope via the ANALYTIC GENERAL SURFACE command block inside the BEGIN CONTACT DEFINITION scope:

```
BEGIN ANALYTIC GENERAL SURFACE <string>surfName
    ANALYTIC SURFACE = <string>geomName
    REFERENCE RIGID BODY = <string>rbName
END
```

The ANALYTIC GENERAL SURFACE command block creates an analytic surface named surfName. The name surfName can be referenced when defining interactions between contact surfaces. The geomName string in the ANALYTIC SURFACE command references the name of an analytic geometry defined via the ANALYTIC SURFACE command block in the sierra scope.

Optionally the analytic surface can be associated with a rigid body, for information on rigid bodies see User's Manual. If an analytic surface is associated with a rigid body, the surface will translate and rotate along with the rigid body. Additionally any contact forces applied to the analytic surface will be assembled to the rigid body reference node causing the rigid body to move.

The VISUALIZE CONTACT FACETS option (See User's Manual) can be used to help confirm that analytic rigid surfaces are being defined as expected. When using the visualize facet option, general analytic surfaces will be represented by an approximate faceted surface in the output meshes.

Example: The example below defines an analytic cylinder. The cylinder is centered at (0.0, 0.0, 0.0). The center axis of the cylinder lies along the z axis. The cylinder has a radius 1.0 and length of 10.0. The cylindrical surface is defined by creating a line in RS space and then revolving that line about the T axis.

The cylinder is attached to a rigid body block_1000, the analytic cylinder around block_1000 impacts the meshed exterior surface of finite element block block_1.

```
BEGIN SIERRA
  BEGIN ANALYTIC SURFACE axleGeom
    ORIGIN          = 0.0  0.0  0.0
    RAXIS           = 1.0  0.0  0.0
    SAXIS           = 0.0  1.0  0.0
```

```
  STARTING POINT = -5.0 1.0
  LINE           =  5.0 1.0
  REVOLVE        = 0.0 360.0
END

BEGIN RIGID BODY axleRB
END

BEGIN SOLID SECTION axleSect
  RIGID BODY = axleSect
END

BEGIN FINITE ELEMENT MODEL mesh1
  BEGIN PARAMETERS FOR BLOCK block_1
  END

  BEGIN PARAMETER FOR BLOCK block_1000
    SECTION = axleSect
  END
END

BEGIN PRESTO PROCEDURE p1
  BEGIN PRESTO REGION r1
    BEGIN CONTACT DEFINITION c1

      BEGIN ANALYTIC GENERAL SURFACE axleSurf
        ANALYTIC SURFACE = axleGeom
        REFERENCE RIGID BODY = block_1000
      END

      CONTACT SURFACE block_1_surf CONTAINS block_1

      BEGIN OUTPUT OPTIONS
        AREA UPDATE FREQUENCY = <integer>numStep(1000)
      END

      BEGIN ENFORCEMENT OPTIONS
        CONTACT FORCE PREDICTOR = OFF|ON(ON)
      END

      BEGIN INTERACTION
        MASTER         = axleSurf
        SLAVE          = block_1_surf
        FRICTION MODEL = frictionless
      END
    END
  END
```

```
  END
END
```

13.1.2 Plane

```
BEGIN ANALYTIC PLANE <string>name
       NORMAL = <string>defined_direction
       POINT = <string>defined_point
       REFERENCE RIGID BODY = <string>rb_name
END [ANALYTIC PLANE <string>name]
```

Analytic planes are not deformable and two analytic planes cannot interact with each other through contact. The `ANALYTIC PLANE` command block for defining an analytic plane begins with the input line shown above:

The string `name` is a user-selected name for this particular analytic plane. This name is used to identify the surface in the interaction definitions. The string `defined_direction` in the `NORMAL` command line refers to a vector that has been defined with a `DEFINE DIRECTION` command line; this vector defines the outward normal to the plane. The string `defined_point` in the `POINT` command line refers to a point in a plane that has been defined with a `DEFINE POINT` command line. The plane is infinite in size. The body the plane is contacting should initially be on the positive outward normal side of the plane. See User's Manual for more information on defining points and directions.

The `REFERENCE RIGID BODY` command can be used to connect the analytic plane to the rigid body block named by `rb_name`. If the rigid body block rotates or translates, the analytic contact plane will rotate and translate with it. The `REFERENCE RIGID BODY` option only works with the Dash search option.

13.1.3 Cylinder

```
BEGIN ANALYTIC CYLINDER <string>name
       CENTER = <string>defined_point
       AXIAL DIRECTION = <string>defined_axis
       RADIUS = <real>cylinder_radius
       LENGTH = <real>cylinder_length
       CONTACT NORMAL = <string>OUTSIDE|INSIDE
END [ANALYTIC CYLINDER <string>name]
```

Analytic cylindrical surfaces are not deformable; they cannot be moved, and two analytic cylindrical surfaces will not interact with each other.

The string `name` is a user-selected name for this particular analytic cylinder. This name is used to identify the surface in the interaction definitions. The cylindrical surface has a finite length. The center point of the cylinder and the direction of the radial axis of the cylinder are defined by the `CENTER` and `AXIAL DIRECTION` command lines, respectively. The string `defined_point` in the `CENTER` command line refers to a point that has been defined with a `DEFINE POINT` command line; the string `defined_axis` in the `AXIAL DIRECTION` command line refers to a direction

that has been defined with a DEFINE DIRECTION command line. See User's Manual for more information on defining points and directions.

The radius of the cylinder is the real value cylinder_radius specified with the RADIUS command line, and the length of the cylinder is the real value cylinder_length specified by the LENGTH command line. The length of the cylinder (cylinder_length) extends a distance of cylinder_length divided by 2 along the cylinder axis in both directions from the center point.

The CONTACT NORMAL command defines whether the normal of the contact cylinder points outward or inward.

```
CONTACT NORMAL = OUTSIDE | INSIDE
```

13.1.4 Other Analytic Surface Options

```
BEGIN OUTPUT OPTIONS
  ARS NODAL AREA UPDATE FREQUENCY = <integer>val(1)
  CONTACT STATUS TYPE = JAS|DEBUG (JAS)
END
ARS CONTACT OUTPUT = OFF|ON(OFF)
```

The nodal area update frequency is a performance option to control how often the ARS surface normals are updated. For a static or semi-static solution increasing this value may increase performance at the potential trade off of a inaccuracy in frictional quantities.

The CONTACT STATUS TYPE controls if the nodal output variable contact_status is written based on JAS conventions (0 not on surface, 0.5, on surface not in contact, 1.0 sliding, -1.0 sticking) or some other convention.

The ARS CONTACT OUTPUT command controls whether ARS specific detailed output variables are computed or not.

13.2 Implicit Solver Control Contact Options

```
BEGIN CONTROL CONTACT
    CONTROL SUBSET = <list>
            controlTypes(ADAGIO, ARS, JAS)
END [CONTROL CONTACT]
```

The CONTROL SUBSET command can be used to cause a control contact block to only apply to some contact enforcement types. The options to the command are ADAGIO to control kinematic and augmented Lagrange contact, JAS to control JAS mode contact, and ARS to control analytic rigid surface contact. By default, the control contact block applies to all three contact types. Use of the control subset logic may be useful if it is desired to have the different enforcement types use different control contact option sets.

The CONTROL CONTACT block is described in [1].

The AREA UPDATE FREQUENCY is a performance option used to control how often the analytic contact surfaces update the local areas and normal directions. Updating these values more frequency (lower numStep) may lower performance but yield greater accuracy (especially in derived output quantities such as contact traction).

If the CONTACT FORCE PREDICTOR option is on the previous step contact forces will be used as an initial guess to the current step contact forces. This could improve results if the contact forces are very stable step to step or make results worse if the contact forces are highly volatile. The default value for this option is ON as ARS contact is often used to model mostly static contacts.

References

[1] Sierra/SolidMechanics Team. Sierra/SolidMechanics 4.46 User's Guide. Technical Report SAND2017-9759, Sandia National Laboratories, Albuquerque, NM, 2017.

Chapter 14

J-Integrals

Sierra/SM provides a capability to compute the J-integral via a domain integral.

Known Issue: Currently, the J-Integral evaluation capability is based on assumptions of elastostatics and a stationary crack, and is only implemented for uniform gradient hex elements.

J is analogous to G from linear elastic fracture mechanics ($-\delta\pi/\delta a$) and is the driving force on the crack tip of length a [1, 2]. Crack propagation occurs when $J(a) \geq R(a)$, where $R(a)$ is the material resistance. For constant R, the resistance is often termed J_c. In the reference configuration, the vector form of the J-integral in finite deformation [3] is

$$\boldsymbol{J} = \int_{\Gamma_0} \boldsymbol{\Sigma} \boldsymbol{N} dA \tag{14.1}$$

where $\boldsymbol{\Sigma} = W\boldsymbol{I} - \boldsymbol{F}^T\boldsymbol{P}$ is called the Eshelby energy-momentum tensor [4]. W is the stored energy density in the reference configuration and $\boldsymbol{F}$ and $\boldsymbol{P}$ are the deformation gradient and first Piola-Kirchhoff stress, respectively. Rice [2] realized that because $\boldsymbol{\Sigma}$ is divergence-free in the absence of body forces, one can examine $\boldsymbol{J}$ in the direction of the defect $\boldsymbol{L}$ (unit vector) and obtain a path-independent integral for traction-free crack faces. J can be written as

$$J = \int_{\Gamma_0} \boldsymbol{L} \cdot \boldsymbol{\Sigma} \boldsymbol{N} dA \tag{14.2}$$

and interpreted as a path-independent driving force in the direction of the defect. We note that one can also express $\boldsymbol{\Sigma}$ in terms of $\bar{\boldsymbol{\Sigma}}$, where $\bar{\boldsymbol{\Sigma}} = W\boldsymbol{I} - \boldsymbol{H}^T\boldsymbol{P}$ and $\boldsymbol{H} = \text{Grad}\,\boldsymbol{u}$. Although $\boldsymbol{\Sigma}$ is symmetric and $\bar{\boldsymbol{\Sigma}}$ is not symmetric, they are equivalent when integrated over the body ($\text{Div}\boldsymbol{P} = \boldsymbol{0}$). In fact, differences in the energy-momentum tensor stem from the functional dependence of the stored energy function W. $\boldsymbol{\Sigma}$ and $\bar{\boldsymbol{\Sigma}}$ derive from $W(\boldsymbol{F})$ and $W(\boldsymbol{H})$, respectively. When integrated, both collapse to the familiar 2-D relation for infinitesimal deformations.

$$J = \int_{\Gamma} \boldsymbol{e}_1 \cdot \boldsymbol{\Sigma} \boldsymbol{n} ds = \int_{\Gamma} (W n_1 - u_{i,1}\sigma_{ij}n_j) \mathrm{d}s \tag{14.3}$$

14.1 Technique for Computing J

J is often expressed as a line (2D) or surface (3D) integral on a ring surrounding the crack tip. Defining a smooth ring over which to compute this surface integral and performing projections of the required field values onto that ring presents many difficulties in the context of a finite element code.

To compute the J-integral in a finite element code, it is more convenient to perform a volume integral over a domain surrounding the crack tip. We can then leverage the information at integration points rather than rely on less accurate projections. To do this, we follow the method described in [5]. We replace $\boldsymbol{L}$ with a smooth function $\boldsymbol{q}$. On the inner contour of the domain Γ_0, $\boldsymbol{q} = \boldsymbol{L}$. On the outer contour of the domain C_0, $\boldsymbol{q} = \boldsymbol{0}$. Because the outer normal of the domain $\boldsymbol{M}$ is equal and opposite of the normal $\boldsymbol{N}$ on Γ_0, there is a change of sign. For traction-free surfaces, we can apply the divergence theorem, enforce $\mathrm{Div}\bar{\boldsymbol{\Sigma}} = \boldsymbol{0}$, and find that the energy per unit length $\bar{J}$ is

$$\bar{J} = -\int_{\Omega_0} (\bar{\boldsymbol{\Sigma}} : \mathrm{Grad}\, \boldsymbol{q}) \mathrm{d}V. \tag{14.4}$$

We can also introduce a correction if we seek to consider cases in which the crack faces, $A_0^+ + A_0^-$, or "caps", $S_0^+ + S_0^-$, of the domain are not traction free. For example, both cases would be satisfied for a thumbnail crack in a pressure vessel. The correction

$$\bar{J} = -\int_{\Omega_0} (\bar{\boldsymbol{\Sigma}} : \mathrm{Grad}\, \boldsymbol{q}) \mathrm{d}V - \int_{S_0^+ + S_0^- + A_0^+ + A_0^-} \boldsymbol{q} \cdot \boldsymbol{H}^T \boldsymbol{T}\, \mathrm{d}A. \tag{14.5}$$

effectively removes the contribution of the applied tractions and ensures that the integral remains path independent. We note that the correction is integrated in the reference configuration with referential traction $\boldsymbol{T}$. When pressure is applied to S_0^+, S_0^-, A_0^+, or A_0^-, Sierra employs Equation (14.5).

We note that all the field quantities are given via simulation and we choose to define $\boldsymbol{q}$ on the nodes of the domain $\boldsymbol{q}^I$. We then employ the standard finite element shape functions to calculate the gradient. We can specify the crack direction $\boldsymbol{L}$ or assume that the crack will propagate in the direction normal to the crack front $-\boldsymbol{M}$. For a "straight" crack front, $\boldsymbol{L} = -\boldsymbol{M}$. If $\boldsymbol{S}$ is tangent to the crack front and $\boldsymbol{T}$ is normal to the lower crack surface, $\boldsymbol{S} \times \boldsymbol{M} = \boldsymbol{T}$. We note that for non-planar, curving cracks, $\boldsymbol{M}$, $\boldsymbol{S}$, and $\boldsymbol{T}$ are functions of the arc length S. For ease, we employ the notation $\boldsymbol{N}$ rather than $-\boldsymbol{M}$. For a crack front S_0, we can define the average driving force J_{avg} as

$$J_{avg} = \frac{\bar{J}}{\int_{S_0} \boldsymbol{L} \cdot \boldsymbol{N} \mathrm{d}S}. \tag{14.6}$$

While the average driving force is useful for interpreting experimental findings and obtaining a macroscopic representation of the driving force, we also seek to examine the local driving force $J(S)$. Using the finite element interpolation functions to discretize $\boldsymbol{L}$ through the smooth function $\boldsymbol{q}$, we find $\boldsymbol{q} = \lambda^I \boldsymbol{q}^I$. For a specific node K, we can define $|\boldsymbol{q}^K| = 1$ and $\boldsymbol{q}^I = \boldsymbol{0}$ for all other $I \neq K$ on S_0. Note that we still need to specify the function $\boldsymbol{q}$ in the $\boldsymbol{S} - \boldsymbol{T}$ plane from the inner contour Γ_0 to the outer contour C_0. The resulting expression for the approximate, point-wise driving force at node K on the crack front is

$$J^K = \frac{\bar{J}}{\int_{S_0} \lambda^K \boldsymbol{q}^K \cdot \boldsymbol{N} \mathrm{d}S}. \tag{14.7}$$

Again, we note that if the direction of propagation $\boldsymbol{L}$ is taken in the direction of the normal $\boldsymbol{N}$, the denominator is $\int_{S_0} \lambda^K \mathrm{d}S$. More information regarding the point-wise approximation of J^K can be found in [6, 7].

Additional information on the J Integral capability can be found in [8].

14.2 Input Commands

Output quantities related to *J*-integrals may be computed during the analysis by including one or more `J INTEGRAL` command blocks in the `REGION` scope. This block can contain the following commands:

```
BEGIN J INTEGRAL <jint_name>
       #
       # Definition of integration domain
       BLOCK = <string list>blockNames
       REMOVE BLOCK = <string list>removeBlocks
       ELEMENT = <int_list>elemNumbers
       INCLUDE ALL BLOCKS
       #
       # integral parameter specification commands
       CRACK PLANE SIDE SET = <string list>side_sets
       CRACK TIP NODE SET = <string list>node_sets
       USE SURFACE FOR EDGE DIRECTION = OFF|ON(ON)
       CRACK DIRECTION = <real>dir_x
                         <real>dir_y
                         <real>dir_z
       INTEGRATION RADIUS = <real>int_radius
       NUMBER OF DOMAINS = <integer>num_domains
       FUNCTION =
          PLATEAU|PLATEAU_RAMP|LINEAR(PLATEAU)
       SYMMETRY = OFF|ON(OFF)
       DEBUG OUTPUT = OFF|ON(OFF) WITH
         <integer>num_nodes NODES ON THE CRACK FRONT
       #
       # time period selection commands
       ACTIVE PERIODS = <string list>period_names
       INACTIVE PERIODS = <string list>period_names
END J INTEGRAL <jint_name>
```

The *J*-integral is performed over a domain defined by a set of elements using the standard element assignment commands. See User's Manual for details.

A set of parameters must be provided to define the crack geometry used in the calculation of the *J*-integral. The *J*-integral command block uses a sideset on one surface of the crack plane behind the crack tip and a nodeset containing the nodes on the crack tip. Both the `CRACK PLANE SIDE SET` and `CRACK TIP NODE SET` commands are required. These commands specify the names of the sideset behind the crack tip and the nodeset on the crack tip, respectively.

By default, the direction of crack propagation is computed from the geometry of the crack plane and tip, as provided in the crack plane sideset and crack tip nodeset ($\boldsymbol{L} = \boldsymbol{N}$). At locations where the crack intersects a surface, the computed $\boldsymbol{N}$ is commonly less accurate. At these locations, the `USE SURFACE FOR EDGE DIRECTION = ON` command will attempt to improve $\boldsymbol{N}$ by projecting it onto the intersected surface. The default is `ON`, and `USE SURFACE FOR EDGE DIRECTION`

= OFF should only be set if the crack tip is known to intersect the surface at a sharp angle. Alternatively, the CRACK DIRECTION command can be used to override the computed direction of crack propagation ($\boldsymbol{L}$). This command takes three real numbers that define the three components of the crack direction vector in the global XYZ coordinate system.

To fully define the domains used for the domain integrals, the radius of the domains and the number of domains must also be specified. A series of disc-shaped integration domains are formed with varying radii going out from the crack tip. The INTEGRATION RADIUS command is used to specify the radius of the outermost domain. The number of integration domains is specified using the NUMBER OF DOMAINS command. The radii of the domains increase linearly going from the innermost to the outermost domain. The domains will only include elements that are included in the overall integration domain defined by the BLOCK command and other related commands.

The weight function $\boldsymbol{q}$ used to calculate the J-integral is specified by use of the FUNCTION command line. The LINEAR function sets the weight function to 1.0 on the crack front Γ_0 and 0.0 at the edge of the domain C_0, int_radius away from the crack tip. The PLATEAU function, which is the default behavior, sets all values of the weight function to 1.0 that lie within the domain of integration and all values outside of the domain are set to 0.0. This allows for integration over a single ring of elements at the edge of the domain. The third option for the FUNCTION command is PLATEAU_RAMP, which for a single domain will take on the same values as the LINEAR function. However, when there are multiple domains over the radius int_radius, the n^{th} domain will have weight function values of 1.0 over the inner (n-1) domains and will vary from 1.0 to 0.0 over the outer n^{th} ring of the domain. These functions can be seen graphically in Figure 14.1.

We note that in employing both the PLATEAU and the PLATEAU_RAMP functions, one is effectively taking a line integral at finite radius (albeit different radii). In contrast, the LINEAR option can be viewed as taking the $lim\ \Gamma_0 \rightarrow 0^+$. If the model is a half symmetry model with the symmetry plane on the plane of the crack, the optional SYMMETRY command can be used to include the symmetry conditions in the formation of the integration domains and in the evaluation of the integral. The default behavior is for symmetry to not be used.

The user may optionally specify the time periods during which the J-integral is computed. The ACTIVE PERIODS and INACTIVE PERIODS command lines are used for this purpose. See User's Manual for more information about these command lines.

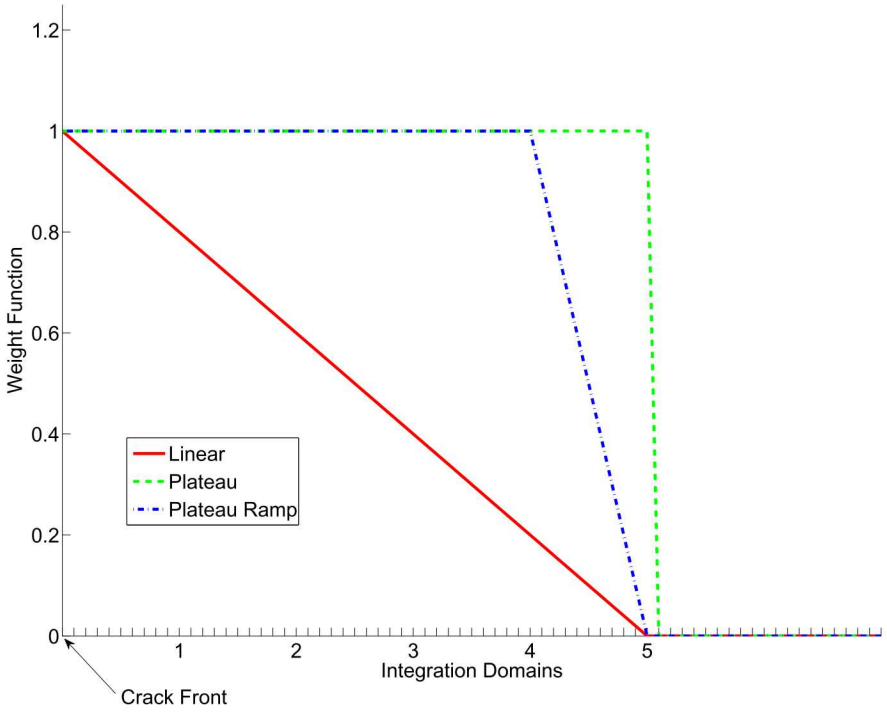

Figure 14.1: Example weight functions for a J-integral integration domain. Weight functions shown for domain 5.

14.3 Output

Many variables are generated for output when the computation of the J-integral is requested. The average value of J for each integration domain is available as a global variable, as described in Table 14.1. The point-wise value of J at nodes along the crack for each integration domain is available as a nodal variable, as shown in Table 14.2. Element variables such as the Eshelby energy-momentum tensor and fields defining the integration domains are also available, as listed in Table 14.3.

The `DEBUG OUTPUT` command can be used to generate output data for debugging the J-integral. If the `DEBUG OUTPUT = ON|OFF(OFF) WITH <integer>num_nodes NODES ON THE CRACK FRONT` line command is set to `ON`, the weight functions, q, will be output for each node-based J value that is calculated. The user must specify `num_nodes`, which represents the number of nodes along the crack front. An internal check is performed during problem initialization that will verify that the number of nodes specified by the user on the command line matches the number of nodes associated with the crack front.

Warning: Using the `DEBUG OUTPUT` command line can potentially result in an extremely large output file because every node in the integration domain will now compute and store $(NumNodeOnCrackFront + 1) * NumDomains$ weight function vectors. This can also potentially exhaust the available memory on the machine.

14.4 Required Discretization

In order to enable the correct construction of the test function $\boldsymbol{q}^I$, the hexahedral mesh should be orthogonal to the crack front. An orthogonal mesh will ensure that the elements are not skewed along the crack front. Because these elements will experience large deformation during crack-tip blunting, well-formed elements increase the accuracy of the solution. We note that this capability is not specific to crack front nodes. Any ellipsoidal surface with a constant bias will generate skewed elements.

In addition, an orthogonal mesh will ensure that the location of a point-wise surface integral will be a closest point projection from the crack-tip node. Consequently, any surface integral via a domain integral at a node along the crack front will be most accurate if the specified radius is a minimum. In addition to increasing the accuracy of point-wise evaluations of the J-integral, an orthogonal mesh will also ease the search algorithm for point-wise evaluations. The search is performed along the normal to the crack front. If the mesh is aligned with the normal, the specification of $\boldsymbol{q}$ is straightforward. Misalignment can result in a "checker boarding" of the integration domains which presents the possibility that $\boldsymbol{q}^I$ will always be one and the J-integral will be zero. Future work may generalize the calculation of J^K, but we are currently limited to hexahedra. Given these requirements, we collaborated with the Cubit team to add the capability to generate meshes that are orthogonal to a surface. The Cubit team implemented the command

```
adjust boundary surface AA snap_to_normal curve A
```

which enables the generated elements on surface `AA` to be "snapped" normal to the curve `A`. For example, one may choose to sweep adjacent squares along the crack front curve `A`. For crack plane surfaces `AA` and `AB` that are joined by the crack front curve `A`, one would issue the following commands in Cubit

```
surface AA AB scheme map
mesh surface AA
node in curve A position fixed
adjust boundary surface AA snap_to_normal curve A
mesh surface AB
node in curve A position fixed
adjust boundary surface AB snap_to_normal curve A
          fixed curve A
```

to obtain an orthogonal mesh. The next step is to sweep that mesh "up" and "down" from the crack surface. To ensure that Cubit employs a "simple" sweep so that the search is consistent through the direction of the sweep, we use

```
volume ABC  scheme sweep source surface AA target
      surface AC
propagate_bias autosmooth_target off sweep_smooth
      linear
sweep_transform translate
```

for volume `ABC`. Because proper mesh construction ensures accuracy and smoothness in J^K, we encourage analysts to use the `snap_to_normal` and `autosmooth_target off` options.

14.5 Results and History Output

This section lists output variables for J-Integral.

- Table 14.1 Global Variables for J-Integral
- Table 14.2 Nodal Variables for J-Integral
- Table 14.3 Element Variables for J-Integral

Table 14.1: Global Variables for J-Integral

Variable Name	Type	Comments
`j_average_<jint_name>`	`Real[]`	Average value of the J-integral over the crack. Array sized to number of integration domains and numbered from inner to outer domain. `<jint_name>` is the name of the `J INTEGRAL` block.

Table 14.2: Nodal Variables for J-Integral

Variable Name	Type	Comments
`j_<jint_name>`	`Real[]`	Point-wise value of J-integral along crack. Array sized to number of integration domains and numbered from inner to outer domain. `<jint_name>` is the name of the `J INTEGRAL` block.

Table 14.3: Element Variables for J-Integral

Variable Name	Type	Comments
`energy_momentum_tensor`	`FullTen36`	Energy momentum tensor
`integration_domains_<jint_name>`	`Integer[]`	Flag indicating elements in integration domains. Set to 1 if in domain, 0 otherwise. Array sized to number of domains and numbered from inner to outer domain. `<jint_name>` is the name of the `J INTEGRAL` block.

References

[1] J.D. Eshelby. The force on an elastic singularity. *Philosophical Transactions of the Royal Society of London A*, 244:87–112, 1951. URL http://dx.doi.org/10.1098/rsta.1951.0016.

[2] J.R. Rice. A path independent integral and the approximate analysis of stress concentration by notches and cracks. *Journal of Applied Mechanics*, 35:379–386, 1968.

[3] G.A. Maugin. *Material Inhomogeneities in Elasticity*. Chapman & Hall/CRC, New York, 1993.

[4] J.D. Eshelby. Energy relations and the energy-momentum tensor in continuum mechanics. In M. Kannien, editor, *Inelastic Behavior of Solids*, pages 77–114. McGraw-Hill, New York, 1970.

[5] F.Z. Li, C.F. Shih, and A. Needleman. A comparison of methods for calculating energy release rates. *Engineering Fracture Mechanics*, 21:405–421, 1985. URL http://dx.doi.org/10.1016/0013-7944(85)90029-3.

[6] C.F. Shih, B. Moran, and T. Nakamura. Energy release rate along a three-dimensional crack front in a thermally stressed body. *International Journal of Fracture*, 30:79–102, 1986. URL http://dx.doi.org/10.1007/BF00034019.

[7] ABAQUS. *Theory Manual*, volume Version 6.7. Hibbitt, Karlsson and Sorensen, Providence, RI, 2007.

[8] Y. Ohashi, J.W. Foulk, and A.J. Lindblad. Verification of J integral capability in sierra mechanics. Technical Report SAND2012-8720, Sandia National Laboratories, Albuquerque, NM, 2012.

Chapter 15

Nonlocal Regularization

Known Issue: Each nonlocal block must be uniquely paired with a material. A single material *cannot* have local and nonlocal blocks. Future work will generalize the methodology.

Using material models that employ strain softening to capture the micromechanics of the failure process will result in mesh-dependent solutions. Fundamentally, the partial differential equation is changing character and the problem becomes ill-posed (for both elliptic and hyperbolic systems). There are multiple methodologies to regularize the solution and nonlocality has been employed to converge to a single solution from a multiplicity of solutions.

15.1 Variational nonlocal method

In the vein of nonlocality, a variational nonlocal method was derived such that one can identify the state variable that controls softening Z and pose a variational principle such that the stored energy is dependent on a nonlocal state variable $\bar{Z}$. At a point, a Lagrange multiplier enforces $\bar{Z} = Z$. When we minimize and discretize, however, we derive an L_2 projection for the "coarser" $\bar{Z}$ and the balance of linear momentum for the "fine" scale. If we assume that the basis functions for the coarser discretization D are constant and discontinuous, we obtain the nonlocal $\bar{Z}$ as a simple volume average of Z.

$$\bar{Z} = \frac{1}{\int_D dV} \int_D Z dV \tag{15.1}$$

In this particular case, less is more. We do not want to recover the mesh-dependent solution inherent in Z with a $\bar{Z}$. Instead, we seek to specify an additional discretization (length scale) independent of the discretization for Z. Because $\bar{Z}$ is just an average, we can consider a coarse domain to be a patch of fine scale elements having volume V that is consistent with a prescribed length scale l where $V = l^3$. For example, one might correlate the mesh dependence in the solution with scalar damage ϕ. The variational nonlocal method would construct a $\bar{\phi}$ for each nonlocal domain D. The stress would then evolve from $\bar{\phi}$ and not ϕ.

Domain decomposition algorithms are invoked to construct coarse scale domains of common volume. For parallel execution, each processor (having nonlocal element blocks) is partitioned during initialization. Nonlocal averages are calculated on the processor and no communication is necessary between processors.

Warning: Because nonlocal domains are initially decomposed on each processor, nonlocal geometries will not a) be consistent with different parallel decompositions and b) admit rebalancing. No infrastructure exists to maintain the character of the nonlocal domains during rebalancing.

15.2 Nonlocal partitioning

Because communication in parallel processing scales with the surface area of the domain, we believed that software designed with the intent of limiting communication would be ideal for application to nonlocal regularization. Hence, graph-based (METIS, Zoltan Hypergraph) and geometric (Zoltan Recursive Coordinate Bisection, Zoltan Recursive Inertial Bisection) decomposition algorithms were implemented and available for the analyst. Figure 15.1 illustrates the Zoltan partitioning methodologies for a circular region surrounding a sharp crack tip. We note that non-contiguous domains can occur in graph-based methodologies. For these reasons, `ZOLTAN_RCB` was selected to be the default partitioning scheme.

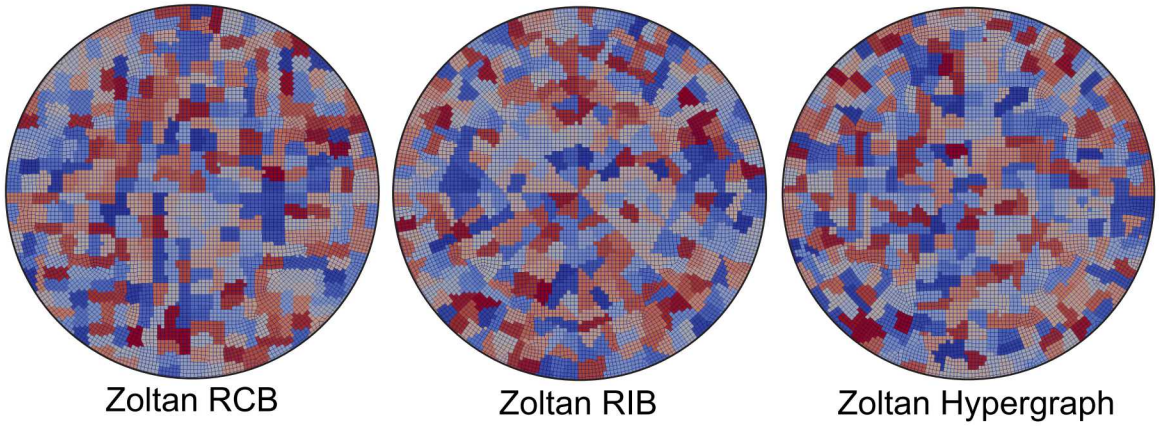

Figure 15.1: Illustration of 400 nonlocal partitions at a sharp crack tip using Zoltan Recursive Coordinate Bisection (RCB), Zoltan Recursive Inertial Bisection (RIB), and Zoltan Hypergraph partitioning methodologies. Note that Zoltan Hypergraph can generate non-contiguous domains. The default partitioning methodology in Sierra is Zoltan RCB.

Initial findings employing geometric partitioning illustrated a sensitivity to domain shape. A re-examination of Figure 15.1 will reveal that the aspect ratios of the domains are significant. Because we are aligning the evolution of a nonlocal variable with the nonlocal domain shape, domains of increasing aspect ratio result in anisotropic evolution. Although other researchers have developed methods for domain decomposition that focus on domain shape [1], we gravitated towards clustering algorithms and the resulting isotropy [2]. Figure 15.2 illustrates the mesh, grid, and result of k-means clustering, a centroid Voronoi Tessellation (CVT). Given a body on processor with mesh size h, we overlay a grid with uniform cell size c. We then find points both inside (red) and outside (blue) the body. After calculating the number of nonlocal volumes N for a body of volume B through $N = B/l^3$, we seed the centroids of the nonlocal domains through Zoltan RCB. K-means clustering of points inside the body evolves the locations of the centroids via Lloyd's algorithm. The algorithm will converge to a CVT, independent of the FE discretization. The tolerance for convergence *tol* is specified as a fraction of the cell size c. The nonlocal domains are then populated by each element's proximity to the nearest CVT centroid. The resulting nonlocal domains are illustrated in Figure 15.2. We note that the nonlocal domain size is only illustrative. Nonlocality in damage, for example, would require a smaller length scale l resulting in a finer discretization of Voronoi polygons.

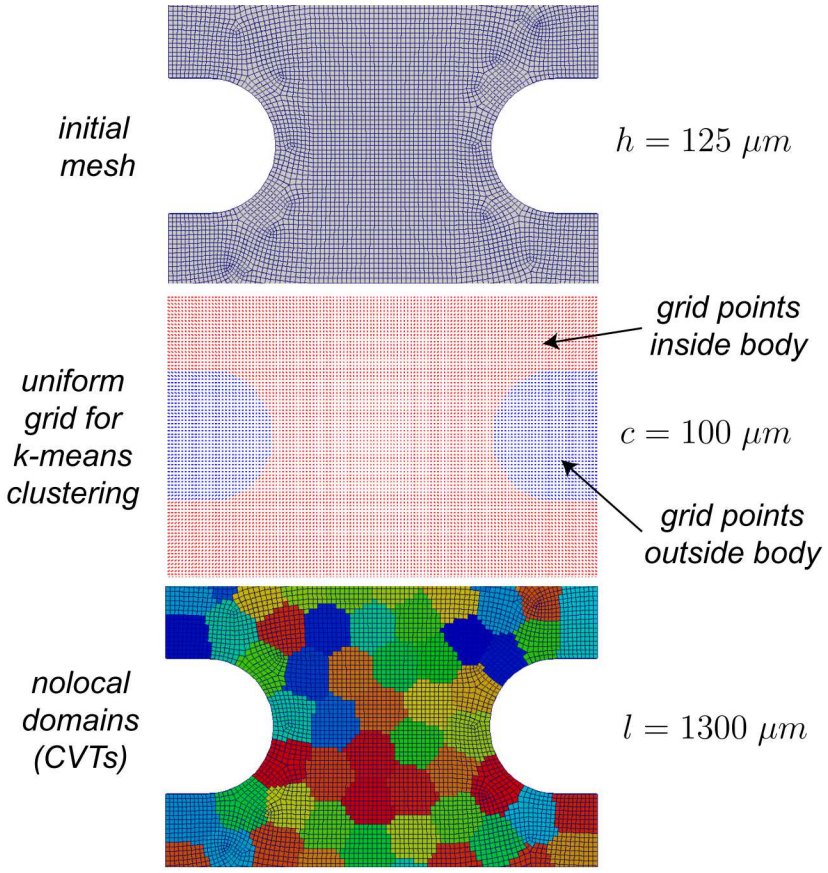

Figure 15.2: Nonlocal domains derive from a Centroidal Voronoi Tessellation (CVT). A partitioned mesh for parallel processing with element size h determines the boundaries of a uniform grid with cell size c. K-means clustering evolves a set of N centroids into a CVT.

15.3 Command summary

In the specification of the block, one can invoke nonlocality in a state variable Z through

```
begin parameters for block block_1
    material ductile_metal
    solid mechanics use model elasto_thermo_visco_poro_plasticity
    section = solid_1
    NONLOCAL REGULARIZATION ON <string>varName WITH LENGTH SCALE =
    <real>length [AND STAGGERING]
    NONLOCAL REGULARIZATION PARTITIONING SCHEME =
    METIS|ZOLTAN_HYPERGRAPH|ZOLTAN_RCB|ZOLTAN_RIB|KMEANS (ZOLTAN_RCB)
#
# Options for k-means clustering
#
    NONLOCAL REGULARIZATION KMEANS CELL SIZE = <real>cell_size
    NONLOCAL REGULARIZATION KMEANS MAXIMUM ITERATIONS = <int>max_iter
    NONLOCAL REGULARIZATION KMEANS TOLERANCE = <real>tol
 end parameters for block block_1
```

where the `varName` is the state variable Z to be averaged and `length` defines the nonlocal volume V = `length`^{3}. The k-means clustering employs a uniform grid having a size `cell_size` and tolerance for convergence `tol`. The maximum number of iterations for k-means clustering is given by `max_iter`. One can output the partitions through the `NONLOCAL_ELEMENT_DOMAIN` element variable. The output of element variables is described in the User's Manual. In addition, each partition and its volume is noted in the log file. The nonlocal variable $\bar{Z}$ can be output through the element variable `NONLOCAL_varName_AVERAGE` while the local variable Z is output through `varName`. We remind the reader that material points contain both Z and $\bar{Z}$. The energy, stress, and tangent depends on $\bar{Z}$. The constitutive update evolves Z. This process, however, is not employed when using `AND STAGGERING`. In this specific case, local variables are averaged after each time step t_n and used as the initial conditions for t_{n+1}. Strictly speaking, `AND STAGGERING` approximates the variational nonlocal method. A fundamental assumption of the nonlocal method is that one is employing a constitutive model in which the state variable update is separate from the evaluation of the energy, stress, or tangent. Currently, only one model in LAME, `HYPERELASTIC_DAMAGE`, separates these functions. All the other constitutive models, however, update the internal state variables and the stress simultaneously. In an attempt to employ the majority of models that do not adhere to this separation, the `AND STAGGERING` option was implemented and does regularize the failure process. This approximation to the nonlocal method is more accurate for small time steps and may require limited hourglass viscosity to stabilize the evolved perturbations (post bifurcation) in uniform-gradient elements. Although we initially envisioned the `AND STAGGERING` option to be most applicable to explicit dynamics, simulations with nonlocal damage evolution for implicit dynamics have illustrated mesh-independent solutions.

Warning: The tangent generated in Adagio currently derives from Z and is local. Future development will implement a nonlocal, finite-difference tangent.

Warning: Element death for nonlocal domains is work in progress. Additionally this capability will not function with 'death on inversion'.

15.4 Usage guidelines

The nonlocal length scale `length` l is a material parameter that will set the length scale over which localization will occur. Although the parameterization of l is indirect, it will control the dissipation and should have an experimental basis.

For a typical application, the analyst might

1. Identify a constitutive model that captures the failure process. This might include a local damage model or any model that employs strain softening to facilitate strain localization.

2. Conduct mesh-dependent simulations with bulk elements of size h to understand potential paths for crack initiation and growth in specimen geometries targeted for parameterizing constitutive model parameters.

3. Invoke nonlocality through a nonlocal length scale l. Mesh-independent solutions stem from resolved nonlocal domains where $l > 3h$. The nonlocal domain size should be small compared to the relevant dimensions (features) of the body.

4. Specify `KMEANS` partitioning. Choose the cell size c such that it is small compared to the nonlocal length scale. We recommend $\frac{1}{20} < \frac{c}{l} < \frac{1}{10}$ for the clustering algorithm to sample between $\sim$ 1000 and $\sim$ 8000 points per nonlocal domain and obtain a converged CVT. Please note that memory requirements will scale geometrically with the cell size. One can easily run out of memory on a cluster given decrements in the cell size. Candidate values for convergence and the maximum number of iterations are 0.02 and 256, respectively. Because the clustering process is only performed during the initialization of the simulation, decreased tolerances and increased iterations are not cost prohibitive.

5. Inspect the character of the nonlocal volumes through `NONLOCAL_ELEMENT_DOMAIN` and determine whether or not there are sufficient nonlocal volumes per partition for parallel processing. Because the nonlocal domains are formed on processor, processor boundaries represent nonlocal domain boundaries. One can enable greater smoothness in the nonlocal response through the mitigation of processor boundaries.

6. Incorporate nonlocality into the fitting process. The fitting process may not be unique in that the same far-field response might be obtained from multiple combinations of both l and the material parameters that govern the failure process.

7. Understand the impact of l. If l is too large, the failure process will be "lumped" over a large region resulting in a non-smooth response. Please consider refitting model parameters with smaller values of l (and h) to obtain the localized nature of the failure process.

8. Explore component or system level geometries with nonlocality. Refine the mesh to ensure that the far-field predictions are indeed mesh independent and that the process zone that evolves from the given micromechanics is resolved.

9. Reflect on the fields employed for model parameterization and the fields evolving in component and system level models. Contrast the evolution of local field variables governed by the

mesh discretization with the nonlocal variable governed by the CVT discretization. If possible, align field evolution in component/system geometries with field evolution in specimen geometries. Disparities may drive the need for additional calibration experiments.

Although these usage guidelines have not focused on incorporating stochastic processes, one may sample distributions in material parameters. The inclusion of a method for regularization enables such findings in that the mesh-dependence associated with fracture/failure is not convoluted with a stochastic representation of the micro mechanical process.

References

[1] H. Meyerhenke, B. Monien, and T. Sauerwald. A new diffusion-based multilevel algorithm for computing graph partitions. *Journal of Parallel Distributed Computing*, (69):750–761, 2009.

[2] J. Burkardt, M. Gunzburger, J. Peterson, and R. Brannon. User manual and supporting information for library of codes for centroidal voronoi point placement and associated zeroth, first, and second moment determination. Technical Report SAND2002-0099, Sandia National Laboratories, Albuquerque, NM, 2002.

Chapter 16

POD

Proper Orthogonal Decomposition (POD) and Explicit Control Modes (ECM, refer to Chapter 7.4.3) should have almost the same name according to the rule

> The name of a method should describe what is done, not how it is done.

A difference from ECM is that POD does not require a coarse finite element mesh. POD is intended for explicit analyses in which the time step is too small, and constructing a coarser mesh for ECM is unfeasible.

Warning: POD is an experimental analysis technique.

16.1 Time Step Control Commands

The larger the time step is, the greater the mass scaling. Part of the Cylinder With Legs test input file invokes POD and controls the way that it works.

```
BEGIN PARAMETERS PRESTO REGION
  #USER TIME STEP = 1.2e-08
END PARAMETERS PRESTO REGION

BEGIN PROPER ORTHOGONAL DECOMPOSITION
  NUMBER OF POD MODES = 21
  SNAPSHOTS INTERVAL = 405
  POD MODES COMPUTATION TIME STEP = 1.e-4
  ENERGY PERCENTAGE = 99.999
  POD FILTER = On
  MODE REFRESH = Off
  #USER FILTER TIME STEP = 1.2327e-08
  USER FILTER TIME STEP = 6.1635e-08 #5X
END PROPER ORTHOGONAL DECOMPOSITION
```

The `USER TIME STEP` overrides the element time step, including any increase in the time step due to POD.

The initialization needs the `NUMBER OF POD MODES` for post-processing. It is the number of fields to allocate that will store POD modes. The way that POD is set up at this time, this is also the number of snapshots and the number of eigenvalue eigenvector pairs.

`SNAPSHOTS INTERVAL` is the number of time steps taken between snapshots used to build the correlation matrix. It is not the number of time steps between adding a POD vector.

`POD MODES COMPUTATION TIME STEP` is the time at which Adagio POD is activated.

`ENERGY PERCENTAGE` is percentage that the sum of the eigenvalues used for the ECM/POD run accounts for with respect to the sum of the total eigenvalue spectrum. It is related to the kinetic energy of the system, but is not the ECM energy percentage [1].

`POD FILTER` activates the high frequency mass scaling. If `OFF`, then the simulation is equivalent to a simulation without ECM/POD.

`MODE REFRESH` This refreshes the number of POD modes throughout the simulation.

`USER FILTER TIME STEP` This is the user defined time step.

In theory the Lanczos algorithm provides the time step, but this has not been implemented.

The Plastic Cylinder test of POD activates the `MODE REFRESH`.

```
MODE REFRESH=ON
```

Snapshots are stored throughout the simulation. At every `POD MODES COMPUTATION TIME STEP`, 10^{-4} seconds here, the POD modes are updated using the new information.

References

[1] G.J. de Frias, W. Aquino, K.H. Pierson, M.W. Heinstein, and B.W. Spencer. A multiscale mass scaling approach for explicit time integration using proper orthogonal decomposition. *International Journal for Numerical Methods in Engineering*, 97(11):799–818, 2014. doi: 10.1002/nme.4608.

Chapter 17

RKPM

Warning: RKPM is a capability still in the development stages. This capability is not yet recommended for general use.

17.1 Formulation

This chapter describes the Reproducing Kernel Particle Method (RKPM) capability. RKPM is a meshfree method that can be constructed such that the approximation can be tailored for arbitrary order of completeness and smoothness [1, 2], using only a scattered set of points. This method reduces the tie between quality of the discretization and quality of the approximation, and is particularly effective for large deformation problems. Currently the RKPM formulation in Sierra/SM uses a Lagrangian description, and is a robust method for modeling large deformation problems where traditional FEM methods may experience mesh distortion issues. Additionally, under the appropriate formulation, it is also very effective at modeling extremely large deformation problems such as fragment/impact/penetration, which is a long term goal of the implementation.

The discrete description of a solid is achieved simply through only a set of nodes, and needs no other information such as a mesh. Each node is associated with a shape function with compact support, with overlap over neighboring nodes naturally determining connectivity. The RKPM shape functions are constructed as follows.

Let the closed domain $\bar{\Omega} \subset \mathbb{R}^d$ with dimension d be discretized by a set of NP nodes $\{\boldsymbol{x}_I | \boldsymbol{x}_I \in \bar{\Omega}\}_{I=1}^{NP}$. The n^{th} order RK approximation of a function $u(\boldsymbol{x})$ in $\bar{\Omega}$ denoted by $u^h(\boldsymbol{x})$ is constructed by the product of a kernel function $\Phi_a(\boldsymbol{x} - \boldsymbol{x}_I)$ with compact support measure a, and a correction function composed of a linear combination of basis functions in the following form [1]:

$$u^h(\boldsymbol{x}) = \sum_{I=1}^{NP} \left\{ \sum_{|\alpha| \leq n} (\boldsymbol{x} - \boldsymbol{x}_I)^\alpha b_\alpha(\boldsymbol{x}) \right\} \Phi_a(\boldsymbol{x} - \boldsymbol{x}_I) u_I \equiv \sum_{I=1}^{NP} \Psi_I(\boldsymbol{x}) u_I. \tag{17.1}$$

Here we have introduced the multi-index notation $\alpha = (\alpha_1, \alpha_2, \ldots, \alpha_d)$ with the length of α defined as $|\alpha| = \sum_{i=1}^{d} \alpha_i$, $\boldsymbol{x}^\alpha \equiv x_1^{\alpha_1} \cdot x_2^{\alpha_2} \cdot \ldots \cdot x_d^{\alpha_d}$, $\boldsymbol{x}_I^\alpha \equiv x_{I1}^{\alpha_1} \cdot x_{I2}^{\alpha_2} \cdot \ldots \cdot x_{Id}^{\alpha_d}$, $b_\alpha = b_{\alpha_1 \alpha_2 \cdots \alpha_d}$, $D_\alpha \equiv \partial_1^{\alpha_1} \partial_2^{\alpha_2} \cdots \partial_d^{\alpha_d} / \partial x_1{}^{\alpha_1} \partial x_2{}^{\alpha_2} \cdots \partial x_d{}^{\alpha_d}$, and u_I are the coefficients of approximation. The term $\{(\boldsymbol{x} - \boldsymbol{x}_I)^\alpha\}_{|\alpha| \leq n}$ is the set of basis functions, and $\{b_\alpha(\boldsymbol{x})\}_{|\alpha| \leq n}$ are coefficients of those basis functions. The kernel function $\Phi_a(\boldsymbol{x} - \boldsymbol{x}_I)$ determines the smoothness of the approximation functions, for example, a cubic b-spline function gives C^2 continuity. The type of kernel function ϕ_a can be chosen by the user. The subscript "a" denotes a measure of influence of the kernel function. The measure is normalized by the minimum nodal spacing, such that $a = 1$ gives the nodal spacing. The details on how to select values of this parameter are given in Section 17.4.

The set of coefficients $\{b_\alpha(\boldsymbol{x})\}_{|\alpha| \leq n}$ are determined by meeting the reproducing conditions

$$\sum_{I=1}^{NP} \Psi_I(\boldsymbol{x}) \boldsymbol{x}_I^\alpha = \boldsymbol{x}^\alpha, \quad |\alpha| \leq n. \tag{17.2}$$

With $\{b_\alpha(\boldsymbol{x})\}_{|\alpha| \leq n}$ obtained from (17.2), the RK shape functions are obtained as

$$u^h(\boldsymbol{x}) = \sum_{I=1}^{NP} \Psi_I(\boldsymbol{x}) u_I \tag{17.3}$$

where

$$\Psi_I(\boldsymbol{x}) = \boldsymbol{H}(\boldsymbol{0})^T \boldsymbol{M}^{-1}(\boldsymbol{x}) \boldsymbol{H}(\boldsymbol{x} - \boldsymbol{x}_I) \Phi_a(\boldsymbol{x} - \boldsymbol{x}_I) \tag{17.4}$$

$$\boldsymbol{M}(\boldsymbol{x}) = \sum_{I=1}^{NP} \boldsymbol{H}(\boldsymbol{x} - \boldsymbol{x}_I) \boldsymbol{H}^T(\boldsymbol{x} - \boldsymbol{x}_I) \Phi_a(\boldsymbol{x} - \boldsymbol{x}_I). \tag{17.5}$$

Here the vector $\boldsymbol{H}^T(\boldsymbol{x} - \boldsymbol{x}_I)$ is the corresponding row vector of $\{(\boldsymbol{x} - \boldsymbol{x}_I)^\alpha\}_{|\alpha| \leq n}$ and $\boldsymbol{M}(\boldsymbol{x})$ is the moment matrix. In this construction, the reproducing conditions (17.2) are met provided the moment matrix (17.5) is invertible, and this requires $(n + d)!/n!d!$ non-collinear points under the cover Φ_a so that the reproducing equations are linearly independent [2]. By direct differentiation, the shape functions also satisfy the property

$$\sum_{I=1}^{NP} D_\beta \Psi_I(\boldsymbol{x}) \boldsymbol{x}_I^\alpha = D_\beta \boldsymbol{x}^\alpha, \quad |\alpha| \leq n. \tag{17.6}$$

where β is a multi-index.

17.2 Domain integration

Domain integration for meshfree methods is most straightforwardly accomplished using Gaussian quadrature over background cells. However due to the complexity of the shape functions, high order quadrature must be employed to ensure sufficient accuracy of the solution [3]. Thus alternative approaches have been proposed to avoid the bottleneck of domain integration, and have been adopted in Sierra/SM. The most effective approach is the stabilized conforming nodal integration (SCNI) method [4, 5], which has been implemented into Sierra/SM as the primary and preferred domain integration method for Lagrangian analysis. This method employs nodal integration, where derivatives evaluated at the nodes are smoothed over conforming nodal representative domains. The strain smoothing serves to both circumvent zero-energy modes associated with nodal integration, as well as provide accuracy by providing linear exactness (passes the patch test) in the Galerkin approximation. The conforming cells required for strain smoothing are simply the elements in the original mesh before it is converted to a particle description. This approach ensures stability and accuracy with optimal convergence, and is also efficient as it employs nodal integration.

While SCNI is an extremely effective technique for Lagrangian analysis, in the presence of fragmentation and material separation the construction of conforming cells is prohibitively expensive. To plan for these future capabilities in Sierra/SM, stabilized non-conforming nodal integration (SNNI) has been implemented, where the conforming condition is relaxed and strains are smoothed over simple box cells constructed around the nodes. This techniques ensures reasonable stability and accuracy, but can suffer from convergence issues due to the failure of the patch test resulting from the relaxation of conforming conditions. The general framework of variationally consistent (VC) integration has been introduced [3] which can restore exactness in the Galerkin approximation, and has been employed for the enhancement of SNNI. The resulting VC-SNNI method (see Section 17.4) performs nearly identically to SCNI, and has been implemented into Sierra/SM.

SCNI and SNNI suppress zero energy modes associated with directly integrating shape functions at nodal points. However spurious low energy oscillatory modes can still exist in both methods when the surface area to volume ratio is small, or when the discretization is fine. To alleviate this issue, an additional stabilization technique has been proposed [6, 7], where the oscillatory modes are penalized in a form which maintains the accuracy of SCNI when it is employed. It is implemented into Sierra/SM and the user can choose to use it by specifying a stabilization coefficient.

17.3 Kinematics for RKPM in SIERRA

For time t^n to time t^{n+1}, objective strain measures are computed with respect to $t^{n+1/2}$ following [8]. With generalized increments $\Delta \boldsymbol{d}^n = \boldsymbol{d}^{n+1} - \boldsymbol{d}^n$ and $\Delta \boldsymbol{v}^n = \boldsymbol{v}^{n+1} - \boldsymbol{v}^n$, the incremental deformation gradient $\boldsymbol{G}_I$ at node I and its rate $\boldsymbol{H}_I$ are computed as

$$\begin{aligned} \boldsymbol{G}_I &= \boldsymbol{D}_I \boldsymbol{A}_I^{-1} \\ \boldsymbol{H}_I &= \boldsymbol{L}_I \boldsymbol{A}_I^{-1} + \tfrac{1}{2} \boldsymbol{D}_I \boldsymbol{L}_I^{-1} \\ \boldsymbol{A}_I &= \boldsymbol{I} + \tfrac{1}{2} \boldsymbol{D}_I \end{aligned} \tag{17.7}$$

where

$$\begin{aligned} (D_I)_{ij} &= \sum_{J=1}^{NP} \Psi_{J,j}(x_I) \Delta d_{Ji} \\ (L_I)_{ij} &= \sum_{J=1}^{NP} \Psi_{J,j}(x_I) \Delta v_{Ji} \end{aligned} \tag{17.8}$$

Kinematic quantities of interest are the strain increment $\boldsymbol{\gamma}_I$ and at node I, strain rate $\dot{\boldsymbol{\gamma}}_I$ and at node I, and deformation gradient $\boldsymbol{F}_I$ at node I:

$$\begin{aligned} \boldsymbol{\gamma}_I &= \tfrac{1}{2} \left(\boldsymbol{G}_I + \boldsymbol{G}_I^T \right) \\ \dot{\boldsymbol{\gamma}}_I &= \tfrac{1}{2} \left(\boldsymbol{H}_I + \boldsymbol{H}_I^T \right) \\ (F_I)_{ij} &= \sum_{J=1}^{NP} \Psi_{J,j}(x_I) d_{Ji}^{n+1} \end{aligned} \tag{17.9}$$

With the Cauchy stress increment $\Delta \boldsymbol{\sigma}_I$ computed by LAME based on these quantities, the update to stress $\boldsymbol{\sigma}_I^{n+1}$ at node I is performed as

$$\begin{aligned} \boldsymbol{\sigma}_I^{n+1} &= \boldsymbol{Q}_I \boldsymbol{\sigma}_I^n \boldsymbol{Q}_I^T + \Delta \boldsymbol{\sigma}_I \\ \boldsymbol{Q}_I &= \boldsymbol{I} + \left(\boldsymbol{I} - \tfrac{1}{2} \boldsymbol{\omega}_I \right)^{-1} \boldsymbol{\omega}_I \\ \boldsymbol{\omega}_I &= \tfrac{1}{2} \left(\boldsymbol{G}_I - \boldsymbol{G}_I^T \right) \end{aligned} \tag{17.10}$$

where $\boldsymbol{Q}_I$ is the rotation matrix computed at node I, and $\boldsymbol{\omega}_I$ is the matrix containing the spin tensor computed at node I.

17.4 Input format

The following parameters can be defined from the input deck:

```
BEGIN RKPM SECTION <string> section_name
  SUPPORT SIZE = <real> normalized_support
  BASIS ORDER = <real>order
  KERNEL TYPE = <real>kernel_type
  KERNEL SHAPE = <string>SPHERE | BOX
  INTEGRATION METHOD = <string>SCNI | SNNI | NSNI | VCSNNI
  STABILIZATION COEFFICIENT = <real> coefficient
  FORMULATION = <string> LAGRANGIAN| SEMI-LAGRANGIAN
  QUASI LINEAR = <string>OFF|ON (OFF)
  QUASI LINEAR COEFFICIENT = <real>quasi_linear_coefficient
  QUASI LINEAR distance = <real>quasi_linear_distance
  FRICTIONAL KERNEL CONTACT = <string> OFF|ON (OFF)
  FRICTIONAL COEFFICIENT = <real> friction_coefficient
END RKPM SECTION <string> section_name
```

- Support Size: This parameter defines the support size of the kernel functions; it controls the locality of the approximation functions. It is a normalized value with respect to the distance to the closest neighboring nodes, and should be greater than 1.5, because of the strain smoothing employed in SCNI and SNNI. For order of approximation (see below) higher than 1, the support size also needs to be increased by unity for each order. For example a normalized support size of 1.6 would be acceptable for linear basis, 2.6 for quadratic basis, 3.6 for cubic basis, and so on. Note that because of the possibility of non-uniform nodal spacing, larger values may be required in more non-uniform discretizations.
- Basis Order: This parameters controls what order of polynomial the approximation space is built upon. RKPM is constructed to reproduce any polynomial function of a given order exactly in the entire domain. The order of reproduction dictates at what rate the solution will converge in the energy norm. A higher basis order will yield better accuracy and faster convergence, but will also increase computational expense.
- Kernel Type: The approximation functions are built from a kernel function and a correction function. The correction function is automatically calculated to meet the required reproducing conditions, but the kernel function can be chosen by the user. The smoothness of the kernel function directly dictates the smoothness of the approximation field. In this implementation, different orders of B-Splines are used. This parameter can be chosen between 1 (linear B-Spline, C^0 continuity) and 5 (quintic B-Spline, C^4 continuity). In problems where the solution is known to be smooth, higher order continuity is more desirable.
- Integration Method: Several RKPM integration schemes are under development in Sierra/SM. Currently, Stabilized Conforming Nodal Integration (SCNI) is the best option. In this case, a conforming mesh is necessary to construct the integration cells. If such information is not available (when the capabilities of the code are extended), Stabilized Non-Conforming Nodal Integration (SNNI) or its VC counterpart, VC-SNNI, can be used instead. For more details, see section 17.2.

- Stabilization Coefficient: This is an optional parameter, and should stay in the range between 0 and 1. If omitted, no additional stabilization is performed. If a coefficient is specified it will be used to perform additional stabilization. If it is set to 0.0, the result will be the same as unstabilized, but the additional stabilization routines will still be called, adding significant computational expense. Therefore, if no stabilization is required, this parameter should be omitted.
- Formulation: Not implemented yet. For now, any RKPM analysis is ran using the Lagrangian description. A semi-Lagrangian formulation is planned for future development. The semi-Lagrangian formulation is better suited to simulations involving very large deformations and material failure.

17.4.1 Converting a mesh to particles

The recommended way to load an RKPM model is to read in a standard hexahedron and/or tetrahedron element mesh and convert the elements to particles at initialization in the region scope using the `BEGIN CONVERSION TO PARTICLES AT INITIALIZATION` (see also the Particle Section command block in Chapter 6 and the peridynamics Chapter 10 of the User's Manual):

```
BEGIN CONVERSION TO PARTICLES AT INITIALIZATION
  BLOCK = <string list>block_names
  SECTION = <string>particle_section
END [CONVERSION TO PARTICLES AT INITIALIZATION]
```

where the `BLOCK` command specifies which blocks are converted to particles, and `SECTION` specifies the peridynamics section.

An alternative way to convert an original mesh to particles is to use the `spheregen.py` routine. The following command will convert an ExodusII file, e.g., `myfile.g` to `myfile.sphere.g`:

```
spheregen.py --nodes_as_attr myfile.g
```

Here, the `--nodes_as_attr` option embeds the original node locations into the sphere mesh as attributes, which is required for RKPM. The sphere mesh, `myfile.sphere.g`, should then be specified as the mesh file in the Sierra/SM input deck. In this implementation, the RKPM nodes are located at the center points of each element constituting the original mesh of the solid. Only the SNNI integration technique is supported for this option.

References

[1] Wing Kam Liu, Sukky Jun, and Yi Fei Zhang. Reproducing kernel particle methods. *International Journal for Numerical Methods in Engineering*, 20(8-9):1081–1106, 1995.

[2] Jiun-Shyan Chen, Chunhui Pan, Cheng-Tang Wu, and Wing Kam Liu. Reproducing kernel particle methods for large deformation analysis of non-linear structures. *Computer Methods in Applied Mechanics and Engineering*, 139(1):195–227, 1996.

[3] Jiun-Shyan Chen, Michael Hillman, and Marcus Rüter. An arbitrary order variationally consistent integration for galerkin meshfree methods. *International Journal for Numerical Methods in Engineering*, 95(5):387–418, 2013.

[4] Jiun-Shyan Chen, Cheng-Tang Wu, Sangpil Yoon, and Yang You. A stabilized conforming nodal integration for galerkin mesh-free methods. *International Journal for Numerical Methods in Engineering*, 50(2):435–466, 2001.

[5] Jiun-Shyan Chen, Sangpil Yoon, and Cheng-Tang Wu. Non-linear version of stabilized conforming nodal integration for galerkin mesh-free methods. *International Journal for Numerical Methods in Engineering*, 53(12):2587–2615, 2002.

[6] J.S. Chen, W. Hu, M.A. Puso, Y. Wu, and X. Zhang. Strain smoothing for stabilization and regularization of galerkin meshfree methods. In *Meshfree Methods for Partial Differential Equations III*, pages 57–75. Springer, 2007.

[7] M.A. Puso, J.S. Chen, E. Zywicz, and W. Elmer. Meshfree and finite element nodal integration methods. *International Journal for Numerical Methods in Engineering*, 74(3):416–446, 2008.

[8] Thomas J.R. Hughes and James Winget. Finite rotation effects in numerical integration of rate constitutive equations arising in large-deformation analysis. *International Journal for Numerical Methods in Engineering*, 15(12):1862–1867, 1980.

Chapter 18

Material Models

The chapter describes materials available in Sierra that are currently under development.

18.1 Elastic Orthotropic Damage Model

```
BEGIN PARAMETERS FOR MODEL ELASTIC_ORTHOTROPIC_DAMAGE
  #
  # Elastic constants
  #
  YOUNGS MODULUS = <real> E
  POISSONS RATIO = <real> ν
  SHEAR MODULUS  = <real> G
  BULK MODULUS   = <real> K
  LAMBDA         = <real> λ
  #
  # Required parameters
  #
  E11    = <real> E11
  E22    = <real> E22
  E33    = <real> E33
  NU12   = <real> ν12
  NU13   = <real> ν13
  NU23   = <real> ν23
  G12    = <real> g12
  G13    = <real> g13
  G23    = <real> g23
  ALPHAD = <real> αd
  BETAD  = <real> βd
  GAMMA0 = <real> γ0
  J1     = <real> j1
  J2     = <real> j2
  J3     = <real> j3
  CN11   = <real> cn11
  CN22   = <real> cn22
  CN33   = <real> cn33
  CS12   = <real> cs12
  CS13   = <real> cs13
  CS23   = <real> cs23
  COORDINATE SYSTEM = <string> coordinate_system_name
  #
  # Optional parameters
  #
  ANGLE_1_ABSCISSA = <real>angle_1_abscissa
  ANGLE_2_ABSCISSA = <real>angle_2_abscissa
  ANGLE_3_ABSCISSA = <real>angle_3_abscissa
  ROTATION_AXIS_1  = <real>rotation_axis_1
  ROTATION_AXIS_2  = <real>rotation_axis_2
  ROTATION_AXIS_3  = <real>rotation_axis_3
  ANGLE_1_FUNCTION = <string>angle_1_function_name
  ANGLE_2_FUNCTION = <string>angle_2_function_name
  ANGLE_3_FUNCTION = <string>angle_3_function_name
```

```
  E11 FUNCTION    = <string>func_name
  E22 FUNCTION    = <string>func_name
  E33 FUNCTION    = <string>func_name
  NU12 FUNCTION   = <string>func_name
  NU13 FUNCTION   = <string>func_name
  NU23 FUNCTION   = <string>func_name
  G12 FUNCTION    = <string>func_name
  G13 FUNCTION    = <string>func_name
  G23 FUNCTION    = <string>func_name
END [PARAMETERS FOR MODEL ELASTIC_ORTHOTROPIC_DAMAGE]
```

The elastic orthotropic damage model is an empirically based constitutive relation that is useful for modeling polymer matrix composite structures. Refer to SAND2013-7257 for a full description of the material model theory and usage.

The command block for an elastic orthotropic damage material starts with the line:

```
BEGIN PARAMETERS FOR MODEL ELASTIC_ORTHOTROPIC_DAMAGE
```

and terminates with the line:

```
END [PARAMETERS FOR MODEL ELASTIC_ORTHOTROPIC_DAMAGE]
```

In the above command block, the required inputs are: two of the five general elastic material constants, directional properties, and the coordinate system. The following is a brief description of each input.

- The density of the material is defined with the `DENSITY` command line.
- The Biot's coefficient of the material is defined with the `BIOTS COEFFICIENT` command line.
- Any two of the following elastic constants are required:
  - Young's modulus is defined with the `YOUNGS MODULUS` command line.
  - Poisson's ratio is defined with the `POISSONS RATIO` command line.
  - The bulk modulus is defined with the `BULK MODULUS` command line.
  - The shear modulus is defined with the `SHEAR MODULUS` command line.
  - Lambda is defined with the `LAMBDA` command line.
- The directional moduli E_{11}, E_{22}, and E_{33} are defined with the `E11`, `E22`, and `E33` command lines.
- The directional Poisson's ratios ν_{12}, ν_{13}, and ν_{23} are defined with the `NU12`, `NU13`, and `NU23` command lines.
- The directional shear moduli G_{12}, G_{13}, and G_{23} are defined with the `G12`, `G13`, and `G23` command lines.
- The specification of the principal material directions begins with the selection of a user specified coordinate system given by the `COORDINATE SYSTEM` command line (see below).
- The damage surface evolution terms are given with the ALPHAD and BETAD command lines.

- The initial damage threshold is defined with the GAMMA0 command line.
- The directional damage surface coefficients with the J1, J2 and J3 command lines.
- The directional normal crack closure coefficients defined with the CN11, CN22 and CN33 command lines.
- The directional shear crack closure coefficients are defined with the CS12, CS13 and CS23 command lines.
- For material orientation definition instructions see the Materials chapter in the Sierra/SM User's Manual.

Warning: The `ELASTIC_ORTHOTROPIC_DAMAGE` model has not been tested in conjunction with the control stiffness implicit solver block.

18.2 Karagozian and Case Concrete Model

```
BEGIN PARAMETERS FOR MODEL KC_CONCRETE
  #
  # Elastic constants
  #
  YOUNGS MODULUS = <real> E
  POISSONS RATIO = <real> ν
  SHEAR MODULUS  = <real> G
  BULK MODULUS   = <real> K
  LAMBDA         = <real> λ
  TWO MU         = <real> 2μ
  #
  #
  #
  COMPRESSIVE STRENGTH = <real>compressive_strength
  FRACTIONAL DILATANCY = <real>omega
  HARDEN-SOFTEN FUNCTION = <string>harden_soften_function_name
  LAMBDAM = <real>lambda_m
  LAMBDAZ = <real>lambda_z
  MAXIMUM AGGREGATE SIZE = <real>max_aggregate_size
  ONE INCH = <real>one_inch
  PRESSURE FUNCTION = <string>pressure_function_name
  RATE SENSITIVITY FUNCTION = <string>rate_function_name
  SINGLE RATE ENHANCEMENT = <enum>TRUE|FALSE
  TENSILE STRENGTH = <real>tensile_strength
  UNLOAD BULK MODULUS FUNCTION = <string>bulk_function_name
END PARAMETERS FOR MODEL KC_CONCRETE
```

The Karagozian & Case (or K&C) concrete model is an inelasticity model appropriate for approximating the constitutive behavior of concrete. Coupled with appropriate elements for capturing the embedded deformation of reinforcing steel, the K&C concrete model can be used effectively for simulating the mechanical response of reinforced concrete structures. The K&C model has several useful characteristics for estimating concrete response, including strain-softening capabilities, some degree of tensile response, and a nonlinear stress-strain characterization that robustly simulates the behavior of plain concrete. This model is described in detail in [1].

In the above command blocks:

- Consult the Sierra/SM User's Guide chapter on Material Models for more information on elastic constants input.
- The compressive strength for a uniaxial compression test is defined with the `COMPRESSIVE STRENGTH` command line.
- The tensile strength for the uniaxial tension test is defined with the `TENSILE STRENGTH` command line.
- The abscissa of the hardening/softening curve where this curve takes on the value of one is termed Lambda-M, and it is defined with the `LAMBDAM` command line (see [1], pg. B-3).
- The abscissa of the hardening/softening curve where this curve takes on the value of zero

after its peak value has been attained is termed Lambda-Z, and it is defined with the LAMBDAZ command line. This parameter should satisfy LAMBDAZ > LAMBDAM (see [1], pg. B-3). This input is Sierra-specific, and differs from the previous PRONTO3D definitions.

- The SINGLE RATE ENHANCEMENT parameter indicates whether the rate enhancement of the model should be independent of the sign of the deformation. If this parameter is set to TRUE, the same enhancement function is used for both compression and tension. If it is set to FALSE, the enhancement function must assign values for both positive and negative values of strain rate (see [1], pg. B-5). This parameter is also Sierra-specific, and is different from the previous PRONTO3D definitions.
- The FRACTIONAL DILATANCY is an estimate of the size of the plastic volume strain increment relative to that corresponding to straining in the hydrostatic plane. This value normally ranges from 0.3 to 0.7, and a value of one-half is commonly used in practice.
- The MAXIMUM AGGREGATE SIZE parameter provides an estimate of the largest length dimension for the aggregate component of the concrete mix. The American Concrete Institute code [2] includes specifications for maximum aggregate size that are based on member depth and clear spacing between adjacent reinforcement elements.
- The parameter ONE INCH provides for conversion to units other than the pounds/inch system commonly used in U.S. concrete venues. This parameter should be set to the equivalent length in the system used for analysis. If centimeters are to be used, for example, then ONE INCH = 2.54.

The following functions describe the evolution of material coefficients in this model:

- The function characterizing the enhancement of strength with strain rate is described via the RATE SENSITIVITY FUNCTION (see [1], pg. B-3).

Warning: The RATE SENSITIVITY FUNCTION command should be used with caution. The implementation appears to overestimate concrete strength in tension, and users are cautioned to provide rate sensitivity function values that have the value of 1.0 for positive (tensile) values of strain rate. These values correspond to no additional strength in tension due to strain rate, and are both physically realistic and conservative.

- The function describing the relationship between pressure and volumetric strain is described via the PRESSURE FUNCTION.
- The function characterizing the relationship between bulk modulus and volumetric strain during unloading is described via the UNLOAD BULK MODULUS FUNCTION.
- The function describing the hardening and softening functions function eta as a function of the material parameters lambda (see LAMBDAM and LAMBDAZ) is defined via the HARDEN-SOFTEN FUNCTION (see [1], pg. B-3).

18.3 Kayenta Model

Note, many parameters of this model are undocumented.

```
BEGIN PARAMETERS FOR MODEL KAYENTA
  B0          = <real> b0
  B1          = <real> b1
  B2          = <real> b2
  B3          = <real> b3
  B4          = <real> b4
  G0          = <real> g0
  G1          = <real> g1
  G2          = <real> g2
  G3          = <real> g3
  G4          = <real> g4
  RJS         = <real> rjs
  RKS         = <real> rks
  RKN         = <real> rkn
  A1          = <real> a1
  A2          = <real> a2
  A3          = <real> a3
  A4          = <real> a4
  P0          = <real> p0
  P1          = <real> p1
  P2          = <real> p2
  P3          = <real> p3
  CR          = <real> cr
  RK          = <real> rk
  RN          = <real> rn
  HC          = <real> hc
  CTPSF       = <real> ctpsf
  CUTPS       = <real> cutps
  CUTI1       = <real> cuti1
  T1          = <real> t1
  T2          = <real> t2
  T3          = <real> t3
  T4          = <real> t4
  T5          = <real> t5
  T6          = <real> t6
  T7          = <real> t7
  J3TYPE      = <real> j3type
  A2PF        = <real> a2pf
  A4PF        = <real> a4pf
  CRPF        = <real> crpf
  RKPF        = <real> rkpf
  FAIL0       = <real> fail0
  FAIL1       = <real> fail1
  FAIL2       = <real> fail2
```

```
  FAIL3     = <real> fail3
  FAIL4     = <real> fail4
  FAIL5     = <real> fail5
  FAIL6     = <real> fail6
  FAIL7     = <real> fail7
  FAIL8     = <real> fail8
  FAIL9     = <real> fail9
  PEAKI1I   = <real> peaki1i
  STRENI    = <real> streni
  FSLOPEI   = <real> fslopei
  PEAKI1F   = <real> peaki1f
  STRENF    = <real> strenf
  FSLOPEF   = <real> fslopef
  SOFTENING = <real> softening
  IEOSID    = <real> ieosid
  DILATLIM  = <real> dilatlim
  NU        = <real> nu
  YSLOPEI   = <real> yslopei
  YSLOPEF   = <real> yslopef
  CKN01     = <real> ckn01
  VMAX1     = <real> vmax1
  SPACE1    = <real> space1
  SHRSTIFF1 = <real> shrstiff1
  CKN01     = <real> ckn02
  VMAX1     = <real> vmax2
  SPACE1    = <real> space2
  SHRSTIFF1 = <real> shrstiff2
  CKN01     = <real> ckn03
  VMAX1     = <real> vmax3
  SPACE1    = <real> space3
  SHRSTIFF1 = <real> shrstiff3
END [PARAMETERS FOR MODEL KAYENTA]
```

Kayenta is an outgrowth of the the Brannon-Fossum-Strack isotropic geomaterial model. that includes features and fitting functions appropriate to a broad class of materials including rocks, rock-like engineered materials (such as concretes and ceramics), and metals. Fundamentally, Kayenta is a computational framework for generalized plasticity models. As such, it includes a yield surface, but the term "yield" is generalized to include any form of inelastic material response including microcrack growth and pore collapse. Kayenta supports optional anisotropic elasticity associated with ubiquitous joint sets. Kayenta supports optional deformation-induced anisotropy through kinematic hardening (in which the initially isotropic yield surface is permitted to translate in deviatoric stress space to model Bauschinger effects). The governing equations are otherwise isotropic. Because Kayenta is a unification and generalization of simpler models, it can be run using as few as 2 parameters (for linear elasticity) to as many as 40 material and control parameters in the exceptionally rare case when all features are used. Isotropic damage is modeled through loss of stiffness and strength. If ever you are unsure of the value of a parameter, leave it unspecified so that Kayenta can use an appropriate default. See [3] for a full description of the model, inputs, and

output variables.

The command block for a Kayenta material starts with the line:

```
BEGIN PARAMETERS FOR MODEL KAYENTA
```

and terminates with the line:

```
END [PARAMETERS FOR MODEL KAYENTA]
```

In the above command blocks:

- The following are valid parameters for the Kayenta material model. If ever you are unsure of the value of a parameter, leave it unspecified so that Kayenta can use an appropriate default.
  - The initial elastic bulk modulus is defined with the `B0` command line.
  - The high pressure coefficient in nonlinear elastic bulk modulus function is defined with the `B1` command line.
  - The curvature parameter in nonlinear elastic bulk modulus function is defined with the `B2` command line.
  - The coefficient in nonlinear elastic bulk modulus to allow for plastic softening is defined with the `B3` command line.
  - The power in bulk modulus softening is defined with the `B4` command line.
  - The initial elastic shear modulus is defined with the `G0` command line.
  - The coefficient in shear modulus hardening is defined with the `G1` command line.
  - The curvature parameter in shear modulus hardening is defined with the `G2` command line.
  - The coefficient in shear modulus softening is defined with the `G3` command line.
  - The power in shear modulus softening is defined with the `G4` command line.
  - The joint spacing is defined with the `RJS` command line.
  - The joint shear stiffness is defined with the `RKS` command line.
  - The joint normal stiffness is defined with the `RKN` command line.
  - The constant term for meridional profile function of ultimate shear limit surface is defined with the `A1` command line.
  - The curvature decay parameter in the meridional profile function is defined with the `A2` command line.
  - The parameter in the meridional profile function is defined with the `A3` command line.
  - The high-pressure slope parameter in meridional profile function is defined with the `A4` command line.
  - One third of the elastic limit pressure parameter at onset of pore collapse is defined with the `P0` command line.
  - One third of slope of porosity vs pressure crush curve at elastic limit is defined with the `P1` command line.
  - The parameter for hydrostatic crush curve is defined with `P2` command line.
  - The asymptote of the plastic volumetric strain for hydrostatic crush is defined with the `P3` command line.
  - The parameter for porosity affecting shear strength is defined with the `CR` command line.

- The triaxial extension strength to compression strength ratio is defined with the `RK` command line.
- The initial shear yield offset [non negative] is defined with the `RN` command line.
- The kinematic hardening parameter is defined with the `HC` command line.
- The tension cut-off value of I1 is defined with the `CUTI1` command line.
- The tension cut-off value of principal stress is defined with the `CUTPS` command line.
- The relaxation time constant 1 is defined with the `T1` command line.
- The relaxation time constant 2 is defined with the `T2` command line.
- The parameter no longer in use. [set to zero] is defined with the `T3` command line.
- The parameter no longer in use. [set to zero] is defined with the `T4` command line.
- The relaxation time constant 5 (stress). is defined with the `T5` command line.
- The relaxation time constant 6 (time). is defined with the `T6` command line.
- The relaxation time constant 7 (1/stress). is defined with the `T7` command line.
- The type of 3^{rd} deviatoric stress invariant function is defined with the `J3TYPE` command line.
- The potential function parameter 1 (default=A2) is defined with the `A2PF` command line.
- The potential function parameter 2 (default=A4) is defined with the `A4PF` command line.
- The potential function parameter 3 (default=CR) is defined with the `CRPF` command line.
- The potential function parameter 4 (default=RK) is defined with the `RKPF` command line.
- The failed speed is defined with the `FSPEED` command line.
- The peak I1 hydrostatic tension strength is defined with the `PEAKI1I` command line.
- The peak (high pressure) shear strength is defined with the `STRENI` command line.
- The initial slope of limit surface at PEAKI1I is defined with the `FSLOPEI` command line.
- `PEAKI1F` is the same as PEAKI1I, but for failed limit surface.
- `STRENF` is the same as STRENI, but for failed limit surface.
- `FSLOPEF` is the same as FSLOPEI, but for failed limit surface.
- The `SOFTENING` command line allows transition of limit surface from intact description to failed description.
- The amount of time that passes with the stress state at the limit surface before the limit surface collapses (i.e., softens) is defined with the `TFAIL` command line.
- The upper limit on plastic volume strain is defined with the `DILATLIM` command line.

18.4 Shape Memory Alloy

```
BEGIN PARAMETERS FOR MODEL SHAPE_MEMORY_ALLOY
  #
  # Elastic constants
  #
  YOUNGS MODULUS = <real> E
  POISSONS RATIO = <real> ν
  SHEAR MODULUS  = <real> G
  BULK MODULUS   = <real> K
  LAMBDA         = <real> λ
  TWO MU         = <real> 2μ
  #
  # Thermoelastic properties of two crystallographic phases
  #
  ELASTIC MODULUS AUSTENITE  = <real> E^A
  POISSON RATIO AUSTENITE    = <real> ν^A
  CTE AUSTENITE              = <real> α^A
  ELASTIC MODULUS MARTENSITE = <real> E^M
  POISSON RATIO MARTENSITE   = <real> ν^M
  CTE MARTENSITE             = <real> α^M
  #
  # Phase diagram parameters
  #
  MARTENSITE START                  = <real> M_s
  MARTENSITE FINISH                 = <real> M_f
  AUSTENITE START                   = <real> A_s
  AUSTENITE FINISH                  = <real> A_f
  STRESS INFLUENCE COEFF MARTENSITE = <real> C^M
  STRESS INFLUENCE COEFF AUSTENITE  = <real> C^A
  #
  # Transformation strain magnitude parameters
  #
  H_MIN          = <real> H_min
  H_SAT          = <real> H_sat
  KT             = <real> k
  SIGMA_CRITICAL = <real> σ^crit
  #
  # Calibration parameters
  #
  N1         = <real> n_1
  N2         = <real> n_2
  N3         = <real> n_3
  N4         = <real> n_4
  SIGMA STAR = <real> σ^*
  T0         = <real> θ_0
  #
  # Initial phase conditions
```

```
  #
  XI0                    = <real> ξ(t = 0)  (0.0)
  PRESTRAIN_DIRECTION    = <int> n^ps  (0)
  PRESTRAIN_MAGNITUDE    = <real> ‖ε_ij^tr (t = 0)‖ (0.0)
  #
END [PARAMETERS FOR MODEL SHAPE_MEMORY_ALLOY]
```

The shape memory alloy (SMA) model is used to describe the thermomechanical response of intermetallics (e.g. NiTi, NiTiCu, NiTiPd, NiTiPt) that can undergo a reversible, diffusionless, solid-to-solid martensitic transformation. Specifically, the materials have a high-symmetry (typically cubic) austenitic crystallographic structure at high temperature and/or low stress. At lower-temperatures and/or high stress the crystallographic structure is transformed to a lower symmetry (typically orthorhombic or monoclinic) martensitic phase. The change in structure and symmetry may be taken advantage of to produce large inelastic strains of $\approx$ 1-8%. Importantly, this class of materials differentiates itself from TRIP steels in that the transformation is *reversible* and a variety of thermomechanical loading paths have been conceived of to take advantage of this behavior. A notable application of these materials is as an actuator in smart, morphing structures.

Phenomenologically, the macroscopic behavior of SMAs is typically discussed in effective stress-temperature space via a *phase diagram* like in Figure 18.1. The four lines denoted M_s, M_f, A_s, and A_f indicate the martensitic start, martensitic finish, austenitic start, and austenitic finish transformation surfaces. *Forward transformation* (from an austenitic to a martensitic state) is described by the martensitic start and finish surfaces. Specifically, the former refers to the thermomechanical conditions at which transformation will initiate while the latter corresponds to complete transformation. The difference between the two surfaces is associated with internal hardening effects due to microstructure (i.e. texture, back stresses). Transformation from martensite to austenite is referred to as *reverse* and is characterized by the austenitic start and finish surfaces. Detailed discussion of the crystallography and phenomenology may be found in [4, 5][1].

Two responses characteristic of SMAs may also be represented via the phase diagram. These are the *actuation response* and the *pseudoelastic* (often referred to as *superelastic* in the literature) responses. The first (actuation) is indicated by path "A" in Figure 18.1. In this case, a mechanical bias load is applied to the SMA and the material is then thermally cycled through forward and reverse transformation. The resulting transformation first produces and then removes the large transformation strains of SMAs and is commonly used for (surprisingly) actuation applications. At higher temperatures ($T > A_f$), mechanical loading may be used induce forward and, upon unloading, reverse transformation as indicated in path "B" of Figure 18.1. Through such a cycle, a distinctive flag shape in the stress strain response is observed through which large amounts of energy may be dissipated while producing no permanent deformations. As such, this loading path is often considered for vibration isolation or damping applications.

In LAMÉ, the response of SMAs is described by the phenomenological model of Lagoudas and coworkers [6]. This model was motivated by actuator applications and it describes the inelastic

[1] In the martensitic configuration, the crystallographic structure can either self-accommodate in a *twinned* configuration producing no macroscopic inelastic strain or an internal or external stress field may be used to *detwin* the microstructure thereby producing the desired inelastic strain. For simplicity, this distinction is bypassed in this brief text and the interested reader should consult the referenced works.

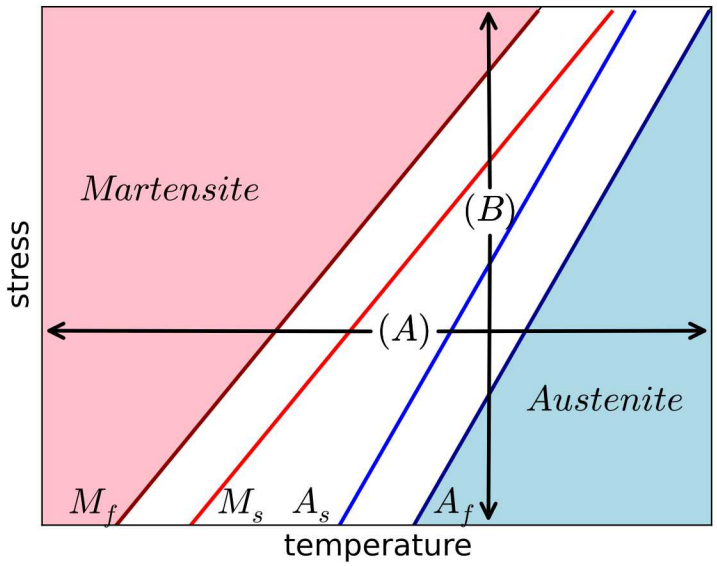

Figure 18.1: Representative phase diagram of shape memory alloys highlighting characteristic loading paths ((*A*) and (*B*)), transformation surfaces, and phases.

deformation associated with martensitic transformation through two internal state variables – the scalar martensitic volume fraction, ξ, and tensorial transformation strain tensor, $\varepsilon_{ij}^{\mathrm{tr}}$. Before proceeding it should be noted that the *structural* response of SMA specimens and components exhibit a rate dependency associated with the strong thermomechanical coupling of SMAs. Specifically, the transformation process gives off/absorbs large amounts of energy via the *latent heat of transformation*. The rate dependence observed is a result of the characteristic time scale associated with thermal transport of this heat. In pure mechanical analyses (like Sierra/SM), this means quasistatics loadings are typically considered (a strain rate of $\approx 1x10^{-4}$ and/or heating/cooling rate of $\approx 2^{\circ}C/\mathrm{min}$). Formulations accounting for the full coupling have been developed but require more complex implementations.

To begin, the model assumes an additive decomposition of the total, elastic, thermal, and transformation deformation (strain) rates respectively denoted by D_{ij}, D_{ij}^{e}, D_{ij}^{th} and D_{ij}^{tr} producing a total deformation rate of the form,

$$D_{ij} = D_{ij}^{\mathrm{e}} + D_{ij}^{\mathrm{th}} + D_{ij}^{\mathrm{tr}}. \tag{18.1}$$

With respect to the thermoelastic deformations, it is noted that the different crystallographic phases have different thermoelastic constants. Previous studies have demonstrated that a rule of mixtures on the compliance and other material properties of the form,

$$\mathbb{S}_{ijkl} = \mathbb{S}_{ijkl}^{A} + \xi\left(\mathbb{S}_{ijkl}^{M} - \mathbb{S}_{ijkl}^{A}\right) = \mathbb{S}_{ijkl}^{A} + \xi\Delta\mathbb{S}_{ijkl}, \tag{18.2}$$

$$\alpha_{ij} = \alpha^{A}\delta_{ij} + \xi\left(\alpha^{M}\delta_{ij} - \alpha^{A}\delta_{ij}\right) = \alpha^{A}\delta_{ij} + \xi\Delta\alpha\delta_{ij}, \tag{18.3}$$

in which $\mathbb{S}_{ijkl}$ and α_{ij} are the current effective compliance and coefficient of thermal expansion and the superscripts "A" and "M" denote thermoelastic properties in the austenitic and martensitic configuration. The symbol "Δ" is used to indicate the difference in a property between the martensitic and austenitic phases while δ_{ij} is the Kronecker delta. Isotropy is assumed for all these properties and the compliances are determined via the definition of elastic moduli and Poisson's ratio of the two phases – E^A, E^M, ν^M, and ν^M. The two Poisson ratios are often the same and take typical values for metals ($\nu^A \approx \nu^M \approx 0.3$) while the elastic moduli can differ by a factor of more than two. For instance the austenitic modulus of NiTi is typically given as ≈ 70 GPa while the martensitic one is ≈ 30 GPa[2]. Importantly, this difference means that the thermoelastic properties and corresponding deformations vary with transformation. As such, the corresponding rates of deformation are given as,

$$D^{\mathrm{e}}_{ij} = \dot{\xi}\Delta\mathbb{S}_{ijkl}\sigma_{kl} + \mathbb{S}_{ijkl}\,\mathring{\sigma}_{kl}, \tag{18.4}$$

$$D^{\mathrm{th}}_{ij} = \dot{\xi}\Delta\alpha\delta_{ij}\left(\theta - \theta_0\right) + \alpha\delta_{ij}\dot{\theta}, \tag{18.5}$$

where θ and θ_0 are the current and reference temperature and σ_{ij} is the symmetric Cauchy stress. Note, in using the SMA model a temperature field *must* be defined. The stress rate may then be shown to be,

$$\mathring{\sigma}_{ij} = \mathbb{C}_{ijkl}\left(D_{kl} - \alpha\delta_{kl}\dot{theta} - \dot{\xi}\left(\Delta\mathbb{S}_{klmn}\sigma_{mn} + \Delta\alpha\delta_{kl}\left(\theta - \theta_0\right)\right) - D^{\mathrm{tr}}_{kl}\right), \tag{18.6}$$

with $\mathbb{C}_{ijkl}$ being the current stiffness tensor defined as $\mathbb{C}_{ijkl} = \mathbb{S}^{-1}_{ijkl}$.

To describe the transformation strain evolution, it is assumed that these deformations evolve with (and only with) the martensitic volume fraction, ξ. The corresponding flow rule is given as,

$$D^{\mathrm{tr}}_{ij} = \dot{\xi}\Lambda_{ij}, \tag{18.7}$$

and Λ_{ij} is the transformation direction tensor assumed to be of the form,

$$\Lambda_{ij} = \begin{cases} H^{\mathrm{cur}}\left(\bar{\sigma}_{vM}\right)\frac{3}{2}\frac{s_{ij}}{\bar{\sigma}_{vM}} & \dot{\xi} \geq 0 \\ \frac{\varepsilon^{\mathrm{tr}-rev}_{ij}}{\xi^{rev}} & \dot{\xi} < 0 \end{cases}. \tag{18.8}$$

In (18.8), H^{cur} is the transformation strain magnitude that is dependent on the von Mises effective stress, $\bar{\sigma}_{vM}$, and s_{ij} is the deviatoric stress. With forward transformation defined in this way, it is assumed that deformation is shear-based and follows a J_2 like flow direction. For reverse transformation ($\dot{\xi} < 0$), the postulated form is utilized to ensure complete recovery of transformation strains with martensitic volume fraction. In other words, all transformation strain components are zero-valued at $\xi = 0$. Without enforcing this condition in this way, non-proportional loading paths could be constructed producing a non-zero transformation strain when the material is austenitic.

[2]Given the lower symmetry of the martensitic phase the determination of an isotropic elastic modulus can vary with characterization methodology. In this case, the apparent elastic modulus measured from macroscopic thermoelastic tests should be used.

The transformation strain at load reversal, $\varepsilon_{ij}^{\text{tr}-rev}$, and martensitic volume fraction at load reversal, ξ^{rev}, are then tracked (via the implementation) and used for this purpose.

The transformation strain magnitude, H^{cur}, is a function of the von Mises effective stress ($\bar{\sigma}_{vM}$) and is introduced to incorporate detwinning effects without introducing an additional internal state variable complicating the model. Specifically, at low stress values, this function returns a minimum value. If the microstructure is self-accommodated this value will be zero. A decaying exponential is used such that as the stress increases the value of the strain magnitude becomes that of the maximum value incorporating both crystallographic and texture effects. The given functional form is,

$$H^{\text{cur}} = \begin{cases} H_{\text{min}} & \bar{\sigma}_{vM} \leq \sigma_{\text{crit}} \\ H_{\text{min}} + (H_{\text{sat}} - H_{\text{min}}) \left(1 - \exp\left(-k\left(\bar{\sigma}_{vM} - \sigma_{\text{crit}}\right)\right)\right) & \bar{\sigma}_{vM} > \sigma_{\text{crit}} \end{cases}, \tag{18.9}$$

where H_{min}, H_{sat}, k, and σ_{crit} are model parameters giving the minimum transformation strain magnitude, maximum transformation strain magnitude, exponential fitting parameter governing the transition zone, and critical stress values (in some ways analogous to the detwinning stress).

The evolution of martensitic transformation process is governed by a transformation function serving an analogous role to the yield function in plasticity. This function is given by,

$$f\left(\sigma_{ij}, \theta, \xi\right) = \pm\phi\left(\sigma_{ij}, \theta, \xi\right) - \bar{\sigma}\left(\sigma_{ij}\right), \tag{18.10}$$

with ϕ begin the thermodynamic driving force for transformation and $\bar{\sigma}$ the critical value. The $\pm$ is used to denote either forward (+) or reverse (−) transformation. This transformation function and the associated forms are derived from continuum thermodynamic considerations and the details of that process are neglected here for brevity but may be found in [6]. The functional forms of these variables are given as,

$$\begin{aligned} \phi\left(\sigma_{ij}, \theta, \xi\right) &= \sigma_{ij}\Lambda_{ij} + \frac{1}{2}\sigma_{ij}\Delta\mathbb{S}_{ijkl}\sigma_{kl} + \sigma_{ij}\Delta\alpha\delta_{ij}\left(\theta - \theta_0\right) + \rho\Delta s_0\theta - \rho\Delta u_0 - f^t\left(\xi\right), \\ \bar{\sigma}\left(\sigma_{ij}\right) &= \sigma_0 + D\sigma_{ij}\Lambda_{ij}, \end{aligned} \tag{18.11}$$

in which $\rho\Delta s_0$ and $\rho\Delta u_0$ are the differences in reference entropy and internal energy of the two phases, D is a calibration parameter intended to capture variations in dissipation with stress, and $f^t\left(\xi\right)$ is the hardening function. With respect to this latter term, empirical observations were used to arrive at a postulated form of,

$$f^t\left(\xi\right) = \begin{cases} \frac{1}{2}a_1\left(1 + \xi^{n_1} - (1-\xi)^{n_2}\right) + a_3 & \dot{\xi} \geq 0 \\ \frac{1}{2}a_2\left(1 + \xi^{n_3} - (1-\xi)^{n_4}\right) - a_3 & \dot{\xi} < 0 \end{cases}, \tag{18.12}$$

with a_1, a_2, and a_3 being fitting parameters and n_1, n_2, n_3, and n_4 are exponents fit to match the smooth transformation from elastic to inelastic deformations at the start of forward, end of forward, start of reverse, and end of reverse transformation respectively.

Before proceeding, one final note should be given in regards to calibration. Specifically, some of the model parameters just listed (a_1, a_2, a_3, D, σ_0, $\rho\Delta s_0$ and $\rho\Delta u_0$) are not easily identified or conceptualized in terms of common thermomechanical experiments. Some easily identifiable parameters (M_s, M_f, A_s, and A_f), however, are not evident in the theoretical formulation. Conditions associated with these terms and some physical constraints may be used to determine the model parameters in terms of these more accessible properties. These relations are,

$$\rho\Delta s_0 = \frac{-2\left(C^M C^A\right)\left[H^{\text{cur}}(\sigma) + \sigma\frac{\partial H^{\text{cur}}}{\partial\sigma} + \sigma\left(\frac{1}{E^M} - \frac{1}{E^A}\right)\right]}{C^M + C^A}\Big|_{\sigma=\sigma^*}, \tag{18.13}$$

$$D = \frac{\left(C^M - C^A\right)\left[H^{\text{cur}}(\sigma) + \sigma\frac{\partial H^{\text{cur}}}{\partial\sigma} + \sigma\left(\frac{1}{E^M} - \frac{1}{E^A}\right)\right]}{\left(C^M + C^A\right)\left[H^{\text{cur}}(\sigma) + \sigma\frac{\partial H^{\text{cur}}}{\partial\sigma}\right]}\Big|_{\sigma=\sigma^*}, \tag{18.14}$$

$$a_1 = \rho\Delta s_0\left(M_f - M_s\right), \qquad a_2 = \rho\Delta s_0\left(A_s - A_f\right), \tag{18.15}$$

$$a_3 = -\frac{a_1}{4}\left(1 + \frac{1}{n_1+1} - \frac{1}{n_2+1}\right) + \frac{a_2}{4}\left(1 + \frac{1}{n_3+1} - \frac{1}{n_4+1}\right), \tag{18.16}$$

$$\rho\Delta u_0 = \frac{\rho\Delta s_0}{2}\left(M_s + A_f\right), \qquad \sigma_0 = \frac{\rho\Delta s_0}{2}\left(M_s - A_f\right) - a_3, \tag{18.17}$$

in which σ^* is the scalar stress measure in which the calibration is performed at. For additional discussion on the characterization of SMAs and calibration of this model, the user is referred to [7, 8].

In the command blocks that define the Shape Memory Alloy model:

- See the User's Guide chapter on Material Models for more information on elastic constants input. Although the thermoelastic constants of the phases are defined separately, the definition of these constants in this form is necessary for the global solver. Typical values of the phases should be applied.

- The isotropic elastic moduli of the austenitic (E^A) and martensitic phases (E^M) are defined with the `ELASTIC MODULUS AUSTENITE` and `ELASTIC MODULUS MARTENSITE` command lines, respectively. Note, alternative elastic constants (e.g. bulk or shear moduli) may not be used.

- The isotropic Poisson's ratio of the austenitic (ν^A) and martensitic phases (ν^M) are defined with the `POISSON RATIO AUSTENITE` and `POISSON RATIO MARTENSITE` command lines, respectively. Note, alternative elastic constants (e.g. lame constant) may not be used.

- The isotropic coefficient of thermal expansion of the austenitic (α^A) and martensitic phases (α^M) are defined with the `CTE AUSTENITE` and `CTE MARTENSITE` command lines, respectively. Note, given the phase and history dependence of the material thermal expansion, the use of artificial or thermal strain functions may not lead to desired results. The use of these constants in encouraged instead.

- The zero stress, smooth transformation temperatures corresponding to the start and end of forward transformation (martensitic start M_s and finish M_f, respectively) and start and end of reverse transformation (austenitic start A_s and finish A_f, respectively) are given by the (in order) command lines `MARTENSITE START`, `MARTENSITE FINISH`, `AUSTENITE START`, and `AUSTENITE FINISH`.

- The stress influence coefficients giving the slope of the forward and reverse transformation surfaces (C^M and C^A, respectively) are given by the `STRESS INFLUENCE COEFF MARTENSITE` and `STRESS INFLUENCE COEFF AUSTENITE`, respectively.

- The stress dependence of the transformation strain magnitude requires four coefficients. These are the minimum transformation strain magnitude (H_{min}), the saturation (or maximum) magnitude (H_{sat}), exponential fitting coefficient (k), and critical effective stress value below which the magnitude is minimum (σ_{crit}). These parameters are defined via the `H_MIN`, `H_SAT`, `KT`, and `SIGMA_CRITICAL` command lines, respectively.

- The smooth hardening fitting constants n_1, n_2, n_3, and n_4 correspond to the degree of smoothness (essentially how gradual the transformation is) of the martensitic start, martensitic finish, austenitic start, and austenitic finish transformation surfaces. They are given by the `N1`, `N2`, `N3`, and `N4` command lines, respectively, and should take values $0 < n_i \leq 1$.

- The stress level of transformation at which calibration is performed is denoted by σ^* and given by the command line `SIGMA STAR`. For thermally induced transformation this corresponds to the bias stress level while in pseudo-elastic loadings it corresponds to the stress level at which the material is roughly evenly split between martensite and austenite.

- The zero-strain reference temperature is denoted θ_0 and prescribed via the `T0` command line.

- Three optional parameters describing the initial state of the material may be input. These parameters are intended for the case in which the material is initially martensite to allow for initial heating and transformation recovery. The first is the initial martensitic volume fraction, $\xi(t = 0)$, input via the `XI0` command line. If this parameter is not specified the default value is 0.0 representative of an austenitic material. A value between 0.0 and 1.0 may be entered to initialize the material to partially (or fully) martensitic. Corresponding initial transformation strains may be entered via the `PRESTRAIN_DIRECTION` (n^{ps}) and `PRESTRAIN_MAGNITUDE` $\left(\|\varepsilon_{ij}^{\text{tr}}(t = 0)\|\right)$ commands. The first (an integer between one and three) gives the direction of transformation (in global Cartesian space) and the magnitude of the inelastic strain in that direction is given by a fraction (between 0 and 1) of H_{sat} via the second `PRESTRAIN_MAGNITUDE` line. As the transformation strain tensor is deviatoric, the other two directions are specified by preserving that the tensor be trace less. Note, the `PRESTRAIN_DIRECTION` and `PRESTRAIN_MAGNITUDE` cannot be specified without a non-zero `XI0` definition. Some additional capabilities in this regard have been developed but the interested users should consult with the developers.

- It is recommended that the `strain incrementation = strongly_objective` section definition always be used in conjunction with the `shape_memory_alloy` model.

- Thermal strains functions and commands in Sierra should not be used in conjunction with the `shape_memory_alloy` model.

Output variables available for this model are listed in Table 18.1.

Table 18.1: State Variables for SHAPE MEMORY ALLOY Model (Section 18.4)

Name	**Description**
`MVF`	martensitic volume fraction, ξ
`TransStrain`	transformation strain tensor, $\varepsilon_{ij}^{\text{tr}}$

18.5 Linear Elastic

```
BEGIN PARAMETERS FOR MODEL LINEAR_ELASTIC
  #
  # Elastic constants
  #
  YOUNGS MODULUS = <real> E
  POISSONS RATIO = <real> ν
  SHEAR MODULUS  = <real> G
  BULK MODULUS   = <real> K
  LAMBDA         = <real> λ
END [PARAMETERS FOR MODEL LINEAR_ELASTIC]
```

The `LINEAR_ELASTIC` material is used for modeling infinitesimal strain elastic response. Generally this model is used for code verification work when comparing to infinitesimal strain solutions. This differs slightly from the standard `ELASTIC` model which is formulated for general finite strain.

18.6 Elastic Three-Dimensional Anisotropic Model

```
BEGIN PARAMETERS FOR MODEL ELASTIC_3D_ANISOTROPIC
  #
  # Elastic constants
  #
  YOUNGS MODULUS = <real> E
  POISSONS RATIO = <real> ν
  SHEAR MODULUS  = <real> G
  BULK MODULUS   = <real> K
  LAMBDA         = <real> λ
  TWO MU         = <real> 2μ
  #
  # Material coordinates system definition
  #
  COORDINATE SYSTEM              = <string>  coordinate_system_name
  DIRECTION FOR ROTATION         = <real>    1|2|3
  ALPHA                          = <real>    α1 (degrees)
  SECOND DIRECTION FOR ROTATION  = <real>    1|2|3
  SECOND ALPHA                   = <real>    α2 (degrees)
  #
  # Required parameters
  #
  STIFFNESS MATRIX 11 = <real> C11
  STIFFNESS MATRIX 22 = <real> C22
  STIFFNESS MATRIX 33 = <real> C33
  STIFFNESS MATRIX 12 = <real> C12
  STIFFNESS MATRIX 13 = <real> C13
  STIFFNESS MATRIX 23 = <real> C23
  STIFFNESS MATRIX 44 = <real> C44
  STIFFNESS MATRIX 55 = <real> C55
  STIFFNESS MATRIX 66 = <real> C55
  STIFFNESS MATRIX 45 = <real> C45
  STIFFNESS MATRIX 46 = <real> C46
  STIFFNESS MATRIX 56 = <real> C56
  STIFFNESS MATRIX 14 = <real> C14
  STIFFNESS MATRIX 15 = <real> C15
  STIFFNESS MATRIX 16 = <real> C16
  STIFFNESS MATRIX 24 = <real> C24
  STIFFNESS MATRIX 25 = <real> C25
  STIFFNESS MATRIX 26 = <real> C26
  STIFFNESS MATRIX 34 = <real> C34
  STIFFNESS MATRIX 35 = <real> C35
  STIFFNESS MATRIX 36 = <real> C36
  #
  # Thermal strain functions
  #
  THERMAL STRAIN 11 FUNCTION = <real> ε11th(θ)
```

```
THERMAL STRAIN 22 FUNCTION = <real> ε22th(θ)
THERMAL STRAIN 33 FUNCTION = <real> ε33th(θ)
THERMAL STRAIN 12 FUNCTION = <real> ε12th(θ)
THERMAL STRAIN 23 FUNCTION = <real> ε23th(θ)
THERMAL STRAIN 13 FUNCTION = <real> ε13th(θ)
#
END [PARAMETERS FOR MODEL ELASTIC_3D_ANISOTROPIC]
```

The ELASTIC 3D ANISOTROPIC model is an extension of the ELASTIC model which allows for full anisotropy in both the material stiffness and thermal expansion. Each stiffness component is labeled with i and j indices which correspond to the components of stress and strain vectors in contracted notation,

$$\begin{bmatrix} \sigma_{11} \\ \sigma_{22} \\ \sigma_{33} \\ \sigma_{12} \\ \sigma_{23} \\ \sigma_{13} \end{bmatrix} = \begin{bmatrix} C_{11} & C_{12} & C_{13} & C_{14} & C_{15} & C_{16} \\ C_{12} & C_{22} & C_{23} & C_{24} & C_{25} & C_{26} \\ C_{13} & C_{23} & C_{33} & C_{34} & C_{35} & C_{36} \\ C_{14} & C_{24} & C_{34} & C_{44} & C_{45} & C_{46} \\ C_{15} & C_{25} & C_{35} & C_{45} & C_{55} & C_{56} \\ C_{16} & C_{26} & C_{36} & C_{46} & C_{56} & C_{66} \end{bmatrix} \begin{bmatrix} \epsilon_{11}^{\text{mech}} \\ \epsilon_{22}^{\text{mech}} \\ \epsilon_{33}^{\text{mech}} \\ \epsilon_{12}^{\text{mech}} \\ \epsilon_{23}^{\text{mech}} \\ \epsilon_{13}^{\text{mech}} \end{bmatrix} ,$$

where the stress and strain components are with respect to principle material directions. The thermal strains are defined in a similar manner,

$$\epsilon = \epsilon^{\text{mech}} + \epsilon^{\text{th}}, \epsilon^{\text{th}} = [\epsilon_{11}^{\text{th}}(\theta)\, \epsilon_{22}^{\text{th}}(\theta)\, \epsilon_{33}^{\text{th}}(\theta)\, \epsilon_{12}^{\text{th}}(\theta)\, \epsilon_{23}^{\text{th}}(\theta)\, \epsilon_{13}^{\text{th}}(\theta)]^{\text{T}} .$$

In a finite strain situation, the anisotropic model is formulated in a hypoelastic manner with a constitutive equation of

$$\dot{\sigma}_{ij} = C_{ijkl} \left(D_{kl} - D_{kl}^{\text{th}} \right) ,$$

where D_{kl} and D_{kl}^{th} are the total and thermal strain rates, respectively, and the components of the fourth order stiffness tensor C_{ijkl} are related to the contracted notation by

$$[\mathbb{C}] = \begin{bmatrix} C_{1111} & C_{1122} & C_{1133} & C_{1112} & C_{1123} & C_{1113} \\ C_{1122} & C_{2222} & C_{2233} & C_{2212} & C_{2223} & C_{2213} \\ C_{1133} & C_{2233} & C_{3333} & C_{3312} & C_{3323} & C_{3313} \\ C_{1112} & C_{2212} & C_{3312} & C_{1212} & C_{1223} & C_{1213} \\ C_{1123} & C_{2223} & C_{3323} & C_{1223} & C_{2323} & C_{2313} \\ C_{1113} & C_{2213} & C_{3313} & C_{1213} & C_{2313} & C_{1313} \end{bmatrix} .$$

18.7 J_2 Plasticity

```
BEGIN PARAMETERS FOR MODEL J2_PLASTICITY
  #
  # Elastic constants
  #
  YOUNGS MODULUS = <real> E
  POISSONS RATIO = <real> ν
  SHEAR MODULUS  = <real> G
  BULK MODULUS   = <real> K
  LAMBDA         = <real> λ
  TWO MU         = <real> 2μ
  #
  # Yield surface parameters
  #
  YIELD STRESS = <real> σ_y
  A            = <real> a (1.0)
  BETA         = <real> β (1.0)
  #
  # Hardening model
  #
  HARDENING MODEL = LINEAR | POWER_LAW | VOCE | USER_DEFINED |
    FLOW_STRESS | DECOUPLED_FLOW_STRESS | CUBIC_HERMITE_SPLINE |
    JOHNSON_COOK | POWER_LAW_BREAKDOWN
  #
  # Linear hardening
  #
  HARDENING MODULUS = <real> H'
  #
  # Power-law hardening
  #
  HARDENING CONSTANT = <real> A
  HARDENING EXPONENT = <real> n (0.5)
  LUDERS STRAIN      = <real> ε_L (0.0)
  #
  # Voce hardening
  #
  HARDENING MODULUS       = <real> A
  EXPONENTIAL COEFFICIENT = <real> n
  #
  # Johnson-Cook hardening
  #
  HARDENING FUNCTION = <string>hardening_function_name
  RATE CONSTANT      = <real> C
  REFERENCE RATE     = <real> ε̇_0
  #
  # Power law breakdown hardening
  #
```

```
HARDENING FUNCTION = <string>hardening_function_name
RATE COEFFICIENT   = <real> g
RATE EXPONENT      = <real> m
#
# User defined hardening
#
HARDENING FUNCTION = <string>hardening_function_name
#
# Spline based hardening curve
#
CUBIC SPLINE TYPE  = <string>
CARDINAL PARAMETER = <real> val
KNOT EQPS          = <real_list> vals
KNOT STRESS        = <real_list> vals
#
#
# Following Commands Pertain to Flow_Stress Hardening Model
#
#    -  Isotropic Hardening model
#
ISOTROPIC HARDENING MODEL = LINEAR | POWER_LAW | VOCE |
                            USER_DEFINED
#
# Specifications for Linear, Power-law, and Voce same as above
#
# User defined hardening
#
ISOTROPIC HARDENING FUNCTION = <string>iso_hardening_fun_name
#
#     - Rate dependence
#
RATE MULTIPLIER = JOHNSON_COOK | POWER_LAW_BREAKDOWN |
   RATE_INDEPENDENT (RATE_INDEPENDENT)
#
# Specifications for Johnson-Cook, Power-law-breakdown
#     same as before EXCEPT no need to specify a
#     hardening function
#
#     - Temperature dependence
#
TEMPERATURE MULTIPLIER = JOHNSON_COOK | USER_DEFINED |
   TEMPERATURE_INDEPENDENT (TEMPERATURE_INDEPENDENT)
#
#  Johnson-Cook temperature dependence
#
MELTING TEMPERATURE   = <real> θ_melt
REFERENCE TEMPERATURE = <real> θ_ref
```

```
 TEMPERATURE EXPONENT  = <real> M
 #
 #  User-defined temperature dependence
 TEMPERATURE MULTIPLIER FUNCTION = <string>temp_mult_function_name
#
 #
 # Following Commands Pertain to Decoupled_Flow_Stress Hardening Model
 #
 #    -  Isotropic Hardening model
 #
 ISOTROPIC HARDENING MODEL = LINEAR | POWER_LAW | VOCE | USER_DEFINED
 #
 # Specifications for Linear, Power-law, and Voce same as above
 #
 # User defined hardening
 #
 ISOTROPIC HARDENING FUNCTION = <string>isotropic_hardening_function_name
 #
 #     - Rate dependence
 #
 YIELD RATE MULTIPLIER = JOHNSON_COOK | POWER_LAW_BREAKDOWN |
             RATE_INDEPENDENT (RATE_INDEPENDENT)
 #
 # Specifications for Johnson-Cook, Power-law-breakdown same as before
 #     EXCEPT no need to specify a hardening function
 #     AND should be preceded by YIELD
 #
 #     As an example for Johnson-Cook yield rate dependence,
 #
 YIELD RATE CONSTANT  = <real> C^y
 YIELD REFERENCE RATE = <real> ε̇_0^y
 #
 HARDENING_RATE MULTIPLIER = JOHNSON_COOK | POWER_LAW_BREAKDOWN |
             RATE_INDEPENDENT (RATE_INDEPENDENT)
 #
 #     Syntax same as for yield parameters but with a HARDENING prefix
 #
 #     - Temperature dependence
 #
 YIELD TEMPERATURE MULTIPLIER = JOHNSON_COOK | USER_DEFINED |
          TEMPERATURE_INDEPENDENT (TEMPERATURE_INDEPENDENT)
 #
 #  Johnson-Cook temperature dependence
 #
 YIELD MELTING TEMPERATURE   = <real> θ_melt^y
 YIELD REFERENCE TEMPERATURE = <real> θ_ref^y
 YIELD TEMPERATURE EXPONENT  = <real> M^y
```

```
  #
  #  User-defined temperature dependence
  YIELD TEMPERATURE MULTIPLIER FUNCTION = <string>yield_temp_mult_fun_name
  #
  HARDENING TEMPERATURE MULTIPLIER = JOHNSON_COOK | USER_DEFINED |
            TEMPERATURE_INDEPENDENT (TEMPERATURE_INDEPENDENT)
  #
  #   Syntax for hardening constants same as for yield but
  #             with HARDENING prefix
#
END [PARAMETERS FOR MODEL J2_PLASTICITY]
```

The J_2 plasticity model is a generic implementation of a von Mises yield surface with kinematic and isotropic hardening features. Unlike similar models (*e.g.* Elastic-Plastic, Elastic-Plastic Power Law) more general, in-development isotropic hardening models are implemented that enable greater flexibility in definition and the possibilities of limited rate and/or temperature dependence. Note, although some testing exists, these feature remain "in-development".

As is common to other plasticity models in Lamé, the J_2 plasticity model is an isotropic, hypoelastic formulation. As such, the total rate of deformation is additively decomposed into an elastic and plastic part such that

$$D_{ij} = D^{\mathrm{e}}_{ij} + D^{\mathrm{p}}_{ij}. \tag{18.18}$$

The objective stress rate, depending only on the elastic deformation, may then be written as,

$$\overset{\circ}{\sigma}_{ij} = \mathbb{C}_{ijkl} D^{\mathrm{e}}_{kl}, \tag{18.19}$$

where $\mathbb{C}_{ijkl}$ is the fourth-order elastic, isotropic stiffness tensor.

The yield surface for the J_2 plasticity model, f, may be written,

$$f\left(\sigma_{ij}, \alpha_{ij}, \bar{\varepsilon}^p, \dot{\bar{\varepsilon}}^p, \theta\right) = \phi\left(\sigma_{ij}, \alpha_{ij}\right) - \bar{\sigma}\left(\bar{\varepsilon}^p, \dot{\bar{\varepsilon}}^p, \theta\right), \tag{18.20}$$

in which α_{ij}, $\bar{\varepsilon}^p$, $\dot{\bar{\varepsilon}}^p$, and θ are the kinematic backstress, equivalent plastic strain, equivalent plastic strain rate, and absolute temperature, respectively, while ϕ and $\bar{\sigma}$ are generically the effective stress and flow stress. Broadly speaking, the effective stress encapsulates directional and kinematic effects while the flow stress gives the size of the current yield surface. It should also be noted that writing the yield surface in this way splits the dependence on the state variables between the effective stress and flow stress functions.

As the current model is for J_2 plasticity, the effective stress is given as,

$$\phi^2\left(\sigma_{ij}, \alpha_{ij}\right) = \frac{3}{2}\left(s_{ij} - \alpha_{ij}\right)\left(s_{ij} - \alpha_{ij}\right), \tag{18.21}$$

with s_{ij} being the deviatoric stress defined as $s_{ij} = \sigma_{ij} - (1/3)\sigma_{kk}\delta_{ij}$. For the flow stress, a general representation of the form,

$$\bar{\sigma}\left(\bar{\varepsilon}^p, \dot{\bar{\varepsilon}}^p, \theta\right) = \sigma_y \hat{\sigma}_{\mathrm{y}}\left(\dot{\bar{\varepsilon}}^p\right) \breve{\sigma}_{\mathrm{y}}(\theta) + K\left(\bar{\varepsilon}^p\right) \hat{\sigma}_{\mathrm{h}}\left(\dot{\bar{\varepsilon}}^p\right) \breve{\sigma}_{\mathrm{h}}(\theta), \tag{18.22}$$

is allowed. In this fashion, the effects of isotropic hardening ($K\left(\bar{\varepsilon}^p\right)$), rate ($\hat{\sigma}_{\mathrm{y,h}}$), and temperature ($\breve{\sigma}_{\mathrm{y,h}}$) are decomposed although separate temperature and rate dependencies may be specified for yield (subscript "y") and hardening ("h"). Such an assumption is an extension of the multiplicative decomposition of the Johnson-Cook model [9, 10]. It should be noted that not all such effects need to be included and the default assumption of the hardening classes is that the response is rate and temperature independent. The following section on plastic hardening will go into more detail on possible choices for functional representations.

An associated flow rule is utilized such that the plastic rate of deformation is normal to the yield surface and is given by,

$$\dot{D}^{\mathrm{p}}_{ij} = \dot{\gamma}\frac{\partial \phi}{\partial \sigma_{ij}}, \tag{18.23}$$

where $\dot{\gamma}$ is the consistency multiplier enforcing $f = 0$ during plastic deformation. Given the form of f, it can also be shown that $\dot{\gamma} = \dot{\bar{\varepsilon}}^p$.

In the command blocks that define the J_2 plasticity model:

- See the User's Guide chapter on Material Models for more information on elastic constants input.
- The reference nominal yield stress, $\bar{\sigma}$, is defined with the `YIELD STRESS` command line.
- The beta parameter defines if hardening is isotropic. Consult the Sierra/SM User Manual chapter on Material Models for more information on the beta parameter.
- The type of hardening law is defined with the `HARDENING MODEL` command line, other hardening commands then define the specific shape of that hardening curve.
- The hardening modulus for a linear hardening model is defined with the `HARDENING MODULUS` command line.
- The hardening constant for a power law hardening model is defined with the `HARDENING CONSTANT` command line.
- The hardening exponent for a power law hardening model is defined with the `HARDENING EXPONENT` command line.
- The Lüders strain for a power law hardening model is defined with the `LUDERS STRAIN` command line.

- The hardening function for a user defined hardening model is defined with the `HARDENING FUNCTION` command line.
- The shape of the spline for the spline based hardening is defined by the `CUBIC SPLINE TYPE`, `CARDINAL PARAMETER`, `KNOT EQPS`, and `KNOT STRESS` command lines.
- The isotropic hardening model for the flow stress hardening model is defined with the `ISOTROPIC HARDENING MODEL` command line.
- The function name of a user-defined isotropic hardening model is defined via the `ISOTROPIC HARDENING FUNCTION` command line.
- The optional rate multiplier for the flow stress hardening model is defined with the `RATE MULTIPLIER` command line.
- The optional temperature multiplier for the flow stress hardening model is defined via the `TEMPERATURE MULTIPLIER` command line.
- The function name of a user-defined temperature multiplier is defined with the `TEMPERATURE MULTIPLIER FUNCTION` command line.
- For a Johnson-Cook temperature multiplier, the melting temperature, θ_{melt}, is defined via the `MELTING TEMPERATURE` command line.
- For a Johnson-Cook temperature multiplier, the reference temperature, θ_{ref}, is defined via the `REFERENCE TEMPERATURE` command line.
- For a Johnson-Cook temperature multiplier, the temperature exponent, M, is defined via the `TEMPERATURE EXPONENT` command line.
- The optional rate multiplier for the yield stress for the decoupled flow stress hardening model is defined with the `YIELD RATE MULTIPLIER` command line.
- The optional rate multiplier for the hardening for the decoupled flow stress hardening model is defined with the `HARDENING RATE MULTIPLIER` command line.
- The optional temperature multiplier for the yield stress for the decoupled flow stress hardening model is defined with the `YIELD TEMPERATURE MULTIPLIER` command line.
- The optional temperature multiplier for the hardening for the decoupled flow stress hardening model is defined via the `HARDENING TEMPERATURE MULTIPLIER` command line.

Output variables available for this model are listed in Table 18.2.

Table 18.2: State Variables for J2 PLASTICITY Model (Section 18.7)

Name	Description
EQPS	equivalent plastic strain, $\bar{\varepsilon}^p$
EQDOT	equivalent plastic strain rate, $\dot{\bar{\varepsilon}}^p$
SEFF	effective stress, ϕ

18.8 Karafillis Boyce Plasticity Model

```
BEGIN PARAMETERS FOR MODEL KARAFILLIS_BOYCE_PLASTICITY
  #
  # Elastic constants
  #
  YOUNGS MODULUS = <real> E
  POISSONS RATIO = <real> ν
  SHEAR MODULUS  = <real> G
  BULK MODULUS   = <real> K
  LAMBDA         = <real> λ
  TWO MU         = <real> 2μ
  #
  # Yield surface parameters
  #
  YIELD STRESS = <real> σ_y
  A            = <real> a (4.0)
  C            = <real> c (0.0)
  COEFF        = <real> C (2.0/3.0)
  ALPHA 1      = <real>  c_1 (1.0)
  ALPHA 2      = <real>  c_2 (1.0)
  GAMMA 1      = <real>  c_1 (1.5)
  GAMMA 2      = <real>  c_2 (1.5)
  GAMMA 3      = <real>  c_3 (1.5)
  #
  # Hardening model
  #
  HARDENING MODEL = LINEAR | POWER_LAW | USER_DEFINED |
    CUBIC_HERMITE_SPLINE
  #
  # Linear hardening
  #
  HARDENING MODULUS = <real> H'
  #
  # Power law hardening
  #
  HARDENING CONSTANT = <real> A
  HARDENING EXPONENT = <real> n (0.5)
  #
  # User defined hardening
  #
  HARDENING FUNCTION = <string>hardening_function_name
  #
  # Spline based hardening curve
  #
  CUBIC SPLINE TYPE  = <string>
  CARDINAL PARAMETER = <real> val
  KNOT EQPS          = <real_list> vals
```

```
  KNOT STRESS        = <real_list> vals
  #
  # Material coordinates system definition
  #
  COORDINATE SYSTEM             = <string> coordinate_system_name
  DIRECTION FOR ROTATION        = <real> 1|2|3
  ALPHA                         = <real> α1 (degrees)
  SECOND DIRECTION FOR ROTATION = <real> 1|2|3
  SECOND ALPHA                  = <real> α2 (degrees)
END [PARAMETERS FOR MODEL KARAFILLIS_BOYCE_PLASTICITY]
```

The Karafillis and Boyce model [11] is an anisotropic plasticity model. The stress is transformed, based on the anisotropy, and the transformed stress is used in the yield function. The transformed stress, using Voigt notation in the material coordinate system, is given by

$$\mathbf{s}' = \mathbf{C} : \boldsymbol{\sigma}$$

$$[\mathbf{C}] = C \begin{bmatrix} 1 & \beta_1 & \beta_2 & 0 & 0 & 0 \\ \beta_1 & \alpha_1 & \beta_3 & 0 & 0 & 0 \\ \beta_2 & \beta_3 & \alpha_2 & 0 & 0 & 0 \\ 0 & 0 & 0 & \gamma_1 & 0 & 0 \\ 0 & 0 & 0 & 0 & \gamma_2 & 0 \\ 0 & 0 & 0 & 0 & 0 & \gamma_3 \end{bmatrix}$$

where the terms β_k are

$$\beta_1 = \frac{\alpha_2 - \alpha_1 - 1}{2}$$

$$\beta_2 = \frac{\alpha_1 - \alpha_2 - 1}{2}$$

$$\beta_3 = \frac{1 - \alpha_1 - \alpha_2}{2}$$

The response is isotropic if $\alpha_1 = \alpha_2 = 1$, $\gamma_1 = \gamma_2 = \gamma_3 = 1.5$, and $C = 2/3$.

The principal stresses of the transformed stress, $\mathbf{s}'$, are used in the yield function

$$\phi = \{(1-c)\,\phi_1 + c\phi_2\}^{1/a}$$

$$\phi_1 = \frac{1}{2}\left(|s_1 - s_2|^a + |s_2 - s_3|^a + |s_3 - s_1|^a\right)$$

$$\phi_2 = \frac{3^a}{2^a + 2}\left(|s_1|^a + |s_2|^a + |s_3|^a\right)$$

The exponent, a, is similar to the exponent in the Hosford plasticity model and the constant, c (not to be confused with C above), is a parameter that provides a mixture of two yield functions.

In the command blocks that define the Hosford plasticity model:

- Consult the Sierra/SM User's Guide chapter on Material Models for more information on elastic constants input.
- The reference nominal yield stress, $\bar{\sigma}$, is defined with the `YIELD STRESS` command line.
- The exponent for the yield surface description, a, is defined with the `A` command line.
- The coefficient C in the stress transformation is defined with the `COEFF` command line.
- The term α_1 in the stress transformation is defined with the `ALPHA 1` command line.
- The term α_2 in the stress transformation is defined with the `ALPHA 2` command line.
- The term γ_1 in the stress transformation is defined with the `GAMMA 1` command line.
- The term γ_2 in the stress transformation is defined with the `GAMMA 2` command line.
- The term γ_3 in the stress transformation is defined with the `GAMMA 3` command line.
- The type of hardening law is defined with the `HARDENING MODEL` command line, other hardening commands then define the specific shape of that hardening curve.
- The hardening modulus for a linear hardening model is defined with the `HARDENING MODULUS` command line.
- The hardening constant for a power law hardening model is defined with the `HARDENING CONSTANT` command line.
- The hardening exponent for a power law hardening model is defined with the `HARDENING EXPONENT` command line.
- The hardening function for a user defined hardening model is defined with the `HARDENING FUNCTION` command line.
- The shape of the spline for the spline based hardening is defined by the `CUBIC SPLINE TYPE`, `CARDINAL PARAMETER`, `KNOT EQPS`, and `KNOT STRESS` command lines.

Output variables available for this model are listed in Table 18.3.

Table 18.3: State Variables for KARAFILLIS_BOYCE_PLASTICITY Model

Index	Name	Variable Description
1	EQPS	equivalent plastic strain, $\bar{\varepsilon}^p$

18.9 Cazacu Plasticity Model

```
BEGIN PARAMETERS FOR MODEL CAZACU_PLASTICITY
  #
  # Elastic constants
  #
  YOUNGS MODULUS = <real> E
  POISSONS RATIO = <real> ν
  SHEAR MODULUS  = <real> G
  BULK MODULUS   = <real> K
  LAMBDA         = <real> λ
  TWO MU         = <real> 2μ
  #
  # Yield surface parameters
  #
  YIELD STRESS = <real> σ_y
  A            = <real> a (1.0)
  #
  # tension/compression assymetry
  #
  RATIO        = <real> r
  #
  # Hardening model
  #
  HARDENING MODEL = LINEAR | POWER_LAW | VOCE | USER_DEFINED |
    FLOW_STRESS | DECOUPLED_FLOW_STRESS | CUBIC_HERMITE_SPLINE |
    JOHNSON_COOK | POWER_LAW_BREAKDOWN
  #
  # Linear hardening
  #
  HARDENING MODULUS = <real> H'
  #
  # Power-law hardening
  #
  HARDENING CONSTANT = <real> A
  HARDENING EXPONENT = <real> n (0.5)
  LUDERS STRAIN      = <real> ε_L (0.0)
  #
  # Voce hardening
  #
  HARDENING MODULUS       = <real> A
  EXPONENTIAL COEFFICIENT = <real> n
  #
  # Johnson-Cook hardening
  #
  HARDENING FUNCTION = <string>hardening_function_name
  RATE CONSTANT      = <real> C
  REFERENCE RATE     = <real> ε̇_0
```

```
#
# Power law breakdown hardening
#
HARDENING FUNCTION = <string>hardening_function_name
RATE COEFFICIENT   = <real> g
RATE EXPONENT      = <real> m
#
# User defined hardening
#
HARDENING FUNCTION = <string>hardening_function_name
#
# Spline based hardening curve
#
CUBIC SPLINE TYPE  = <string>
CARDINAL PARAMETER = <real> val
KNOT EQPS          = <real_list> vals
KNOT STRESS        = <real_list> vals
#
#
# Following Commands Pertain to Flow_Stress Hardening Model
#
#    -  Isotropic Hardening model
#
ISOTROPIC HARDENING MODEL = LINEAR | POWER_LAW | VOCE |
                            USER_DEFINED
#
# Specifications for Linear, Power-law, and Voce same as above
#
# User defined hardening
#
ISOTROPIC HARDENING FUNCTION = <string>iso_hardening_fun_name
#
#     - Rate dependence
#
RATE MULTIPLIER = JOHNSON_COOK | POWER_LAW_BREAKDOWN |
   RATE_INDEPENDENT (RATE_INDEPENDENT)
#
# Specifications for Johnson-Cook, Power-law-breakdown
#     same as before EXCEPT no need to specify a
#     hardening function
#
#     - Temperature dependence
#
TEMPERATURE MULTIPLIER = JOHNSON_COOK | USER_DEFINED |
   TEMPERATURE_INDEPENDENT (TEMPERATURE_INDEPENDENT)
#
#  Johnson-Cook temperature dependence
```

```
 #
 MELTING TEMPERATURE   = <real> θ_melt
 REFERENCE TEMPERATURE = <real> θ_ref
 TEMPERATURE EXPONENT  = <real> M
 #
 #  User-defined temperature dependence
 TEMPERATURE MULTIPLIER FUNCTION = <string>temp_mult_function_name
#
 #
 # Following Commands Pertain to Decoupled_Flow_Stress Hardening Model
 #
 #    -  Isotropic Hardening model
 #
 ISOTROPIC HARDENING MODEL = LINEAR | POWER_LAW | VOCE | USER_DEFINED
 #
 # Specifications for Linear, Power-law, and Voce same as above
 #
 # User defined hardening
 #
 ISOTROPIC HARDENING FUNCTION = <string>isotropic_hardening_function_name
 #
 #     - Rate dependence
 #
 YIELD RATE MULTIPLIER = JOHNSON_COOK | POWER_LAW_BREAKDOWN |
             RATE_INDEPENDENT (RATE_INDEPENDENT)
 #
 # Specifications for Johnson-Cook, Power-law-breakdown same as before
 #     EXCEPT no need to specify a hardening function
 #     AND should be preceded by YIELD
 #
 #     As an example for Johnson-Cook yield rate dependence,
 #
 YIELD RATE CONSTANT  = <real> C^y
 YIELD REFERENCE RATE = <real> ε̇_0^y
 #
 HARDENING_RATE MULTIPLIER = JOHNSON_COOK | POWER_LAW_BREAKDOWN |
             RATE_INDEPENDENT (RATE_INDEPENDENT)
 #
 #     Syntax same as for yield parameters but with a HARDENING prefix
 #
 #     - Temperature dependence
 #
 YIELD TEMPERATURE MULTIPLIER = JOHNSON_COOK | USER_DEFINED |
           TEMPERATURE_INDEPENDENT (TEMPERATURE_INDEPENDENT)
 #
 #  Johnson-Cook temperature dependence
 #
```

```
  YIELD MELTING TEMPERATURE   = <real> θ^y_melt
  YIELD REFERENCE TEMPERATURE = <real> θ^y_ref
  YIELD TEMPERATURE EXPONENT  = <real> M^y
  #
  #  User-defined temperature dependence
  YIELD TEMPERATURE MULTIPLIER FUNCTION = <string>yield_temp_mult_fun_name
  #
  HARDENING TEMPERATURE MULTIPLIER = JOHNSON_COOK | USER_DEFINED |
            TEMPERATURE_INDEPENDENT (TEMPERATURE_INDEPENDENT)
  #
  #   Syntax for hardening constants same as for yield but
  #            with HARDENING prefix
#
END [PARAMETERS FOR MODEL CAZACU_PLASTICITY]
```

The Cazacu plasticity model is an isotropic plasticity model that accounts for tension/compression asymmetry in yield.. This model is used primarily for modeling the plastic deformation of HCP metals which can show significant tension/compression asymmetry. As is common to other plasticity models in Lamé, the Cazacu plasticity model uses a hypoelastic formulation. As such, the total rate of deformation is additively decomposed into an elastic and plastic part such that

$$D_{ij} = D^{\mathrm{e}}_{ij} + D^{\mathrm{p}}_{ij}. \tag{18.24}$$

The objective stress rate, depending only on the elastic deformation, may then be written as,

$$\overset{\circ}{\sigma}_{ij} = \mathbb{C}_{ijkl} D^{\mathrm{e}}_{kl}, \tag{18.25}$$

where $\mathbb{C}_{ijkl}$ is the fourth-order elastic, isotropic stiffness tensor.

The yield surface for the Cazacu plasticity model, f, may be written,

$$f\left(\sigma_{ij}, \bar{\varepsilon}^p, \dot{\bar{\varepsilon}}^p\right) = \phi\left(\sigma_{ij}\right) - \bar{\sigma}\left(\bar{\varepsilon}^p, \dot{\bar{\varepsilon}}^p\right), \tag{18.26}$$

in which $\bar{\varepsilon}^p$ and $\dot{\bar{\varepsilon}}^p$ are the equivalent plastic strain and equivalent plastic strain rate respectively, while ϕ and $\bar{\sigma}$ are generically the effective stress and flow stress. Broadly speaking, the flow stress gives the size of the current yield surface. For the Cazacu plasticity model, the effective stress is given as,

$$\phi\left(\sigma_{ij}\right) = \left\{ h(a,k)\left[\left(|s_1| - k s_1\right)^a + \left(|s_2| - k s_2\right)^a + \left(|s_3| - k s_3\right)^a \right] \right\}^{1/a} \tag{18.27}$$

with s_i being the principal deviatoric stresses, k and a are model parameters describing asymmetry in tension/compression along with the shape of the yield surface. The function $h(a,k)$ is a normalizing factor that is set so that the effective stress for a uniaxial stress state is σ

$$h = \frac{3^a}{((2(1-k))^a + 2(1+k)^a)} \tag{18.28}$$

The parameter k is calculated from the tension/compression asymmetry. The ratio of the yield stress in tension to the yield stress in compression is

$$r = \sigma_y^T / \sigma_y^C \tag{18.29}$$

The value of k is

$$k = \frac{1 - h(r)}{1 + h(r)} \quad ; \quad h(r) = \left[\frac{2^a - 2r^a}{(2r)^a - 2} \right]^{1/a} \tag{18.30}$$

An associated flow rule is utilized such that the plastic rate of deformation is normal to the yield surface and is given by,

$$\dot{D}_{ij}^{\mathrm{p}} = \dot{\gamma} \frac{\partial \phi}{\partial \sigma_{ij}}, \tag{18.31}$$

where $\dot{\gamma}$ is the consistency multiplier enforcing $f = 0$ during plastic deformation. Given the form of f, it can also be shown that $\dot{\gamma} = \dot{\bar{\varepsilon}}^p$, i.e. the consistency parameter is equal to the rate of the equivalent plastic strain.

In the command blocks that define the Cazacu plasticity model:

- See the User's Guide chapter on Material Models for more information on elastic constants input.
- The reference nominal yield stress, $\bar{\sigma}$, is defined with the `YIELD STRESS` command line.
- The type of hardening law is defined with the `HARDENING MODEL` command line, other hardening commands then define the specific shape of that hardening curve.
- The hardening modulus for a linear hardening model is defined with the `HARDENING MODULUS` command line.
- The hardening constant for a power law hardening model is defined with the `HARDENING CONSTANT` command line.
- The hardening exponent for a power law hardening model is defined with the `HARDENING EXPONENT` command line.
- The Lüders strain for a power law hardening model is defined with the `LUDERS STRAIN` command line.
- The hardening function for a user defined hardening model is defined with the `HARDENING FUNCTION` command line.

- The shape of the spline for the spline based hardening is defined by the `CUBIC SPLINE TYPE`, `CARDINAL PARAMETER`, `KNOT EQPS`, and `KNOT STRESS` command lines.
- The isotropic hardening model for the flow stress hardening model is defined with the `ISOTROPIC HARDENING MODEL` command line.
- The function name of a user-defined isotropic hardening model is defined via the `ISOTROPIC HARDENING FUNCTION` command line.
- The optional rate multiplier for the flow stress hardening model is defined with the `RATE MULTIPLIER` command line.
- The optional temperature multiplier for the flow stress hardening model is defined via the `TEMPERATURE MULTIPLIER` command line.
- The function name of a user-defined temperature multiplier is defined with the `TEMPERATURE MULTIPLIER FUNCTION` command line.
- For a Johnson-Cook temperature multiplier, the melting temperature, θ_{melt}, is defined via the `MELTING TEMPERATURE` command line.
- For a Johnson-Cook temperature multiplier, the reference temperature, θ_{ref}, is defined via the `REFERENCE TEMPERATURE` command line.
- For a Johnson-Cook temperature multiplier, the temperature exponent, M, is defined via the `TEMPERATURE EXPONENT` command line.
- The optional rate multiplier for the yield stress for the decoupled flow stress hardening model is defined with the `YIELD RATE MULTIPLIER` command line.
- The optional rate multiplier for the hardening for the decoupled flow stress hardening model is defined with the `HARDENING RATE MULTIPLIER` command line.
- The optional temperature multiplier for the yield stress for the decoupled flow stress hardening model is defined with the `YIELD TEMPERATURE MULTIPLIER` command line.
- The optional temperature multiplier for the hardening for the decoupled flow stress hardening model is defined via the `HARDENING TEMPERATURE MULTIPLIER` command line.

Output variables available for this model are listed in Table 18.4.

Table 18.4: State Variables for CAZACU PLASTICITY Model (Section 18.9)

Name	Description
EQPS	equivalent plastic strain, $\bar{\varepsilon}^p$
EQDOT	equivalent plastic strain rate, $\dot{\bar{\varepsilon}}^p$
SEFF	effective stress, ϕ

18.10 Cazacu Orthotropic Plasticity Model

```
BEGIN PARAMETERS FOR MODEL CAZACU_ORTHOTROPIC_PLASTICITY
  #
  # Elastic constants
  #
  YOUNGS MODULUS = <real> E
  POISSONS RATIO = <real> ν
  SHEAR MODULUS  = <real> G
  BULK MODULUS   = <real> K
  LAMBDA         = <real> λ
  TWO MU         = <real> 2μ
  #
  # Yield surface parameters
  #
  YIELD STRESS = <real> σ_y
  A            = <real> a (4.0)
  #
  # tension/compression asymmetry
  #
  KP           = <real> k'
  KPP          = <real> k''
  #
  # orthotroppic parameters
  #
  CP11         = <real> c'_11
  CP22         = <real> c'_22
  CP33         = <real> c'_33
  CP12         = <real> c'_12
  CP23         = <real> c'_23
  CP31         = <real> c'_31
  CP44         = <real> c'_44
  CP55         = <real> c'_55
  CP66         = <real> c'_66
  CPP11        = <real> c''_11
  CPP22        = <real> c''_22
  CPP33        = <real> c''_33
  CPP12        = <real> c''_12
  CPP23        = <real> c''_23
  CPP31        = <real> c''_31
  CPP44        = <real> c''_44
  CPP55        = <real> c''_55
  CPP66        = <real> c''_66
  #
  # Hardening model
  #
  HARDENING MODEL = LINEAR | POWER_LAW | VOCE | USER_DEFINED |
    FLOW_STRESS | DECOUPLED_FLOW_STRESS | CUBIC_HERMITE_SPLINE |
```

```
  JOHNSON_COOK | POWER_LAW_BREAKDOWN
#
# Linear hardening
#
HARDENING MODULUS = <real> H'
#
# Power-law hardening
#
HARDENING CONSTANT = <real> A
HARDENING EXPONENT = <real> n (0.5)
LUDERS STRAIN      = <real> ε_L (0.0)
#
# Voce hardening
#
HARDENING MODULUS       = <real> A
EXPONENTIAL COEFFICIENT = <real> n
#
# Johnson-Cook hardening
#
HARDENING FUNCTION = <string>hardening_function_name
RATE CONSTANT      = <real> C
REFERENCE RATE     = <real> ε̇_0
#
# Power law breakdown hardening
#
HARDENING FUNCTION = <string>hardening_function_name
RATE COEFFICIENT   = <real> g
RATE EXPONENT      = <real> m
#
# User defined hardening
#
HARDENING FUNCTION = <string>hardening_function_name
#
# Spline based hardening curve
#
CUBIC SPLINE TYPE  = <string>
CARDINAL PARAMETER = <real> val
KNOT EQPS          = <real_list> vals
KNOT STRESS        = <real_list> vals
#
#
# Following Commands Pertain to Flow_Stress Hardening Model
#
#    -  Isotropic Hardening model
#
ISOTROPIC HARDENING MODEL = LINEAR | POWER_LAW | VOCE |
                            USER_DEFINED
```

```
 #
 # Specifications for Linear, Power-law, and Voce same as above
 #
 # User defined hardening
 #
 ISOTROPIC HARDENING FUNCTION = <string>iso_hardening_fun_name
 #
 #     - Rate dependence
 #
 RATE MULTIPLIER = JOHNSON_COOK | POWER_LAW_BREAKDOWN |
    RATE_INDEPENDENT (RATE_INDEPENDENT)
 #
 # Specifications for Johnson-Cook, Power-law-breakdown
 #     same as before EXCEPT no need to specify a
 #     hardening function
 #
 #     - Temperature dependence
 #
 TEMPERATURE MULTIPLIER = JOHNSON_COOK | USER_DEFINED |
    TEMPERATURE_INDEPENDENT (TEMPERATURE_INDEPENDENT)
 #
 #  Johnson-Cook temperature dependence
 #
 MELTING TEMPERATURE   = <real> θ_melt
 REFERENCE TEMPERATURE = <real> θ_ref
 TEMPERATURE EXPONENT  = <real> M
 #
 #  User-defined temperature dependence
 TEMPERATURE MULTIPLIER FUNCTION = <string>temp_mult_function_name
#
 #
 # Following Commands Pertain to Decoupled_Flow_Stress Hardening Model
 #
 #    -  Isotropic Hardening model
 #
 ISOTROPIC HARDENING MODEL = LINEAR | POWER_LAW | VOCE | USER_DEFINED
 #
 # Specifications for Linear, Power-law, and Voce same as above
 #
 # User defined hardening
 #
 ISOTROPIC HARDENING FUNCTION = <string>isotropic_hardening_function_name
 #
 #     - Rate dependence
 #
 YIELD RATE MULTIPLIER = JOHNSON_COOK | POWER_LAW_BREAKDOWN |
             RATE_INDEPENDENT (RATE_INDEPENDENT)
```

```
  #
  # Specifications for Johnson-Cook, Power-law-breakdown same as before
  #     EXCEPT no need to specify a hardening function
  #     AND should be preceded by YIELD
  #
  #     As an example for Johnson-Cook yield rate dependence,
  #
  YIELD RATE CONSTANT  = <real> C^y
  YIELD REFERENCE RATE = <real> ε̇_0^y
  #
  HARDENING_RATE MULTIPLIER = JOHNSON_COOK | POWER_LAW_BREAKDOWN |
              RATE_INDEPENDENT (RATE_INDEPENDENT)
  #
  #     Syntax same as for yield parameters but with a HARDENING prefix
  #
  #     - Temperature dependence
  #
  YIELD TEMPERATURE MULTIPLIER = JOHNSON_COOK | USER_DEFINED |
            TEMPERATURE_INDEPENDENT (TEMPERATURE_INDEPENDENT)
  #
  #  Johnson-Cook temperature dependence
  #
  YIELD MELTING TEMPERATURE   = <real> θ_melt^y
  YIELD REFERENCE TEMPERATURE = <real> θ_ref^y
  YIELD TEMPERATURE EXPONENT  = <real> M^y
  #
  #  User-defined temperature dependence
  YIELD TEMPERATURE MULTIPLIER FUNCTION = <string>yield_temp_mult_fun_name
  #
  HARDENING TEMPERATURE MULTIPLIER = JOHNSON_COOK | USER_DEFINED |
            TEMPERATURE_INDEPENDENT (TEMPERATURE_INDEPENDENT)
  #
  #   Syntax for hardening constants same as for yield but
  #            with HARDENING prefix
#
END [PARAMETERS FOR MODEL CAZACU_ORTHOTROPIC_PLASTICITY]
```

The orthotropic Cazacu plasticity model is an extension of the tension/compression asymmetry model of Cazacu to account for orthotropic response. As is common to other plasticity models in Lamé, the Cazacu plasticity model uses a hypoelastic formulation. As such, the total rate of deformation is additively decomposed into an elastic and plastic part such that

$$D_{ij} = D^{\mathrm{e}}_{ij} + D^{\mathrm{p}}_{ij}. \tag{18.32}$$

The objective stress rate, depending only on the elastic deformation, may then be written as,

$$\overset{\circ}{\sigma}_{ij} = \mathbb{C}_{ijkl} D^{\mathrm{e}}_{kl}, \tag{18.33}$$

where $\mathbb{C}_{ijkl}$ is the fourth-order elastic, isotropic stiffness tensor.

The yield surface for the orthotropic Cazacu plasticity model, f, may be written,

$$f\left(\sigma_{ij}, \bar{\varepsilon}^p, \dot{\bar{\varepsilon}}^p\right) = \phi\left(\sigma_{ij}\right) - \bar{\sigma}\left(\bar{\varepsilon}^p, \dot{\bar{\varepsilon}}^p\right), \tag{18.34}$$

in which $\bar{\varepsilon}^p$ and $\dot{\bar{\varepsilon}}^p$ are the equivalent plastic strain and equivalent plastic strain rate respectively, while ϕ and $\bar{\sigma}$ are generically the effective stress and flow stress. Broadly speaking, the flow stress gives the size of the current yield surface. For the orthotropic Cazacu plasticity model, the effective stress is given as,

$$\begin{aligned}\phi^2\left(\sigma_{ij}\right) = \Big\{ h(a,k',k'',c'_{ij},c''_{ij}) \Big[&\left(|s'_1| - k's'_1\right)^a + \left(|s'_2| - k's'_2\right)^a + \left(|s'_3| - k's'_3\right)^a \\ &+ \left(|s''_1| - k''s''_1\right)^a + \left(|s''_2| - k''s''_2\right)^a + \left(|s''_3| - k''s''_3\right)^a \Big] \Big\}^{1/a}\end{aligned} \tag{18.35}$$

with s'_i and s''_i being the principal transformed stresses, and k', k'' and a are model parameters describing the asymmetry in tension/compression along with the general shape of the yield surface. The transformed stresses, which account for the anisotropy, are given by

$$s'_{ij} = C'_{ijkl} s_{kl} \quad ; \quad s''_{ij} = C''_{ijkl} s_{kl} \tag{18.36}$$

In matrix notation in the material coordinate system, these transformations are

$$\begin{Bmatrix} s'_{11} \\ s'_{22} \\ s'_{33} \\ s'_{12} \\ s'_{23} \\ s'_{31} \end{Bmatrix} = \begin{bmatrix} c'_{11} & c'_{12} & c'_{31} & 0 & 0 & 0 \\ c'_{12} & c'_{22} & c'_{23} & 0 & 0 & 0 \\ c'_{31} & c'_{23} & c'_{33} & 0 & 0 & 0 \\ 0 & 0 & 0 & c'_{44} & 0 & 0 \\ 0 & 0 & 0 & 0 & c'_{55} & 0 \\ 0 & 0 & 0 & 0 & 0 & c'_{66} \end{bmatrix} \begin{Bmatrix} s_{11} \\ s_{22} \\ s_{33} \\ s_{12} \\ s_{23} \\ s_{31} \end{Bmatrix} \tag{18.37}$$

and

$$\begin{Bmatrix} s''_{11} \\ s''_{22} \\ s''_{33} \\ s''_{12} \\ s''_{23} \\ s''_{31} \end{Bmatrix} = \begin{bmatrix} c''_{11} & c''_{12} & c''_{31} & 0 & 0 & 0 \\ c''_{12} & c''_{22} & c''_{23} & 0 & 0 & 0 \\ c''_{31} & c''_{23} & c''_{33} & 0 & 0 & 0 \\ 0 & 0 & 0 & c''_{44} & 0 & 0 \\ 0 & 0 & 0 & 0 & c''_{55} & 0 \\ 0 & 0 & 0 & 0 & 0 & c''_{66} \end{bmatrix} \begin{Bmatrix} s_{11} \\ s_{22} \\ s_{33} \\ s_{12} \\ s_{23} \\ s_{31} \end{Bmatrix} \tag{18.38}$$

The c'_{ij} and c''_{ij} are model parameters governing the anisotropy. The normalizing coefficient, h, depends on the model parameters and is computed so that the effective stress for a uniaxial stress state is σ.

An associated flow rule is utilized such that the plastic rate of deformation is normal to the yield surface and is given by,

$$\dot{D}^{\mathrm{p}}_{ij} = \dot{\gamma}\frac{\partial \phi}{\partial \sigma_{ij}}, \tag{18.39}$$

where $\dot{\gamma}$ is the consistency multiplier enforcing $f = 0$ during plastic deformation. Given the form of f, it can also be shown that $\dot{\gamma} = \dot{\bar{\varepsilon}}^{p}$, i.e. the consistency parameter is equal to the rate of the equivalent plastic strain.

In the command blocks that define the orthotropic Cazacu plasticity model:

- See the User's Guide chapter on Material Models for more information on elastic constants input.
- The reference nominal yield stress, $\bar{\sigma}$, is defined with the `YIELD STRESS` command line.
- The type of hardening law is defined with the `HARDENING MODEL` command line, other hardening commands then define the specific shape of that hardening curve.
- The hardening modulus for a linear hardening model is defined with the `HARDENING MODULUS` command line.
- The hardening constant for a power law hardening model is defined with the `HARDENING CONSTANT` command line.
- The hardening exponent for a power law hardening model is defined with the `HARDENING EXPONENT` command line.
- The Lüders strain for a power law hardening model is defined with the `LUDERS STRAIN` command line.
- The hardening function for a user defined hardening model is defined with the `HARDENING FUNCTION` command line.
- The shape of the spline for the spline based hardening is defined by the `CUBIC SPLINE TYPE`, `CARDINAL PARAMETER`, `KNOT EQPS`, and `KNOT STRESS` command lines.
- The isotropic hardening model for the flow stress hardening model is defined with the `ISOTROPIC HARDENING MODEL` command line.
- The function name of a user-defined isotropic hardening model is defined via the `ISOTROPIC HARDENING FUNCTION` command line.
- The optional rate multiplier for the flow stress hardening model is defined with the `RATE MULTIPLIER` command line.

- The optional temperature multiplier for the flow stress hardening model is defined via the `TEMPERATURE MULTIPLIER` command line.
- The function name of a user-defined temperature multiplier is defined with the `TEMPERATURE MULTIPLIER FUNCTION` command line.
- For a Johnson-Cook temperature multiplier, the melting temperature, θ_{melt}, is defined via the `MELTING TEMPERATURE` command line.
- For a Johnson-Cook temperature multiplier, the reference temperature, θ_{ref}, is defined via the `REFERENCE TEMPERATURE` command line.
- For a Johnson-Cook temperature multiplier, the temperature exponent, M, is defined via the `TEMPERATURE EXPONENT` command line.
- The optional rate multiplier for the yield stress for the decoupled flow stress hardening model is defined with the `YIELD RATE MULTIPLIER` command line.
- The optional rate multiplier for the hardening for the decoupled flow stress hardening model is defined with the `HARDENING RATE MULTIPLIER` command line.
- The optional temperature multiplier for the yield stress for the decoupled flow stress hardening model is defined with the `YIELD TEMPERATURE MULTIPLIER` command line.
- The optional temperature multiplier for the hardening for the decoupled flow stress hardening model is defined via the `HARDENING TEMPERATURE MULTIPLIER` command line.

Output variables available for this model are listed in Table 18.5.

Table 18.5: State Variables for CAZACU ORTHOTROPIC PLASTICITY Model (Section 18.10)

Name	**Description**
`EQPS`	equivalent plastic strain, $\bar{\varepsilon}^p$
`EQDOT`	equivalent plastic strain rate, $\dot{\bar{\varepsilon}}^p$
`SEFF`	effective stress, ϕ

18.11 Skorohod-Olevsky Viscous Sintering (SOVS)

```
BEGIN PARAMETERS FOR MODEL SOVS
  #
  #  Elastic constants
  #
  YOUNGS MODULUS = <real> E
  POISSONS RATIO = <real> ν
  SHEAR MODULUS  = <real> G
  BULK MODULUS   = <real> K
  LAMBDA         = <real> λ
  TWO MU         = <real> 2μ
  #
  #  Initial relative density
  #
  RHO0     = <real> ρ0
  #
  #  Normalized shear viscosity relative density dependence
  #
  A1       = <real> a1
  B1       = <real> b1
  #
  #  Normalized bulk viscosity relative density dependence
  #
  A2       = <real> a2
  B2       = <real> b2
  C2       = <real> c2
  #
  #  Effective sinter stress relative density dependence
  #
  SIGMA_S0 = <real> σs0
  A3       = <real> a3
  B3       = <real> b3
  #
  #  Skeleton shear viscosity temperature dependence
  #
  A4       = <real> a4
  B4       = <real> b4
  C4       = <real> c4
  T0       = <real> θ0
  #
  #  Numerical integration parameters
  #
  BETA     = <real> β (0.5)
  TOL      = <real> tol (1.0E6)
END [PARAMETERS FOR MODEL SOVS]
```

The Skorohod-Olevsky viscous sintering (SOVS) model is a continuum scale model for the evolution of porosity and deformation of ceramic materials through sintering. This implementation is intended to capture geometric evolution of a body through such a process thereby enabling the design and manufacture of complex 3D components and/or structures.

Here, the model is a linear-viscous form of the non-linear viscous incompressible model of Olevsky [12] based on the concepts of plastic porous bodies. The specific implementation used here is that of Argüello and coworkers [13]. Like other inelastic models, an additive split in the rate of deformation,

$$D_{ij} = D^{\mathrm{e}}_{ij} + D^{\mathrm{in}}_{ij}, \tag{18.40}$$

is used in which the elastic constitutive relation may be written as,

$$\overset{\circ}{\sigma}_{ij} = \mathbb{C}_{ijkl} D^{\mathrm{e}}_{kl}. \tag{18.41}$$

For the inelastic response, a constitutive relation may be derived via thermodynamic analysis and dissipation considerations (see [12]) producing an inelastic (viscous) strain rate, D^{in}_{ij}, of the form,

$$D^{\mathrm{in}}_{ij} = \frac{\sigma'_{ij}}{2\eta_0(\theta)\,\phi(\rho)} + \frac{\sigma_{kk}/3 - \sigma_s(\rho)}{6\eta_0(\theta)\,\psi(\rho)}\delta_{ij}, \tag{18.42}$$

with η_0, ϕ, σ_s, and ψ, being the shear viscosity of the fully dense skeleton, normalized shear viscosity, sintering stress, and normalized bulk viscosity. A split between the contributions of the deviatoric, σ'_{ij}, and volumetric, $\sigma_{kk}/3$, components of the Cauchy stress, $\sigma_{ij} = \sigma'_{ij} + (1/3)\,\sigma_{kk}\delta_{ij}$, is also utilized. Note, in (18.42) explicit dependencies of the various terms on relative density, ρ, and absolute temperature, θ, are indicated although for simplicity will be neglected in the remainder. Importantly, the relative density, ρ, is defined as,

$$\rho = \frac{\rho_t}{\rho_T}, \tag{18.43}$$

where ρ_T is the theoretical density and ρ_t is the current material density at time t. Conservation of mass may be invoked to show the time rate of change of the relative density, $\dot{\rho}$, is simply,

$$\dot{\rho} = -\rho D^{\mathrm{in}}_{kk}. \tag{18.44}$$

Based on previously performed kinetic Monte-Carlo analysis, Argüello and coworkers [13] used the following density dependent relations,

$$\phi(\rho) = a_1 \rho^{b_1}, \tag{18.45}$$

$$\psi(\rho) = a_2 \frac{\rho^{b_2}}{(1-\rho)^{c_2}}, \tag{18.46}$$

$$\sigma_s(\rho) = \sigma_{s0} \bar{\sigma}_s(\rho), \tag{18.47}$$

$$\bar{\sigma}_s(\rho) = a_3 \rho^{b_3}. \tag{18.48}$$

In (18.47) it can be observed that the sintering stress is decomposed into two parts: (*i*) the local sintering stress, σ_{s0}, and (*ii*) the relative density dependent normalized effective sintering stress, $\bar{\sigma}_s$. With respect to the latter, the functional representation is given in (18.48). For the former, the value may be approximated as,

$$\sigma_{s0} = \frac{3\alpha}{r_0}, \tag{18.49}$$

with α being the surface tension and r_0 the average grain size. In the current implementation, only the local sintering stress is input to the model as the surface tension and grain size are unneeded elsewhere.

The temperature dependence of the shear viscosity of the fully dense skeleton was proposed in a previous effort by Olevsky *et al.* [14] and is given as,

$$\eta_0(\theta) = a_4 \left(\frac{\theta}{\theta_0}\right)^2 + b_4 \frac{\theta}{\theta_0} + c_4, \tag{18.50}$$

in which θ_0 is a reference temperature. During the efforts of Argüello *et al.* [13], alternative forms of this dependence based on either an Arrhenius relationship or the introduction of an additional variable for grain growth were put forth. Notably, the latter showed good agreement with experimental measurements although at the time only a 1D form was considered as alterations to the numerical scheme were needed for the 3D implementation. For the current model, the previous quadratic form is used as that was the expression validated against experiments.

For details on the SOVS model, please see [13].

In the command blocks that define the SOVS model:

- See the User's Guide chapter on Material Models for more information on elastic constants input.
- The initial relative density, ρ_0, ($0 \leq \rho_0 \leq 1$) is defined with the `RHO0` command line.
- The modulus of the relative density dependence of the normalized shear viscosity, a_1, is defined with the `A1` command line.
- The exponent of the relative density dependence of the normalized shear viscosity, b_1, is defined with the `B1` command line.

- The modulus of the relative density dependence of the normalized bulk viscosity, a_2, is defined with the `A2` command line.
- The exponent of the relative density dependence of the normalized bulk viscosity, b_2, is defined with the `B2` command line.
- The exponent of the relative porosity dependence of the normalized bulk viscosity, c_2, is defined with the `C2` command line.
- The local sintering stress, σ_{s0}, is defined with the `SIGMA_S0` command line.
- The modulus of the relative density dependence of the normalized effective sintering stress, a_3, is defined with the `A3` command line.
- The exponent of the relative density dependence of the normalized effective sintering stress, b_3, is defined with the `B3` command line.
- The quadratic constant of the skeleton shear viscosity on normalized temperature, a_4, is defined with the `A4` command line.
- The linear constant of the skeleton shear viscosity on normalized temperature, b_4, is defined with the `B4` command line.
- The constant of the skeleton shear viscosity on normalized temperature, c_4, is defined with the `C4` command line.
- The reference temperature used with the skeleton shear viscosity, θ_0, is defined with the `T0` command line.
- The type of integration is controlled by the integration selection parameter, β ($0 \leq \beta \leq 1$), is defined with the `BETA` command line. A value of one corresponds to implicit constitutive integration while zero is specified for explicit integration. The default value is 0.5.
- The tolerance of convergence for the non-linear problem associated with constitutive model integration, tol, may be specified by the `TOL` command line. A default value of 1.0×10^6 is used if no value is specified.
- It is recommended that the default values of constitutive integration parameters (β, tol) be used. Alternative selections remain an unverified development option.

Output variables available for this model are listed in Table 18.6.

Table 18.6: State Variables for SOVS Model (Section 18.11)

Name	Description
RHO	relative density, ρ
RHO_DOT	time rate of change of density, $\dot{\rho}$
EPSILON_IN_DOT	inelastic strain rate, $\dot{\varepsilon}_{ij}^{\text{in}}$
ITERATIONS	constitutive integration convergence iterations, iter

18.12 Hydra Plasticity

18.12.1 Summary

The hydra plasticity model has the following features:

- Isotropic elastic behavior, with elastic constants that may optionally depend on temperature,
- A Hill yield surface that may undergo isotropic hardening,
- Tabular definition of the material's hardening behavior, with dependence on equivalent plastic strain and optional dependence on temperature, and/or equivalent plastic strain rate,
- Option inclusion of material failure,
- Tabular definition of the material's failure strain, with dependence on stress triaxiality and optional dependence on temperature, equivalent plastic strain rate, and/or Lode angle (via a Lode parameter),
- Linear material strength and stiffness degradation following failure initiation that is based on the fracture energy for the material and is normalized to the element characteristic length to reduce mesh dependencies,
- User specified value of decay at which an integration point is flagged for removal from the analysis, and
- Optional inclusion of heating caused by plastic deformation of the material.

18.12.2 User Guide

```
BEGIN PARAMETERS FOR MODEL HYDRA_PLASTICITY
  #
  # Elastic Constants
  #
  YOUNGS MODULUS     = <real> E
  YOUNGS FUNCTION    = <string> youngs_func_name f_E(T_t)
  POISSONS RATIO     = <real> ν
  POISSONS FUNCTION  = <string> poissons_func_name f_ν(T_t)
  #
  # Material Coordinates System Definition
  #
  COORDINATE SYSTEM             = <string> coordinate_system_name
  DIRECTION FOR ROTATION        = <real> 1|2|3
  ALPHA                         = <real> α_1 (degrees)
  SECOND DIRECTION FOR ROTATION = <real> 1|2|3
  SECOND ALPHA                  = <real> α_2 (degrees)
  #
  # Yield Surface Parameters
  #
```

```
  R11             = <real> R11
  R22             = <real> R22
  R33             = <real> R33
  R12             = <real> R12
  R23             = <real> R23
  R31             = <real> R31
  #
  # Hardening Parameters
  #
  HARDENING FUNCTION = <string> hardening_func_name f_H(ε̄^p, ε̇^p, T_t)
  PLASTIC STRAIN RATE LOG FLAG = <bool> true or false
  #
  # Plastic Heating Parameters
  #
  SPECIFIC HEAT            = <real> C
  SPECIFIC HEAT FUNCTION   = <string> specific_heat_func_name f_C(T_t)
  INELASTIC HEAT FRACTION = <real> η
  ADIABATIC ANALYSIS FLAG = <bool> true or false
  #
  # Failure Parameters
  #
  FAILURE FUNCTION            = <string> failure_func_name f_F(κ, ε̇^p, Θ_p, T_t)
  FRACTURE ENERGY             = <real> G_f
  ELEMENT REMOVAL DECAY VALUE = <real> φ_r
  FAILURE ANALYSIS FLAG       = <bool> true or false
END [PARAMETERS FOR MODEL HYDRA_PLASTICITY]
```

- The elastic constants, E and ν, are defined by the `YOUNGS MODULUS` and `POISSONS RATIO` command lines, respectively. Both of these values must be defined by the user, there are no defaults.

- The temperature scaling factor functions for E and ν are defined by the `YOUNGS MODULUS FUNCTION` and `POISSONS RATIO FUNCTION` command lines, respectively. The `youngs_func_name` and `poissons_func_name` reference functions defined by separate `FUNCTION` command blocks. These functions should define temperature dependent scaling factors that when applied to E and ν (defined by the `YOUNGS MODULUS` and `POISSONS RATIO` command lines) will produce temperature adjusted E and ν values. Definition of these functions is optional. If not defined by the user a constant temperature scaling factor of 1.0 will be used.

- The hydra plasticity material model uses an element specific coordinate frame. The coordinate frame used is specified by the `COORDINATE SYSTEM` command line, where the `coordinate_system_name` references a coordinate system defined by a separate `COORDINATE SYSTEM` command block. For the hydra plasticity model, this coordinate system can be either a rectangular or a cylindrical coordinate system. The `COORDINATE`

SYSTEM defines a local R, S, and T frame at each element. This initial coordinate system can be additionally rotated to give the final material directions at each material point.

The first rotation of the initial coordinate system is defined using the DIRECTION FOR ROTATION and ALPHA command lines. The axis for rotation of the initial coordinate system is specified by the DIRECTION FOR ROTATION command line, 1 corresponds to the initial coordinate system local R axis, 2 corresponds to the initial coordinate system local S axis, and 3 corresponds to the initial coordinate system local T axis. The right hand rule angle of rotation about this axis is given by ALPHA. This rotation yields an intermediate coordinate system.

A secondary rotation of the intermediate coordinate system may be defined using the SECOND DIRECTION FOR ROTATION and SECOND ALPHA command lines. The axis for rotation of the intermediate coordinate system is specified by the SECOND DIRECTION FOR ROTATION command line, 1 corresponds to the intermediate coordinate system local R axis, 2 corresponds to the intermediate coordinate system local S axis, and 3 corresponds to the intermediate coordinate system local T axis. The right hand rule angle of rotation about this axis is given by SECOND ALPHA. The resulting coordinate system gives the final R, S, and T coordinate frame for the material directions.

At a minimum, the COORDINATE SYSTEM command line must be specified. The DIRECTION FOR ROTATION, ALPHA, SECOND DIRECTION FOR ROTATION, and SECOND ALPHA command lines are optional, and default to 1, 0.0, 2, and 0.0, respectively (effectively specifying no additional rotations of the coordinate system specified by the COORDINATE SYSTEM command line).

- The ratio of the normal yield stress to the reference yield stress ($\bar{\sigma}_r$) in the $\bar{\mathbf{e}}_1\bar{\mathbf{e}}_1$ material direction is defined with the R11 command line. The default is 1.0.

- The ratio of the normal yield stress to the reference yield stress ($\bar{\sigma}_r$) in the $\bar{\mathbf{e}}_2\bar{\mathbf{e}}_2$ material direction is defined with the R22 command line. The default is 1.0.

- The ratio of the normal yield stress to the reference yield stress ($\bar{\sigma}_r$) in the $\bar{\mathbf{e}}_3\bar{\mathbf{e}}_3$ material direction is defined with the R33 command line. The default is 1.0.

- The ratio of the shear yield stress to the reference shear yield stress in the $\bar{\mathbf{e}}_1\bar{\mathbf{e}}_2$ material direction is defined with the R12 command line. The default is 1.0. Note that the reference shear stress is equal to $\frac{1}{\sqrt{3}}\bar{\sigma}_r$.

- The ratio of the shear yield stress to the reference shear yield stress in the $\bar{\mathbf{e}}_2\bar{\mathbf{e}}_3$ material direction is defined with the R23 command line. The default is 1.0. Note that the reference shear stress is equal to $\frac{1}{\sqrt{3}}\bar{\sigma}_r$.

- The ratio of the shear yield stress to the reference shear yield stress in the $\bar{\mathbf{e}}_3\bar{\mathbf{e}}_1$ material direction is defined with the R31 command line. The default is 1.0. Note that the reference shear stress is equal to $\frac{1}{\sqrt{3}}\bar{\sigma}_r$.

- The hardening function is defined with the HARDENING FUNCTION command line. The hardening_func_name references a function defined by a separate FUNCTION command

block. The hardening function must be defined using a piecewise multivariate function (`TYPE = PIECEWISE MULTIVARIATE`). The piecewise multivariate function allows the user to define the behavior of a single dependent variable with respect to one or more independent variables. In this case, hardening (which defines the reference yield stress) can be defined with dependencies on equivalent plastic strain $\bar{\varepsilon}^p$, and optionally on equivalent plastic strain rate $\dot{\bar{\varepsilon}}^p$, and temperature T_t. The hardening function must be defined by the user and must include dependence of the reference yield stress on equivalent plastic strain. All other dependencies are optional.

Shown below is an example of the format required to define a hardening function using a piecewise multivariate function:

```
begin function multivariate_hardening_function
  type = piecewise multivariate
  column titles plastic_strain plastic_strain_rate temperature \#
    yield_stress
  begin values
    0.00  -3.0   100.0   1.52294e+09
    0.10  -3.0   100.0   1.76488e+09
    0.20  -3.0   100.0   1.78225e+09
    0.30  -3.0   100.0   1.79298e+09
    0.40  -3.0   100.0   1.80086e+09
    0.50  -3.0   100.0   1.80713e+09
                .
                .
                .
  end
end
```

The `column titles` line contains the dependent variable `yield_stress` in the last column and the independent variables `plastic_strain`, `plastic_strain_rate`, and `temperature` in the first three columns. The specific column name shown must be used if dependency on the variable is desired. The piecewise multivariate function requires that the independent variables create a fully populated grid where points in each dimension are evenly spaced. For performance reasons, the independent variables that are expected to vary the most in the analyses should be placed in the left columns, and variables that are expected to vary the least in the right columns.

- The flag `PLASTIC STRAIN RATE LOG FLAG` is used to specify whether the data for $\dot{\bar{\varepsilon}}^p$ provided in the hardening function is $\log_{10}$ or not. If the command line `PLASTIC STRAIN RATE LOG FLAG` is set equal to *true*, the values provided in the piecewise multivariate function defining the hardening for the material are $\log_{10}\left(\dot{\bar{\varepsilon}}^p\right)$. This is the case in the example provided above, where the equivalent plastic strain rate value given as -3.0 corresponds to an actual strain rate of 0.001 1/s. The default setting is $false$.

- The value for the specific heat, C, which is the amount of heat required to change the temperature of a unit mass of the material by one degree, is defined with the `SPECIFIC HEAT` command line. The specific heat must be specified by the user, there is no default value.

- The temperature scaling factor function for C is defined by the `SPECIFIC HEAT FUNCTION`

command line. The specific_heat_func_name references a function defined by a separate FUNCTION command block. The function should define temperature dependent scaling factors that when applied to C (defined by the SPECIFIC HEAT command line) will produce the temperature adjusted C value. Definition of this function is optional. If not defined by the user, a constant temperature scaling factor of 1.0 will be used.

- The value for the inelastic heat fraction, η, is defined with the INELASTIC HEAT FRACTION command line. The inelastic heat fraction defines the fraction of plastic work that acts to heat the material. The default value is 1.0.

- The flag ADIABATIC ANALYSIS FLAG is used to specify whether an adiabatic analysis should be performed. If the command line ADIABATIC ANALYSIS FLAG is set equal to *true*, the material model will calculate a change in temperature in the material due to plastic work, and add the plastic work temperature change to the externally defined temperature, before determining temperature dependent material properties. If the command line ADIABATIC ANALYSIS FLAG is set equal to $false$, the material model will still calculate the plastic work performed on the material, but will make no adjustment to the externally defined temperature before determining temperature dependent material properties. The material model will continue to calculate the plastic work heat increment and heat flux, making them available through state variables for coupled analysis. The default setting is $false$.

- The failure function is defined with the FAILURE FUNCTION command line. The failure_func_name references a function defined by a separate FUNCTION command block. The failure function, like the hardening function, must be defined using a piecewise multivariate function (TYPE = PIECEWISE MULTIVARIATE). The failure function defines the failure strain, with dependencies on stress triaxiality $\varkappa$, and optionally on equivalent plastic strain rate $\dot{\bar{\varepsilon}}^p$, temperature T_t, and Lode parameter Θ_p (where Θ_p is calculated as $\cos(3\Theta)$ and Θ is the Lode angle). The failure function need only be defined when FAILURE ANALYSIS FLAG is set equal to *true*. When defined, the failure function must include dependence of the failure strain on stress triaxiality. All other dependencies are optional.

  Shown below is an example of the format required to define a failure function using a piecewise multivariate function:

```
begin function multivariate_failure_function
  type = piecewise multivariate
  column titles stress_triaxiality plastic_strain_rate temperature \#
    lode_parameter failure_strain
  begin values
    -0.333  -3.0   100.0  -1.00   102.816
     0.000  -3.0   100.0  -1.00   0.288
     0.333  -3.0   100.0  -1.00   0.431
     0.666  -3.0   100.0  -1.00   0.395
     0.999  -3.0   100.0  -1.00   0.275
                .
                .
                .
  end
end
```

The `column titles` line contains the dependent variable `failure_strain` in the last column and the independent variables `stress_triaxiality`, `plastic_strain_rate`, `temperature`, and `lode_parameter` in the first four columns. The specific column name shown must be used if dependency on the variable is desired. The piecewise multivariate function requires that the independent variables create a fully populated grid where points in each dimension are evenly spaced. For performance reasons, the independent variables that are expected to vary the most in the analyses should be placed in the left columns, and variables that are expected to vary the least in the right columns.

- The fracture energy for the material, G_f, the energy required to form a unit area of crack surface, is defined with the `FRACTURE ENERGY` command line. This default value is 1.0.
- The decay value at which an element or integration point is flagged for removal from the analysis, φ_r, is specified by the `ELEMENT REMOVAL DECAY VALUE` command line. The default value is 0.001.
- The flag `FAILURE ANALYSIS FLAG` is used to specify whether the failure modeling capabilities of the material model should be enabled. If the command line `FAILURE ANALYSIS FLAG` is set equal to *true*, the material model will include failure. If the command line `FAILURE ANALYSIS FLAG` is set equal to $false$, the failure capabilities of the material model will be disabled. In the latter case, the user need not define a failure function, fracture energy, or element removal decay value. The default setting is $false$.

Output variables available for this model are listed in Table 18.7.

18.12.3 Theory

Strain Decomposition

The hydra plasticity model makes use of an additive decomposition of the strain tensor into elastic and inelastic (plastic) components. The rate form of the additive decomposition is given by:

$$\dot{\varepsilon} = \dot{\varepsilon}^e + \dot{\varepsilon}^p \tag{18.51}$$

where $\dot{\varepsilon}$ is the total strain rate that consists of an elastic ($\dot{\varepsilon}^e$) and plastic ($\dot{\varepsilon}^p$) component.

Elasticity

In the elastic regime, the true stress σ is related to the total strain ε, by Hooke's law:

$$\sigma = \mathbb{C}(T_t)\varepsilon \tag{18.52}$$

where $\mathbb{C}(T_t)$ is the fourth order elastic moduli tensor that may optionally depend on the material temperature T_t. Isotropic elasticity is assumed, so the elastic moduli tensor is fully defined by two elastic constants. In the hydra plasticity model the two elastic constants are constrained to be Young's modulus and Poisson's ratio. These constants each may optionally depend on temperature T_t.

Table 18.7: State Variables for HYDRA PLASTICITY Model (Section 18.12)

Name	Description
ITERATIONS	Number of iterations required for convergence of the Newton algorithm.
SEFF	Effective Stress $\phi(\sigma)$, note may $\neq \sigma_e = \sqrt{3J_2}$
SBAR	Yield stress based on the current size of the yield surface. $\bar{\sigma}$
EQPS	Equivalent Plastic Strain $\bar{\varepsilon}^p = \int_0^t \dot{\bar{\varepsilon}}^p \mathrm{d}t$
EQPS_RATE	Equivalent Plastic Strain Rate $\dot{\bar{\varepsilon}}^p = \sqrt{\frac{2}{3}\dot{\varepsilon}^p : \dot{\varepsilon}^p}$
HEAT_FLUX	Heat Flux $r^p = \eta(\sigma : \dot{\varepsilon}^p)$
HEAT_INCREMENT	Heat Increment Δr^p
TEMP_TOTAL	Total temperature including change in temperature due to plastic heating. $T_t = T + \Delta T_p$, where T is the externally defined temperature.
EQPS_DT	Total accumulated change in temperature due to plastic heating. ΔT_p
FAIL_STRESS	Effective stress at the time of failure initiation. $\sigma_e^f = \sqrt{3J_2^f}$
UFAIL	Displacement over which the integration point's strength and stiffness are reduced to zero following failure initiation. $u^f = \frac{2G_f}{\sigma_e^f}$
DAMAGE	Damage, equal to 0 at failure initiation, increasing to 1 at full material strength and stiffness degradation. D
PRESSURE	Pressure $p = -\frac{1}{3}\mathrm{tr}(\sigma)$
SECOND_STRESS_INVARIANT	Second Stress Invariant $J_2 = \frac{1}{2}\left[\mathrm{tr}\left(\sigma^2\right) - \frac{1}{3}\mathrm{tr}(\sigma)^2\right]$
THIRD_STRESS_INVARIANT	Third Stress Invariant $J_3 = \frac{1}{3}\left[\mathrm{tr}\left(\sigma^3\right) - \mathrm{tr}\left(\sigma^2\right)\mathrm{tr}(\sigma) + \frac{2}{9}\mathrm{tr}(\sigma)^3\right]$
STRESS_TRIAXIALITY	Stress Triaxiality $\varkappa = -\frac{p}{\sigma_e}$
LODE_PARAMETER	Lode Parameter $\Theta_p = \cos(3\Theta)$, where $\Theta = \left(\frac{J_3}{2}\right)\left(\frac{3}{J_2}\right)^{1.5}$ is the Lode angle.

Yield Surface

The hydra plasticity model makes use of the Hill yield surface. The Hill yield surface may be orthotropic, and assumes orthogonal principal material directions. The yield surface is defined as follows,

$$\begin{aligned}\phi^2\left(\sigma_{ij}\right) &= F\left(\sigma_{22}-\sigma_{33}\right)^2 + G\left(\sigma_{33}-\sigma_{11}\right)^2 + H\left(\sigma_{11}-\sigma_{22}\right)^2 \\ &+2L\sigma_{23}^2 + 2M\sigma_{31}^2 + 2N\sigma_{12}^2\end{aligned} \tag{18.53}$$

where the coefficients F, G, H, L, M, and N are given by the following.

$$\begin{aligned}F &= \frac{(\bar{\sigma}_r)^2}{2}\left[\frac{1}{\left(\sigma_{22}^y\right)^2}+\frac{1}{\left(\sigma_{33}^y\right)^2}-\frac{1}{\left(\sigma_{11}^y\right)^2}\right] \quad ; \quad L = \frac{(\bar{\sigma})^2}{2}\left[\frac{1}{\left(\tau_{23}^y\right)^2}\right] \\ G &= \frac{(\bar{\sigma}_r)^2}{2}\left[\frac{1}{\left(\sigma_{33}^y\right)^2}+\frac{1}{\left(\sigma_{11}^y\right)^2}-\frac{1}{\left(\sigma_{22}^y\right)^2}\right] \quad ; \quad M = \frac{(\bar{\sigma}_r)^2}{2}\left[\frac{1}{\left(\tau_{31}^y\right)^2}\right] \\ H &= \frac{(\bar{\sigma}_r)^2}{2}\left[\frac{1}{\left(\sigma_{11}^y\right)^2}+\frac{1}{\left(\sigma_{22}^y\right)^2}-\frac{1}{\left(\sigma_{33}^y\right)^2}\right] \quad ; \quad N = \frac{(\bar{\sigma}_r)^2}{2}\left[\frac{1}{\left(\tau_{12}^y\right)^2}\right]\end{aligned} \tag{18.54}$$

In Equation 18.54, σ_{11}^y, σ_{22}^y, σ_{33}^y, τ_{12}^y, τ_{23}^y, and τ_{31}^y represent the three normal and three shear yield stresses in the three material coordinate directions, and $\bar{\sigma}_r$ a reference yield stress that is defined by the hardening function. The six independent yield stresses, are specified by the user through the definition of the following six yield ratios.

$$\begin{aligned}R_{11} &= \frac{\sigma_{11}^y}{\bar{\sigma}} \quad ; \quad R_{12} = \sqrt{3}\frac{\tau_{12}^y}{\bar{\sigma}} \\ R_{22} &= \frac{\sigma_{22}^y}{\bar{\sigma}} \quad ; \quad R_{23} = \sqrt{3}\frac{\tau_{23}^y}{\bar{\sigma}} \\ R_{33} &= \frac{\sigma_{33}^y}{\bar{\sigma}} \quad ; \quad R_{31} = \sqrt{3}\frac{\tau_{31}^y}{\bar{\sigma}}\end{aligned} \tag{18.55}$$

If all of the above ratios are set equal to 1.0 ($R_{ij} = 1$) the Mises yield surface is recovered.

Hardening

The hydra plasticity model assumes isotropic hardening. Hardening of the material is defined by a hardening function.

$$\bar{\sigma}_r = f_H\left(\bar{\varepsilon}^p, \dot{\bar{\varepsilon}}^p, T_t\right) \tag{18.56}$$

The hardening function defines the reference yield stress ($\bar{\sigma_r}$) for the material. The hardening function has dependence on the equivalent plastic strain ($\bar{\varepsilon}^p$), and optionally may depend on the equivalent plastic strain rate ($\dot{\bar{\varepsilon}}^p$) and/or temperature ($T_t$). The equivalent plastic strain is defined as follows:

$$\bar{\varepsilon}^p = \int_0^t \dot{\bar{\varepsilon}}^p \mathrm{d}t \tag{18.57}$$

where $\dot{\bar{\varepsilon}}^p$ is the equivalent plastic strain rate calculated from the plastic strain rates ($\dot{\varepsilon}^p$) as follows.

$$\dot{\bar{\varepsilon}}^p = \sqrt{\frac{2}{3}\dot{\varepsilon}^p : \dot{\varepsilon}^p} \tag{18.58}$$

Failure

Failure in the hydra plasticity model is comprised of two distinct phases. The first, pre-failure initiation phase, involves the calculation of a failure initiation metric that is used to determine when the failure initiation criterion has been met. The second, post-failure initiation phase, involves the accumulation of damage in the material (with increasing plastic deformation) and the degradation of the material's strength and stiffness.

The failure initiation criterion is strain based. The criterion is satisfied when the failure measure (fm) equation is satisfied.

$$fm = \int \frac{\mathrm{d}\bar{\varepsilon}^p}{\bar{\varepsilon}_f^p\left(\varkappa, \dot{\bar{\varepsilon}}^p, \Theta_p, T_t\right)} \geq 1.0 \tag{18.59}$$

The failure strain $\bar{\varepsilon}_f^p\left(\varkappa, \dot{\bar{\varepsilon}}^p, \Theta_p, T_t\right)$ is provided by the failure function f_F, and is dependent on stress triaxiality ($\varkappa$), and optionally on plastic strain rate ($\dot{\bar{\varepsilon}}^p$), Lode angle ($\Theta$, through the Lode parameter, Θ_p), and/or temperature (T_t). Stress triaxiality is calculated as follows:

$$\varkappa = -\frac{p}{\sigma_e} \tag{18.60}$$

where p is the pressure and σ_e is the effective stress. The pressure is given by the following,

$$p = -\frac{1}{3}\mathrm{tr}\left(\sigma\right) \tag{18.61}$$

and the effective stress by the following.

$$\sigma_e = \sqrt{3J_2} \tag{18.62}$$

In the above equation J_2 is the second stress invariant and is calculated from the stress σ as follows.

$$J_2 = \frac{1}{2}\left[\mathrm{tr}\left(\sigma^2\right) - \frac{1}{3}\mathrm{tr}\left(\sigma\right)^2\right] \tag{18.63}$$

The Lode parameter (Θ_p) is a function of the Lode angle (Θ),

$$\Theta = \left(\frac{J_3}{2}\right)\left(\frac{3}{J_2}\right)^{1.5} \tag{18.64}$$

where J_3 is the third stress invariant calculated from the stress σ as follows.

$$J_3 = \frac{1}{3}\left[\text{tr}\left(\sigma^3\right) - \text{tr}\left(\sigma^2\right)\text{tr}\left(\sigma\right) + \frac{2}{9}\text{tr}\left(\sigma\right)^3\right] \tag{18.65}$$

The Lode parameter is then calculated as follows.

$$\Theta_p = \cos\left(3\Theta\right) \tag{18.66}$$

Note that the Lode parameter can vary from -1.0 (triaxial compression) to 1.0 (triaxial tension), with a value of 0.0 representing the pure shear stress state.

Once the failure initiation criterion has been satisfied, increasing plastic deformation of the material results in the accumulation of damage (D). The rate of damage accumulation is governed by the following rate equation:

$$\dot{D} = \frac{L\dot{\bar{\varepsilon}}_f^p}{u^f} \tag{18.67}$$

where $\dot{\bar{\varepsilon}}_f^p$ is the equivalent plastic strain rate associated with plastic deformation of the material occurring after the initiation of failure, L is the characteristic length associated with the material integration point (taken as $\sqrt[3]{V_{ipt}}$, where V_{ipt} is the volume of material associated with the material integration point), and u^f is the failure displacement. The failure displacement is calculated based on the state of the material at the time of failure initiation as follows:

$$u^f = \frac{2G_f}{\sigma_e^f} \tag{18.68}$$

where G_f is the material's fracture energy and σ_e^f is the effective stress at the instant of failure initiation. The instantaneous damage value is therefore given by the following.

$$D = \int_0^t \dot{D}\text{d}t \tag{18.69}$$

It is important to note that the use of the characteristic length (L) associated with the material integration point in Equation 18.67 is an approximate way to remove some of the mesh sensitivity effects associated with material softening. The implementation attempts to get the amount of energy dissipated by the failure process to match the fracture energy for the material, regardless of the mesh size selected.

As damage accumulates in the material, both the strength and stiffness of the material are degraded. This degradation takes the following form,

$$\bar{\sigma_r}^D = (1 - D)\sigma_e^f = \varphi\sigma_e^f \tag{18.70}$$

$$\mathbb{C}^D = (1 - D)\mathbb{C} = \varphi\mathbb{C} \tag{18.71}$$

where $\varphi = (1 - D)$ defines the decay value for the damaged material, and $\bar{\sigma_r}^D$ and $\mathbb{C}^D$ define the damaged yield strength and elastic moduli tensor, respectively. The material strength and stiffness are continually degraded with increasing plastic deformation until the material is fully damage ($D = 1$) or the decay value (φ) has reached a critical decay value specified by the user (φ_r), at which point the material point is flagged for removal from the analysis. It is important to note that the pressure stresses are only degraded when the pressure is tensile (negative pressures). When the pressure is compressive, the pressure stresses are not degraded, which results in the material behaving increasingly like an incompressible fluid as damage is accumulated.

Plastic Heating

The hydra plasticity model includes the ability to calculate changes in the material's temperature due to heating resulting from plastic deformation of the material. The heat flux (r^p) per unit volume associated with a given plastic strain rate ($\dot{\varepsilon}^p$) is calculated as:

$$r^p = \eta\sigma\dot{\varepsilon}^p \tag{18.72}$$

where η is a user defined inelastic heat fraction and σ is the instantaneous stress. Given the specific heat $C(T_t)$ for the material, which may be a function of the temperature (T_t), the heat equation to be solved at each material integration point is,

$$\dot{T}_t C(T_t)\rho = r^p \tag{18.73}$$

where T_t is the temperature and $\dot{T}_t$ is the rate of change of the temperature.

18.12.4 Implementation

Trial Stress

The hydra plasticity model uses a predictor-corrector algorithm for integrating the constitutive model. Since the elastic constants of the hydra plasticity model may depend on temperature, the fourth order elastic moduli tensor $\mathbb{C}$ is first updated to account for the current (step n) temperature (T_t^n). If `ADIABATIC ANALYSIS FLAG` is set equal to *true*, the current temperature is calculated as follows:

$$T_t^{(n)} = T^{(n)} + \Delta T_p^{(n-1)} \tag{18.74}$$

where $T^{(n)}$ is the current time step (n) externally defined temperature, and $T_p^{(n-1)}$ is the accumulated temperature change in the material resulting from plastic work up through the previous time step

$(n-1)$. If ADIABATIC ANALYSIS FLAG is set equal to $false$, the current temperature is taken directly as the externally defined temperature.

$$T_t^{(n)} = T^{(n)} \tag{18.75}$$

Given the current step strain rate $\dot{\varepsilon}^{(n)}$, time increment $\Delta t^{(n)}$, and temperature adjusted elastic moduli tensor $\mathbb{C}\left(T_t^{(n)}\right)$, a trial stress is calculated assuming an elastic response:

$$\sigma_{tr}^{(n)} = \sigma^{(n-1)} + \mathbb{C}\left(T_t^{(n)}\right)\Delta t^{(n)}\dot{\varepsilon}^{(n)} \tag{18.76}$$

where $\sigma^{(n-1)}$ is the converged stress state from the previous time step. If the trial stress lies inside the yield surface (i.e. if $\phi(\sigma_{tr}^{(n)}) \leq \bar{\sigma}(\bar{\varepsilon}^{p^{(n)}}, \dot{\bar{\varepsilon}}^{p^{(n)}}, T_t^{(n)})$), then the step is elastic, the plastic strain increment and plastic strain rate are zero, and the stress is given by the trial stress ($\sigma_{tr}^{(n)}$). If the trial stress is outside of the yield surface (i.e. if $\phi(\sigma_{tr}^{(n)}) > \bar{\sigma}(\bar{\varepsilon}^{p^{(n)}}, \dot{\bar{\varepsilon}}^{p^{(n)}}, T_t^{(n)})$) then the step will include plastic deformation of the material.

Return Mapping Algorithm

When the elastic trial stress falls outside of the yield surface, the model uses an iterative algorithm to determine the increment of plastic strain that occurs during the time step and the final stress state in the material. During the solution process, normality is enforced:

$$R = \Delta\varepsilon^{p^{(n)}} - \Delta\gamma^{(n)}\frac{\partial\phi}{\partial\sigma} = 0 \tag{18.77}$$

and the final stress state for the increment (n) is required to resides on the yield surface.

$$f = \phi\left(\sigma^{(n)}\right) - \bar{\sigma}\left(\bar{\varepsilon}^{p^{(n)}}, \dot{\bar{\varepsilon}}^{p^{(n)}}, T_t^{(n)}\right) = 0 \tag{18.78}$$

A Newton-Raphson search algorithm is implemented. Using $\Delta\gamma^{(k)}$ (which conveniently is equal to $\Delta\bar{\varepsilon}^{p^{(k)}}$) and σ^k as the solution variables, the iterative algorithm is as follows:

$$\begin{aligned}
\Delta\gamma^{(k+1)} &= \Delta\gamma^{(k)} + \Delta\left(\Delta\gamma\right)^{(k)} \\
\sigma^{(k+1)} &= \sigma^{(k)} + \Delta\sigma^{(k)} \\
\Delta\varepsilon^{p^{(k)}} &= \mathbb{C}\left(T_t^{(n,k=0)}\right)^{-1}\left(\sigma_{tr}^{(n)} - \sigma^{(k)}\right)
\end{aligned} \tag{18.79}$$

where $\Delta\gamma^{(0)} = 0$ and $\sigma^{(0)} = \sigma_{tr}$. The increment in plastic strain is given by:

$$\Delta\left(\Delta\gamma\right)^{(k)} = \frac{f^{(k)} - R^{(k)}\mathscr{L}^{(k)}\dfrac{\partial\phi^{(k)}}{\partial\sigma}}{\dfrac{\partial\phi^{(k)}}{\partial\sigma}\mathscr{L}^{(k)}\dfrac{\partial\phi^{(k)}}{\partial\sigma} + H'^{(k)}} \tag{18.80}$$

where $f^{(k)}$ and $R^{(k)}$ are defined for the k^{th} increment using Equation 18.78 and 18.77 as follows:

$$\begin{aligned} f^{(k)} &= \phi\left(\sigma^{(k)}\right) - \bar{\sigma}\left(\bar{\varepsilon}^{p^{(k)}}, \dot{\bar{\varepsilon}}^{p^{(k)}}, T_t^{(k)}\right) \\ R^{(k)} &= \Delta\varepsilon^{p^{(k)}} - \Delta\gamma^{(k)} \frac{\partial\phi}{\partial\sigma}^{(k)} \end{aligned} \tag{18.81}$$

and the elastoplastic tangent ($\mathscr{L}^{(k)}$) for the k^{th} increment, as follows.

$$\mathscr{L}^{(k)} = \mathbb{C}\left(T_t^{(n,k=0)}\right)^{-1} + \Delta\gamma \frac{\partial^2\phi^{(k)}}{\partial\sigma\partial\sigma} \tag{18.82}$$

In Equation 18.80 the slope of the hardening curve ($H'^{(k)}$) is required. Because the hardening behavior in the hydra plasticity model may depend on a number of variables defined in a multivariate function, the calculation of $H'^{(k)}$ is performed using a finite difference approximation. This is handle by incrementing the current equivalent plastic strain ($\bar{\varepsilon}^{p^{(k)}}$) and updating the other parameters ($T_t^{(k)}$ and $\dot{\bar{\varepsilon}}^{p^{(k)}}$) upon which the hardening function depends based on the incremented plastic strain, before the hardening function is evaluated to obtain the values used in the finite difference calculation. This approach ensures that the hardening slope appropriately captures not only the effect of the change in plastic strain, but also the change in material temperature and strain rate generated by a change in the plastic strain. Equations 18.80 and 18.82 also require the first and second partial derivatives of $\phi^{(k)}$. Since ϕ is known, the values are calculated at each step using the current stress state ($\sigma^{(k)}$) and predetermined analytical expressions (not described here). Finally, the search direction in stress space ($\Delta\sigma^{(k)}$) utilized in Equation 18.79 is given by the following.

$$\Delta\sigma^{(k)} = -\mathscr{L}^{(k)}\left(R^{(k)} + \Delta\left(\Delta\gamma\right)^{(k)} \frac{\partial\phi^{(k)}}{\partial\sigma}\right) \tag{18.83}$$

It has been observed that the Newton-Raphson algorithm described above does not always converge when non von Mises yield surfaces are employed. To improve the robustness of the return mapping algorithm, a line search is performed during each Newton-Raphson (k) iteration. This algorithm takes the following form.

$$\begin{aligned} \Delta\gamma^{(j)} &= \Delta\gamma^{(k)} + \alpha^{(j)}\Delta\left(\Delta\gamma\right)^{(k)} \\ \sigma^{(j)} &= \sigma^{(k)} + \alpha^{(j)}\Delta\sigma^{(k)} \end{aligned} \tag{18.84}$$

where $\alpha^{(j)} \in (0, 1]$ is the line search parameter that is determined iteratively using a simple algorithm not described here. $\alpha^{(0)} = 1$ is used to initialize the line search. Note that if $\alpha^{(j)} = 1$ then the exact Newton-Raphson algorithm search direction and magnitude is recovered. The $\Delta\gamma^{(k+1)}$ and $\sigma^{(k+1)}$ values are then given by the converged ($\alpha^{(j=\text{converged})}$) lines search values.

$$\Delta\gamma^{(k+1)} = \Delta\gamma^{(k)} + \alpha^{(j=\text{converged})}\Delta\left(\Delta\gamma\right)^{(k)}$$
$$\sigma^{(k+1)} = \sigma^{(k)} + \alpha^{(j=\text{converged})}\Delta\sigma^{(k)} \tag{18.85}$$

During each Newton-Raphson (k) and line search (j) iteration, the variables that affect the material hardening and failure parameters are updated, and the hardening and failure functions re-evaluated. These parameters include the plastic strain ($\bar{\varepsilon}^p$), plastic strain rate ($\dot{\bar{\varepsilon}}^p$), temperature ($T_t$), stress triaxiality ($\varkappa$), and lode parameter ($\Theta_p$). These parameters are calculated as follows, where m is equal to either k or j depending on whether the process is occurring during the Newton-Raphson (k outer) loop or the line search (j inner) loop of the return mapping algorithm.

$$\bar{\varepsilon}^{p^{(m)}} = \Delta\gamma^{(m)} \tag{18.86}$$

$$\dot{\bar{\varepsilon}}^{p^{(m)}} = \frac{\Delta\gamma^{(m)}}{\Delta t^{(n)}} \tag{18.87}$$

$$T_t^{(m)} = T^{(n)} + \Delta T_p^{(m)} \tag{18.88}$$

$$\varkappa^{(m)} = -\frac{p^{(m)}}{\sigma_e^{(m)}} \tag{18.89}$$

$$\Theta_p^{(m)} = \cos\left(3\Theta^{(m)}\right) \tag{18.90}$$

In the above equations, the pressure ($p^{(m)}$) is calculated as follows,

$$p^{(m)} = -\frac{1}{3}\text{tr}\left(\sigma^{(m)}\right) \tag{18.91}$$

the effective stress is calculated as follows,

$$\sigma_e^{(m)} = \sqrt{3J_2^{(m)}} \tag{18.92}$$

and the lode angle is calculated as follows.

$$\Theta^{(m)} = \left(\frac{J_3^{(m)}}{2}\right)\left(\frac{3}{J_2^{(m)}}\right)^{1.5} \tag{18.93}$$

$J_2^{(m)}$ and $J_3^{(m)}$ are the second and third stress invariants, respectively, that are calculated as follows.

$$J_2^{(m)} = \frac{1}{2}\left[\text{tr}\left(\sigma^{(m)^2}\right) - \frac{1}{3}\text{tr}\left(\sigma^{(m)}\right)^2\right] \tag{18.94}$$

$$J_3^{(m)} = \frac{1}{3}\left[\text{tr}\left(\sigma^{(m)^3}\right) - \text{tr}\left(\sigma^{(m)^2}\right)\text{tr}\left(\sigma^{(m)}\right) + \frac{2}{9}\text{tr}\left(\sigma^{(m)}\right)^3\right] \tag{18.95}$$

Plastic Heating

The hydra plasticity model includes the ability to calculate heating of the material resulting from its plastic deformation. The heat flux increment ($r^{p^{(n)}}$) per unit volume for a given time step n is calculated as:

$$r^{p^{(n)}} = \eta \frac{\left(\sigma^{(n)} + \sigma^{(n-1)}\right)}{2} : \Delta\varepsilon^{p^{(n)}} \tag{18.96}$$

where η is a user defined inelastic heat fraction, $\sigma^{(n)}$ is the current time step's stress, $\sigma^{(n-1)}$ is the previous time step's stress, and $\Delta\varepsilon^{p^{(n)}}$ is the current time step's increment in plastic strain. The temperature change added to the integration point resulting from plastic heating ($\Delta T_p^{(n)}$) is given by the following:

$$\Delta T_p^{(n)} = \Delta T_p^{(n-1)} + \Delta\left(\Delta T_p\right)^{(n)} \tag{18.97}$$

where $\Delta T_p^{(n-1)}$ is the accumulated temperature change added to the integration point resulting from plastic heating up through the previous time step, and $\Delta\left(\Delta T_p\right)^{(n)}$ is the additional increment in temperature change resulting from the plastic deformation of the material during the current time step, which is calculated as follows.

$$\Delta\left(\Delta T_p\right)^{(n)} = \frac{r^{p^{(n)}}}{\rho C\left(\frac{T_t^{(n)} + T_t^{(n-1)}}{2}\right)} \tag{18.98}$$

In Equation 18.98 ρ is the material density. Because the specific heat may be temperature dependent, this equation is iteratively solved, with each successive iteration providing an updated $T_t^{(n)}$.

Failure

Material failure is initiated in the model when the failure measure reaches or exceeds 1.0 ($fm \geq 1.0$). The failure measure is calculated as follows:

$$fm^{(n)} = fm^{(n-1)} + \Delta fm^{(n)} \tag{18.99}$$

The increment in the failure measure associated with the current time step ($\Delta fm^{(n)}$) is calculated as follows:

$$\Delta fm^{(n)} = \frac{\Delta\bar{\varepsilon}^{p^{(n)}}}{\bar{\varepsilon}_f^p\left(\varkappa^{(n)}, \dot{\bar{\varepsilon}}^{p^{(n)}}, \Theta_p^{(n)}, T_t^{(n)}\right)} \tag{18.100}$$

where $\Delta\bar{\varepsilon}^{p^{(n)}}$ is the current step's increment in equivalent plastic strain, and $\bar{\varepsilon}_f^p\left(\varkappa^{(n)}, \dot{\bar{\varepsilon}}_{p^{(n)}}, \Theta_p^{(n)}, T_t^{(n)}\right)$ is the failure strain for the current increment, provided by the failure function.

During the time step in which the failure measure just reaches or exceeds the failure initiation criterion, the failure stress (σ_e^f) and failure displacement (u^f) are determined. This is done iteratively during the line search portion of the return mapping algorithm, and consists of a process where the line search parameter ($\alpha^{(j)}$) is successively modified until the failure measure just equals 1.0.The value returned by the hardening function when this occurs is the stress utilized as the failure stress (σ_e^f) and the failure displacement is calculated as follows.

$$u^f = \frac{2G_f}{\sigma_e^f} \tag{18.101}$$

where G_f is the material's fracture energy.

Once the failure initiation criterion has been satisfied, the yield strength of the material remains constant and is set equal to the failure stress. In addition, increasing plastic deformation of the material results in the accumulation of damage (D). Damage is calculated as follows:

$$D^{(n)} = D^{(n-1)} + \frac{L\Delta\bar{\varepsilon}_f^{p^{(n)}}}{u^f} \tag{18.102}$$

where $D^{(n-1)}$ is the damage accumulated in the material through the previous time step, $\Delta\bar{\varepsilon}_f^{p^{(n)}}$ is the change in the equivalent plastic strain associated with the current time step (including only plastic strains that have occurred after the failure initiation criterion has been satisfied), and L is the characteristic length associated with the material integration point (taken as $\sqrt[3]{V_{ipt}}$, where V_{ipt} is the volume of material associated with the material integration point). As damage accumulates in the material, both the strength, and indirectly, the stiffness of the material are degraded. This degradation is accomplished by returning the damage adjusted stresses (σ_D) at the conclusion of the material integration step, as follows.

$$\sigma_D^{(n)} = (1 - D)\sigma^{(n)} = \varphi\sigma^{(n)} \tag{18.103}$$

where $\varphi = (1 - D)$ defines the decay value for the damaged material. This effectively results in a response where the material strength and stiffness are degraded. It is important to note that the pressure stresses are only degraded when the pressure is tensile (negative pressures). When the pressure is compressive, the pressure stress components of $\sigma^{(n)}$ are not degraded as indicated in Equation 18.103. The material strength and stiffness are continually degraded with increasing plastic deformation until the material is fully damage ($D = 1$) or the decay value (φ) has reached a critical decay value specified by the user (φ_r), at which point the material point is flagged for removal from the analysis.

18.12.5 Verification

The hydra plasticity model was verified through comparison of results from the material model with results obtained from the general metal plasticity model in Abaqus/Explicit (Version 6.14). A series of six element tests were designed to verify all of the hydra plasticity model's capabilities.

Description of Six Element Test Cases

Five test cases in total were performed. For each of the five test cases, six elements were loaded using six different prescribed velocities - the goal being to test the hydra plasticity model performs as expected for a variety of different stress states. These elements are not connected in any way, so each of the six element test cases are actually six single element tests performed at the same time. Elements 1, 2, and 3 were loaded to cause a tension stress state in the σ_{xx}, σ_{yy}, and σ_{zz} components respectively. Elements 4, 5, and 6 were loaded to cause shear dominated stress states - though not pure shear - with the dominant component of stress in the τ_{xx}, τ_{yy}, and τ_{zz} and component respectively. Figure 18.2 shows the six elements in an undeformed (top) and deformed (bottom) configuration. The deformed configuration shown is chosen from an arbitrary state in time prior to the failure of any of the elements and is intended only to illustrate the types of loadings applied.

A test case matrix was developed to verify the capabilities of the hydra plasticity model over a range of inputs. Table 18.8 below shows the five test cases developed. Test cases 1 through 4 test different combinations of low (300 K) and high (700 K) temperatures and load and high load rates (resulting in a range of strain rates tested). Test cases 1 through 4 all have Hill ratios that vary between 0.90 and 1.20. Test case 5 tests the adiabatic heating capability of the hydra plasticity model. Because Abaqus does not allow adiabatic heating for a Hill surface all of the Hill ratios were set to 1.0 in the hydra plasticity model to create a Mises yield surface.

Table 18.8: Hydra plasticity test case matrix

Test Case	Temp (K)	load rate (m/s)	Failure Included	Adiabatic Heating Included	Hill Ratios (R11, R22, R33, R12, R23, R31)
1	300	1	Yes	No	1.00, 1.15, 0.90, 1.00, 1.20, 0.95
2	700	1	Yes	No	1.00, 1.15, 0.90, 1.00, 1.20, 0.95
3	300	10	Yes	No	1.00, 1.15, 0.90, 1.00, 1.20, 0.95
4	700	10	Yes	No	1.00, 1.15, 0.90, 1.00, 1.20, 0.95
5	300	1	Yes	Yes	all 1.00 = Mises

A set of hardening data was defined for all five test cases. A python script was used to generate the same data formatted for the hydra plasticity model and an Abaqus general metal plasticity model. The hardening data used for the test cases was dependent on equivalent plastic strain, temperature, and equivalent plastic strain rate. Figure 18.3 shows the data points used to define yield stress as a function equivalent plastic strain at various temperatures and equivalent plastic strain rates. Both the hydra plasticity model and the Abaqus general metal plasticity model use linear interpolation between most of the data points to obtain the yield stress (the exception being the equivalent plastic strain rate direction which for the test cases include the hydra plasticity model had the PLASTIC STRAIN RATE LOG FLAG set to true and Abaqus by default uses log interpolation between for

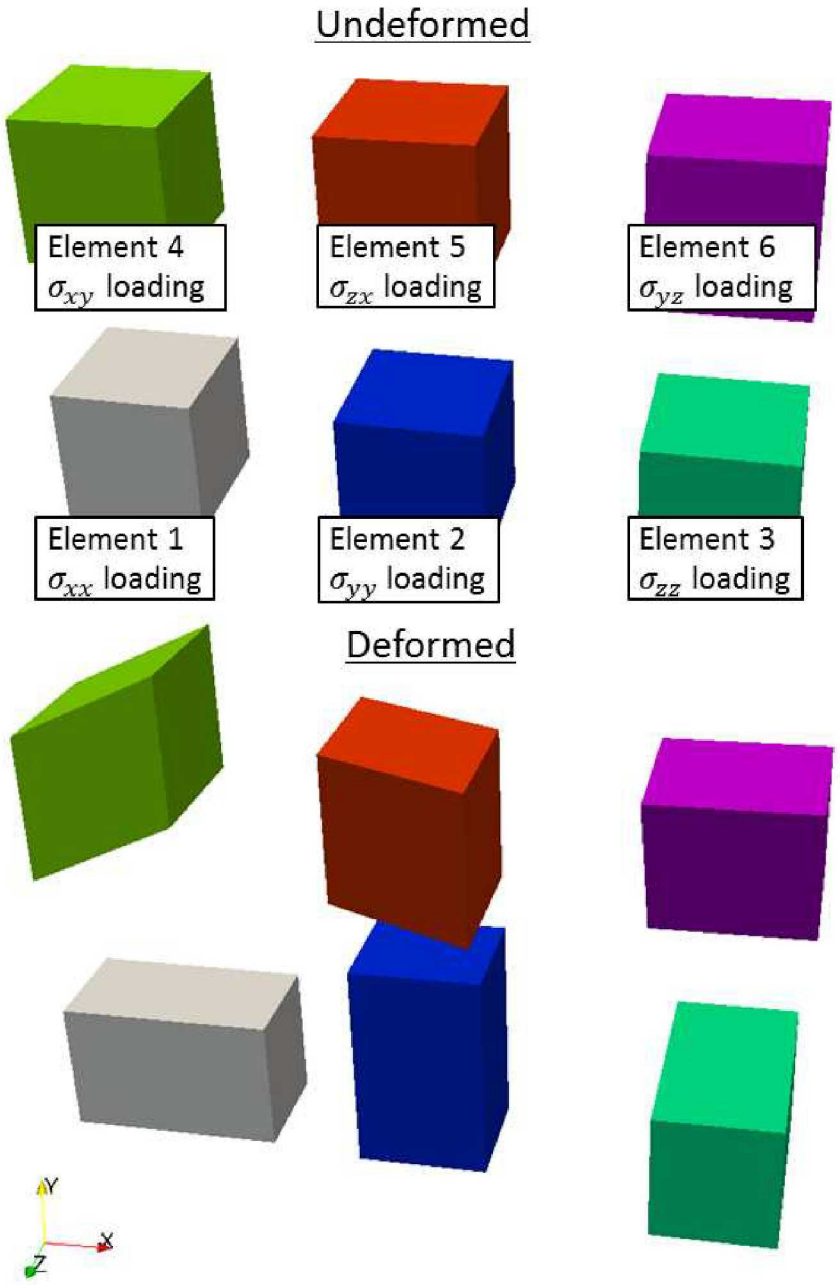

Figure 18.2: Undeformed (top) and deformed (bottom) shapes for the six element tests.

strain rate data).

A set of failure data was also defined for all five test cases. Again, a python script was used to generate the same data formatted for the hydra plasticity model and an Abaqus general metal plasticity model. The failure data used for the test cases was dependent on stress triaxiality, temperature, equivalent plastic strain rate, and Lode angle (via the Lode parameter). Figure 18.4 shows the data points used to define failure strain as a function of stress triaxiality at various temperatures, equivalent plastic strain rates, and Lode parameters. Again, both the hydra plasticity model and the

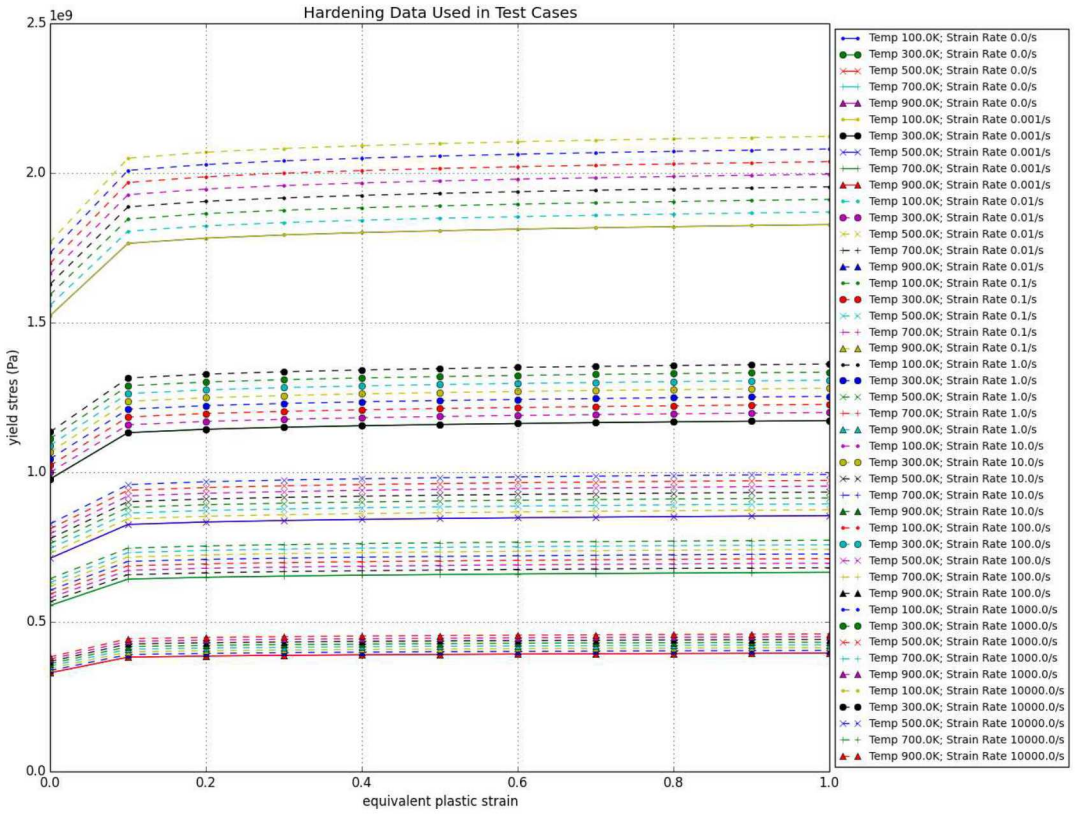

Figure 18.3: Hardening data used in all five test cases.

Abaqus general metal plasticity model use linear interpolation between the data points to obtain the failure strain.

Comparison of Results

The five test cases were each run in Sierra using the hydra plasticity model, and Abaqus using the general plasticity model. The results of the five test cases are presented in Figures 4 through 8. Each of these figures presents the equivalent plastic strain in an element versus the unrotated stress in the element in the dominant loading direction. For example, for element 1 which is loaded in the σ_{xx} component the y-axis represents the unrotated stress σ_{xx}; for element 4 which is dominantly loaded in the component the y-axis represents the unrotated stress τ_{xx}; etc.

Figure 18.5 shows the results from test case 1, where the temperature was set to 300 K and the loading rate was 1 m/s. The figure shows that there is near perfect agreement between Sierra and Abaqus for all of the tension loaded elements (elements 1, 2, and 3). As expected, the tension loaded elements all fail at the same equivalent plastic strain since they all use the same failure data. The agreement between Sierra and Abaqus is very close for the shear dominated loading elements (elements 4, 5, and 6) with less agreement as the plastic strain increases.

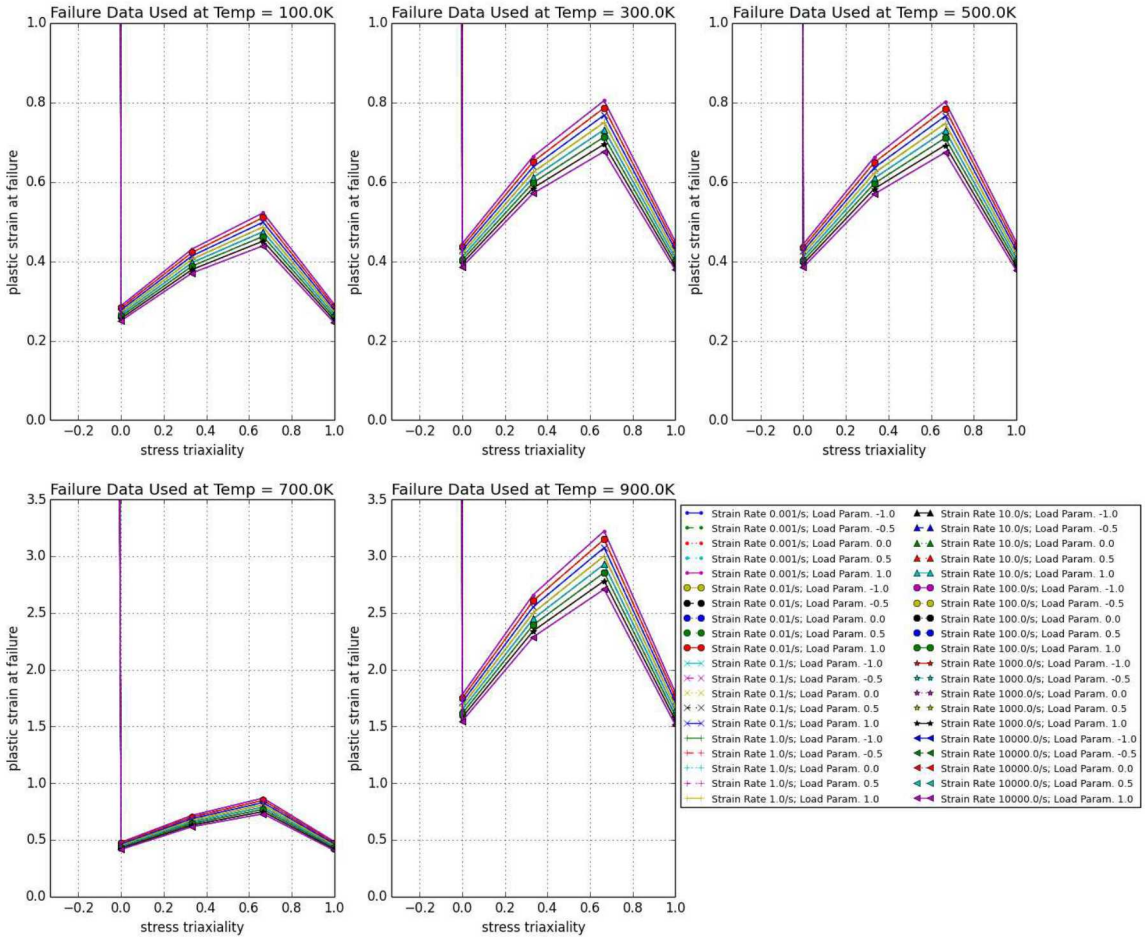

Figure 18.4: Failure data used in all five test cases.

Figure 18.6 shows the results from test case 2, where the temperature was set to 700 K and the loading rate was 1 m/s. Again, the figure shows that there is near perfect agreement between Sierra and Abaqus for all of the tension loaded elements (elements 1, 2, and 3). And again, as expected the tension loaded elements all fail at the same equivalent plastic strain since they all use the same failure data. Also, the agreement between Sierra and Abaqus is very close for the shear dominated loading elements (elements 4, 5, and 6) with less agreement as the plastic strain increases.

Figure 18.7 shows the results from test case 3, where the temperature was set to 300 K and the loading rate was 10 m/s. The figure shows that there is very close agreement between Sierra and Abaqus for all of the tension loaded elements (elements 1, 2, and 3). However, there is some minor disagreement between the two sets at very low plastic strains. And again, as expected the tension loaded elements all fail at the same equivalent plastic strain since they all use the same failure data. Also, the agreement between Sierra and Abaqus is very close for the shear dominated loading

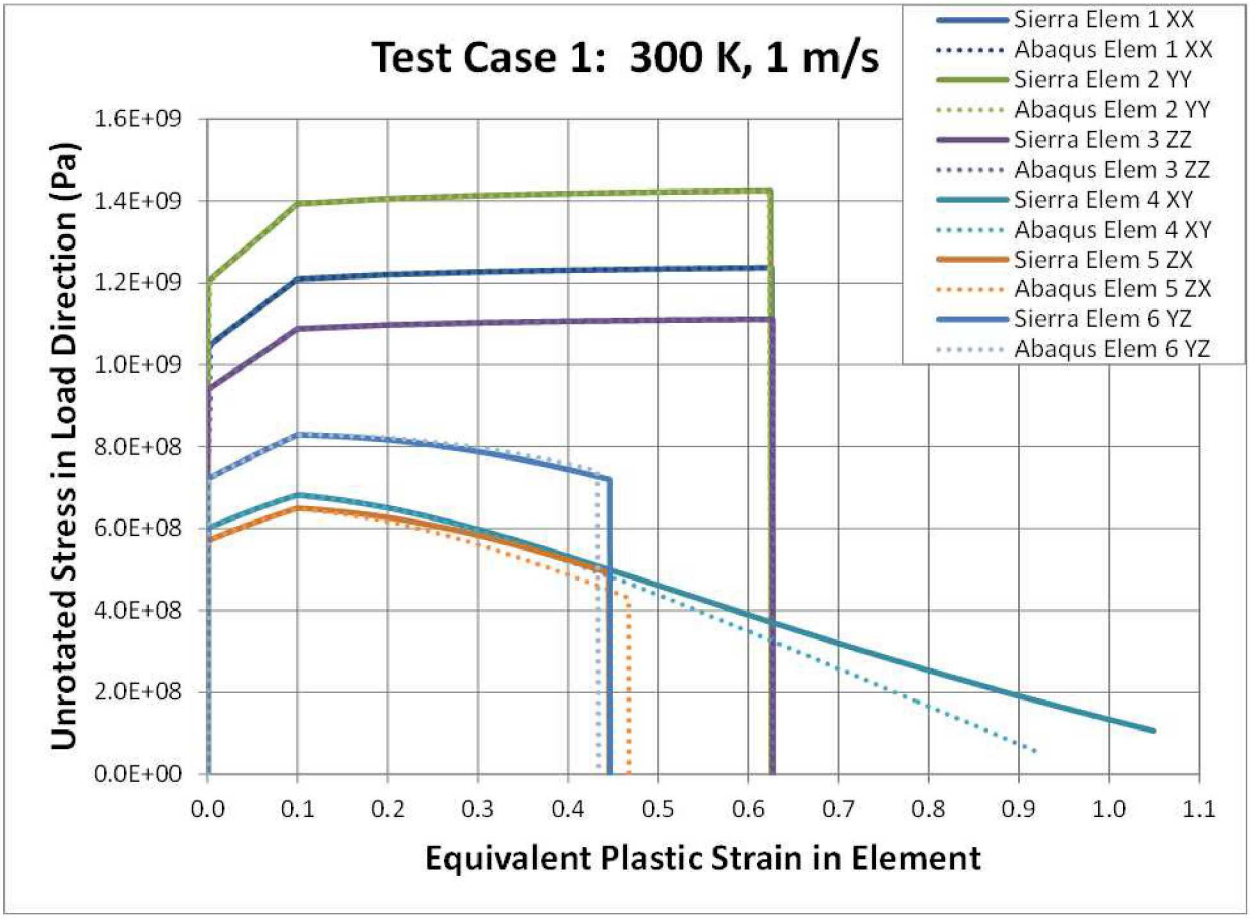

Figure 18.5: Comparison of results from test case 1.

elements (elements 4, 5, and 6) with less agreement as the plastic strain increases.

Figure 18.8 shows the results from test case 4, where the temperature was set to 700 K and the loading rate was 10 m/s. Again, the figure shows that there is good agreement between Sierra and Abaqus for all of the tension loaded elements (elements 1, 2, and 3). However, there is more discrepancy between the two sets of data at low plastic strains. And again, as expected the tension loaded elements all fail at the same equivalent plastic strain since they all use the same failure data. Also, the agreement between Sierra and Abaqus is very close for the shear dominated loading elements (elements 4, 5, and 6) with less agreement as the plastic strain increases.

Figure 18.9 shows the results from test case 5, the test case that includes adiabatic heating and the Hill ratios are all set to 1.0 (which is equivalent to the Mises surface). For this case the temperature was set to 300 K and the loading rate was 1 m/s. Because the Hill ratios are all the same the results from the three tension elements all lie right on top of each other in the figure; likewise the results from the three shear elements all lie right on top of each other. The figure shows that there is very good agreement between Sierra and Abaqus for all of the tension loaded elements (elements 1, 2, and 3). As expected, the tension loaded elements all fail at the same equivalent plastic strain since they all use the same failure data. The agreement between Sierra and Abaqus is very close for the shear dominated loading elements (elements 4, 5, and 6) with less agreement as the plastic strain

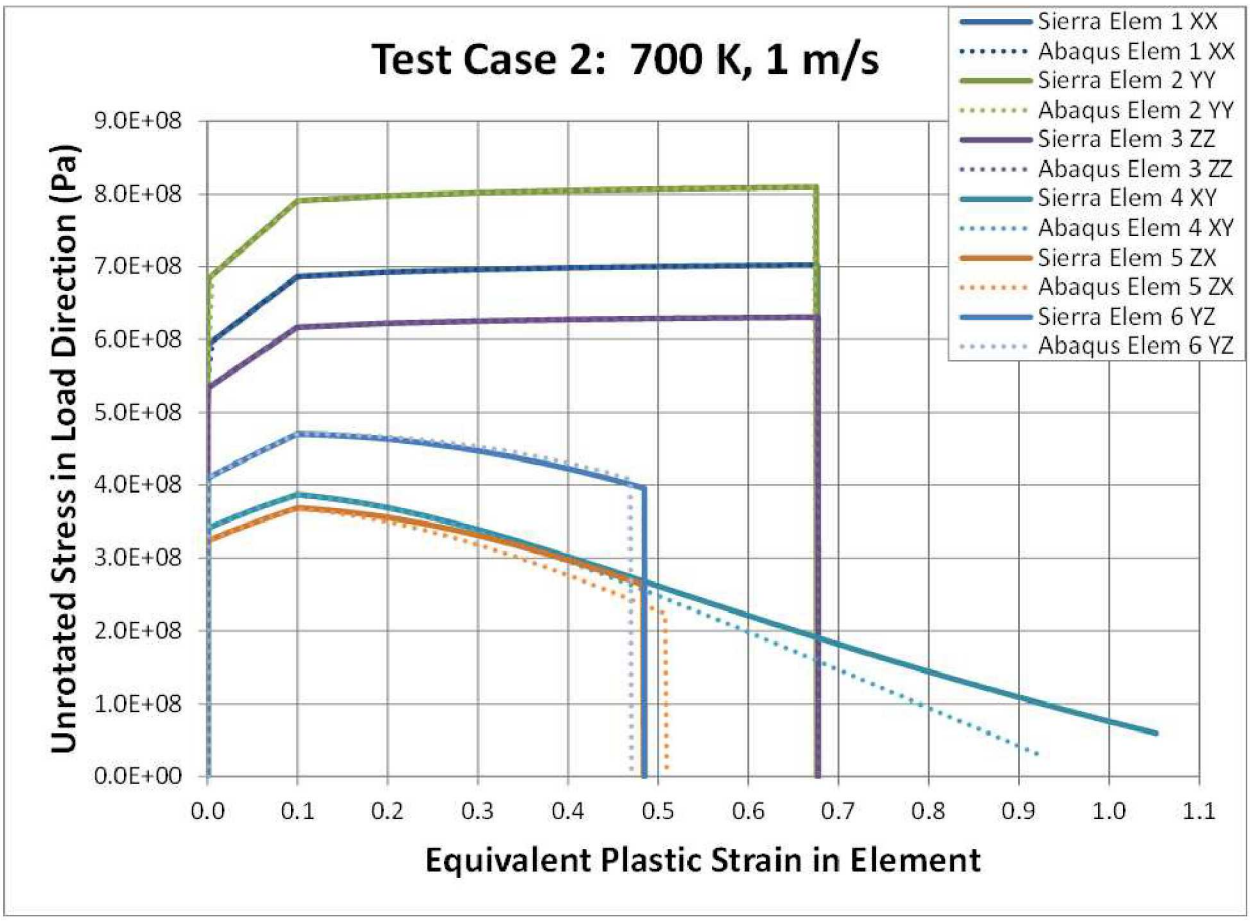

Figure 18.6: Comparison of results from test case 2.

increases.

Conclusions

The hydra plasticity model was verified by comparing the hydra plasticity model to a similar model in Abaqus. Five sets of six single element tests that exercised a range of features in the hydra plasticity model were used for the verification. Nearly perfect agreement between the hydra plasticity model and the Abaqus model was found in the tensile loaded elements. At higher temperatures, some minor differences between the two models was seen at low plastic strains. Good agreement was found between the two models in the shear loaded elements; however, there are non-trivial differences at larger strains. While every attempt was made to make the models in Sierra using hydra plasticity and the models Abaqus/Explicit using the generalized plasticity model to be the same there may be some differences in non-material model algorithms or options that would result in discrepancies.

While the above tests are comprehensive, additional verification may benefit the model. Additional verification should focus on the hydra plasticity model's ability to recovering the data input by the hardening and failure functions under simple loading conditions.

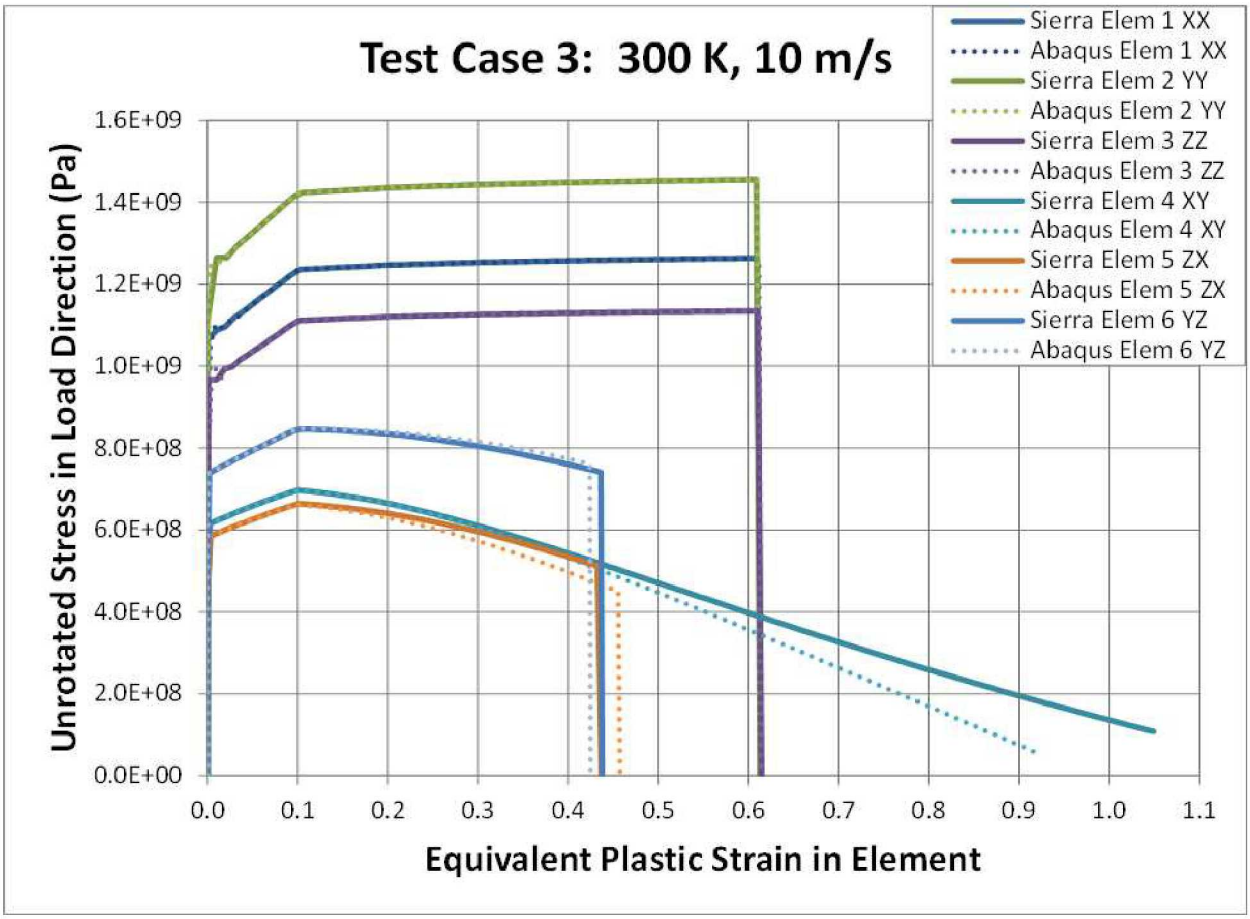

Figure 18.7: Comparison of results from test case 3.

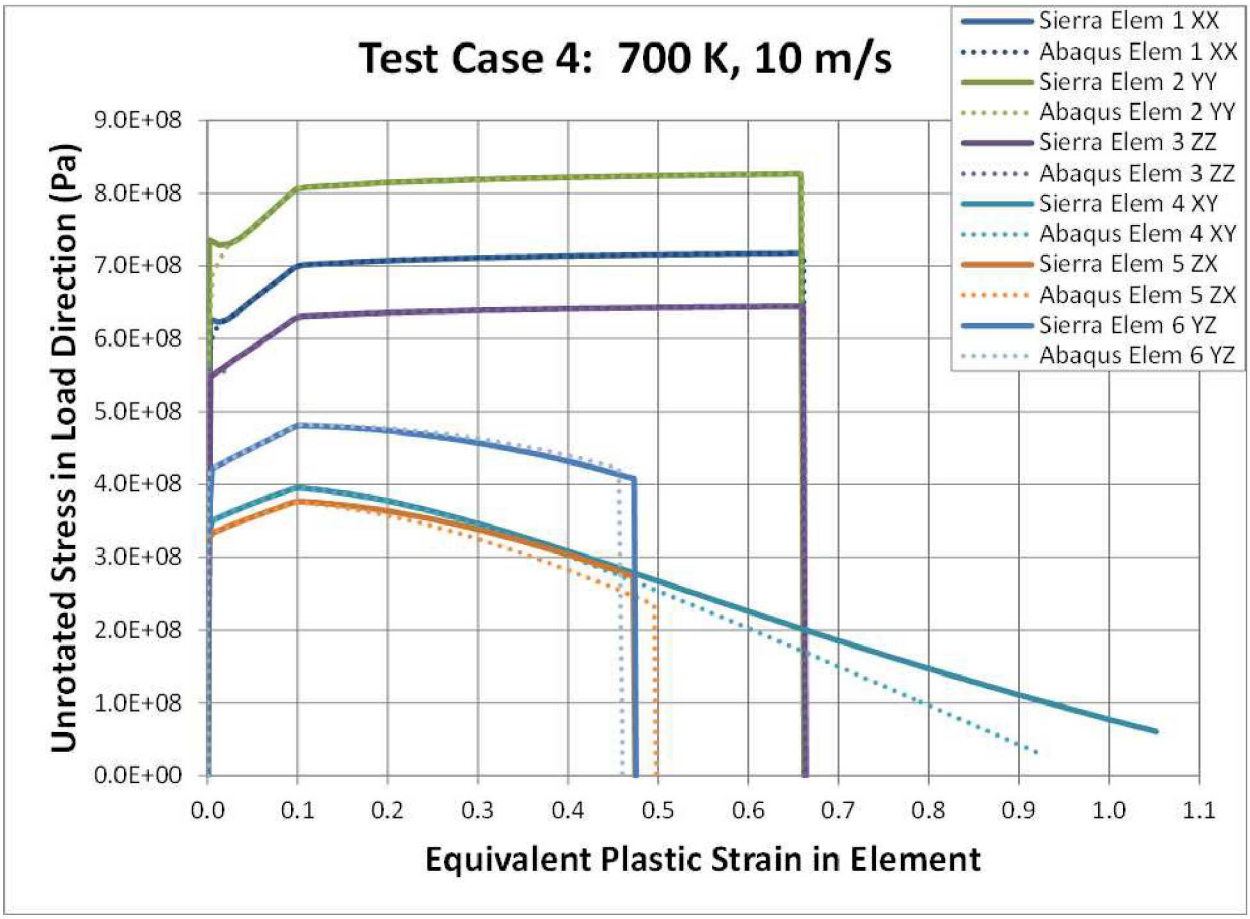

Figure 18.8: Comparison of results from test case 4.

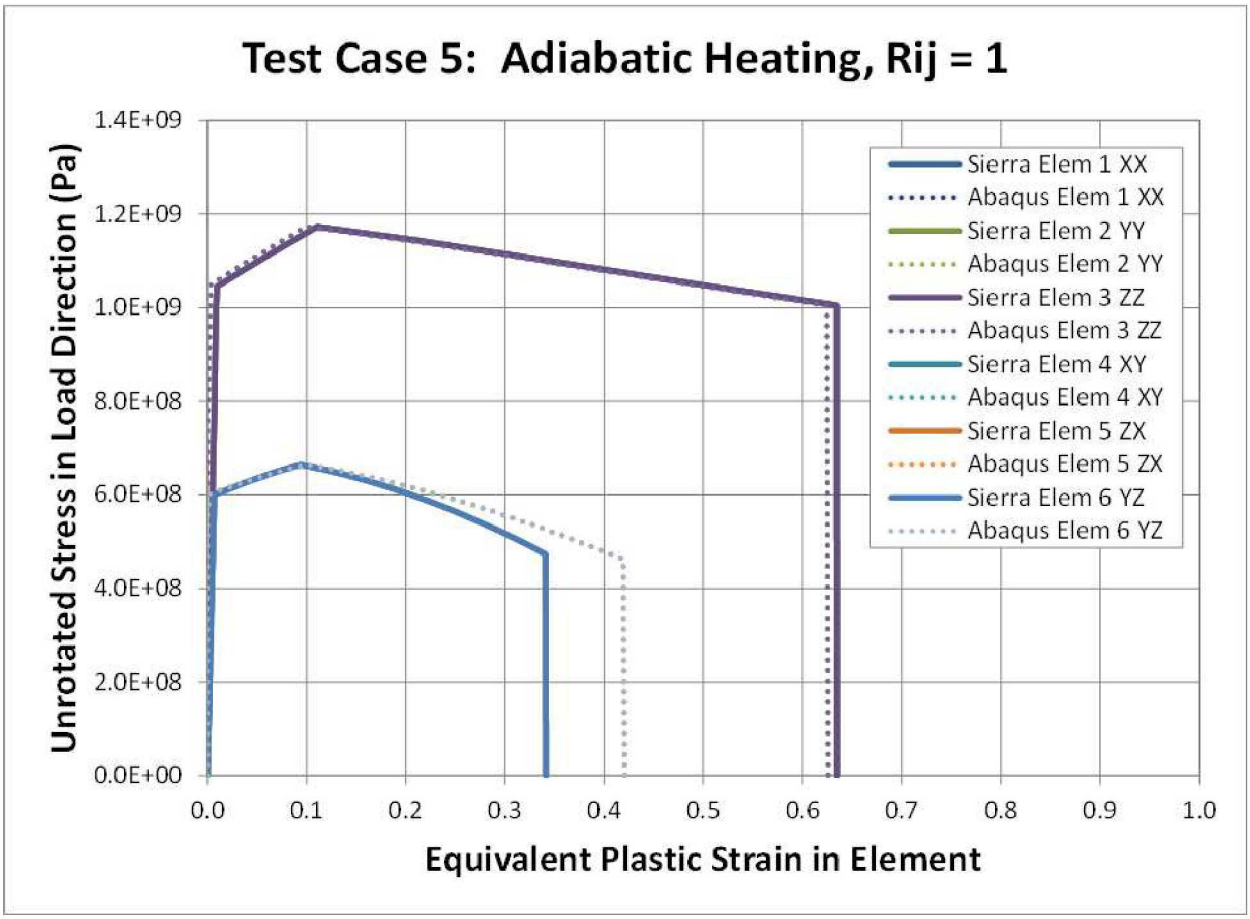

Figure 18.9: Comparison of results from test case 5.

18.13 NLVE 3D Orthotropic Model

```
BEGIN PARAMETERS FOR MODEL NLVE_3D_ORTHOTROPIC
  #
  # Elastic constants
  #
  YOUNGS MODULUS = <real> E
  POISSONS RATIO = <real> ν
  SHEAR MODULUS  = <real> G
  BULK MODULUS   = <real> K
  LAMBDA         = <real> λ
  TWO MU         = <real> 2μ
  #
  # Material coordinates system definition
  #
  COORDINATE SYSTEM             = <string> coordinate_system_name
  DIRECTION FOR ROTATION        = <real> 1|2|3
  ALPHA                         = <real> α1 (degrees)
  SECOND DIRECTION FOR ROTATION = <real> 1|2|3
  SECOND ALPHA                  = <real> α2 (degrees)
  #
  #
  #
  FICTITIOUS LOGA FUNCTION = <string>fict_loga_function_name
  FICTITIOUS LOGA SCALE FACTOR = <real>fict_loga_scale_factor
  #
  # In each of the five "PRONY" command lines and in
  # the RELAX TIME command line, the value of i can be from
  # 1 through 30
  #
  1PSI PRONY <integer>i = <real>psi1_i
  2PSI PRONY <integer>i = <real>psi2_i
  3PSI PRONY <integer>i = <real>psi3_i
  4PSI PRONY <integer>i = <real>psi4_i
  5PSI PRONY <integer>i = <real>psi5_i
  RELAX TIME <integer>i = <real>tau_i
  REFERENCE TEMP = <real>tref
  REFERENCE DENSITY = <real>rhoref
  WLF C1 = <real>wlf_c1
  WLF C2 = <real>wlf_c2
  B SHIFT CONSTANT = <real>b_shift
  SHIFT REF VALUE = <real>shift_ref
  WWBETA 1PSI = <real>wwb_1psi
  WWTAU 1PSI = <real>wwt_1psi
  WWBETA 2PSI = <real>wwb_2psi
  WWTAU 2PSI = <real>wwt_2psi
  WWBETA 3PSI = <real>wwb_3psi
  WWTAU 3PSI = <real>wwt_3psi
```

```
WWBETA 4PSI = <real>wwb_4psi
WWTAU 4PSI = <real>wwt_4psi
WWBETA 5PSI = <real>wwb_5psi
WWTAU 5PSI = <real>wwt_5psi
DOUBLE INTEG FACTOR = <real>dble_int_fac
REF RUBBERY HCAPACITY = <real>hcapr
REF GLASSY HCAPACITY = <real>hcapg
GLASS TRANSITION TEM = <real>tg
REF GLASSY C11 = <real>c11g
REF RUBBERY C11 = <real>c11r
REF GLASSY C22 = <real>c22g
REF RUBBERY C22 = <real>c22r
REF GLASSY C33 = <real>c33g
REF RUBBERY C33 = <real>c33r
REF GLASSY C12 = <real>c12g
REF RUBBERY C12 = <real>c12r
REF GLASSY C13 = <real>c13g
REF RUBBERY C13 = <real>c13r
REF GLASSY C23 = <real>c23g
REF RUBBERY C23 = <real>c23r
REF GLASSY C44 = <real>c44g
REF RUBBERY C44 = <real>c44r
REF GLASSY C55 = <real>c55g
REF RUBBERY C55 = <real>c55r
REF GLASSY C66 = <real>c66g
REF RUBBERY C66 = <real>c66r
REF GLASSY CTE1 = <real>cte1g
REF RUBBERY CTE1 = <real>cte1r
REF GLASSY CTE2 = <real>cte2g
REF RUBBERY CTE2 = <real>cte2r
REF GLASSY CTE3 = <real>cte3g
REF RUBBERY CTE3 = <real>cte3r
LINEAR VISCO TEST = <real>lvt
T DERIV GLASSY C11 = <real>dc11gdT
T DERIV RUBBERY C11 = <real>dc11rdT
T DERIV GLASSY C22 = <real>dc22gdT
T DERIV RUBBERY C22 = <real>dc22rdT
T DERIV GLASSY C33 = <real>dc33gdT
T DERIV RUBBERY C33 = <real>dc33rdT
T DERIV GLASSY C12 = <real>dc12gdT
T DERIV RUBBERY C12 = <real>dc12rdT
T DERIV GLASSY C13 = <real>dc13gdT
T DERIV RUBBERY C13 = <real>dc13rdT
T DERIV GLASSY C23 = <real>dc23gdT
T DERIV RUBBERY C23 = <real>dc23rdT
T DERIV GLASSY C44 = <real>dc44gdT
T DERIV RUBBERY C44 = <real>dc44rdT
```

```
T DERIV GLASSY C55 = <real>dc55gdT
T DERIV RUBBERY C55 = <real>dc55rdT
T DERIV GLASSY C66 = <real>dc66gdT
T DERIV RUBBERY C66 = <real>dc66rdT
T DERIV GLASSY CTE1 = <real>dcte1gdT
T DERIV RUBBERY CTE1 = <real>dcte1rdT
T DERIV GLASSY CTE2 = <real>dcte2gdT
T DERIV RUBBERY CTE2 = <real>dcte2rdT
T DERIV GLASSY CTE3 = <real>dcte3gdT
T DERIV RUBBERY CTE3 = <real>dcte3rdT
T DERIV GLASSY HCAPACITY = <real>dhcapgdT
T DERIV RUBBERY HCAPACITY = <real>dhcaprdT
REF PSIC = <real>psic_ref
T DERIV PSIC = <real>dpsicdT
T 2DERIV PSIC = <real>d2psicdT2
PSI EQ 2T = <real>psitt
PSI EQ 3T = <real>psittt
PSI EQ 4T = <real>psitttt
PSI EQ XX 11 = <real>psiXX11
PSI EQ XX 22 = <real>psiXX22
PSI EQ XX 33 = <real>psiXX33
PSI EQ XX 12 = <real>psiXX12
PSI EQ XX 13 = <real>psiXX13
PSI EQ XX 23 = <real>psiXX23
PSI EQ XX 44 = <real>psiXX44
PSI EQ XX 55 = <real>psiXX55
PSI EQ XX 66 = <real>psiXX66
PSI EQ XXT 11 = <real>psiXXT11
PSI EQ XXT 22 = <real>psiXXT22
PSI EQ XXT 33 = <real>psiXXT33
PSI EQ XXT 12 = <real>psiXXT12
PSI EQ XXT 13 = <real>psiXXT13
PSI EQ XXT 23 = <real>psiXXT23
PSI EQ XXT 44 = <real>psiXXT44
PSI EQ XXT 55 = <real>psiXXT55
PSI EQ XXT 66 = <real>psiXXT66
PSI EQ XT 1 = <real>psiXT1
PSI EQ XT 2 = <real>psiXT2
PSI EQ XT 3 = <real>psiXT3
PSI EQ XTT 1 = <real>psiXTT1
PSI EQ XTT 2 = <real>psiXTT2
PSI EQ XTT 3 = <real>psiXTT3
REF PSIA 11 = <real>psiA11
REF PSIA 22 = <real>psiA22
REF PSIA 33 = <real>psiA33
REF PSIA 12 = <real>psiA12
REF PSIA 13 = <real>psiA13
```

```
  REF PSIA 23 = <real>psiA23
  REF PSIA 44 = <real>psiA44
  REF PSIA 55 = <real>psiA55
  REF PSIA 66 = <real>psiA66
  T DERIV PSIA 11 = <real>dpsiA11dT
  T DERIV PSIA 22 = <real>dpsiA22dT
  T DERIV PSIA 33 = <real>dpsiA33dT
  T DERIV PSIA 12 = <real>dpsiA12dT
  T DERIV PSIA 13 = <real>dpsiA13dT
  T DERIV PSIA 23 = <real>dpsiA23dT
  T DERIV PSIA 44 = <real>dpsiA44dT
  T DERIV PSIA 55 = <real>dpsiA55dT
  T DERIV PSIA 66 = <real>dpsiA66dT
  REF PSIB 1     = <real> psiB1
  REF PSIB 2     = <real> psiB2
  REF PSIB 3     = <real> psiB3
  T DERIV PSIB 1 = <real> dpsiB1dT
  T DERIV PSIB 2 = <real> dpsiB2dT
  T DERIV PSIB 3 = <real> dpsiB3dT
  PSI POT TT     = <real> psipotTT
  PSI POT TTT    = <real> psipotTTT
  PSI POT TTTT   = <real> psipotTTTT
  PSI POT XT 1   = <real> psipotXT1
  PSI POT XT 2   = <real> psipotXT2
  PSI POT XT 3   = <real> psipotXT3
  PSI POT XTT 1  = <real> psipotXTT1
  PSI POT XTT 2  = <real> psipotXTT2
  PSI POT XTT 3  = <real> psipotXTT3
  PSI POT XXT 11 = <real> psipotXXT11
  PSI POT XXT 22 = <real> psipotXXT22
  PSI POT XXT 33 = <real> psipotXXT33
  PSI POT XXT 12 = <real> psipotXXT12
  PSI POT XXT 13 = <real> psipotXXT13
  PSI POT XXT 23 = <real> psipotXXT23
  PSI POT XXT 44 = <real> psipotXXT44
  PSI POT XXT 55 = <real> psipotXXT55
  PSI POT XXT 66 = <real> psipotXXT66
END [PARAMETERS FOR MODEL NLVE_3D_ORTHOTROPIC]
```

The NLVE three-dimensional orthotropic model is a nonlinear viscoelastic orthotropic continuum model that describes the behavior of fiber-reinforced polymer-matrix composites. In addition to being able to model the linear elastic and linear viscoelastic behaviors of such composites, it also can capture both “weak” and “strong” nonlinear viscoelastic effects such as stress dependence of the creep compliance and viscoelastic yielding. This model can be used in both Presto and Adagio.

Because the NLVE model is still under active development and also because it has an extensive list of command lines, we have not followed the typical approach in documenting this model.

18.14 Honeycomb Model

```
BEGIN PARAMETERS FOR MODEL HONEYCOMB
  #
  # Elastic constants
  #
  YOUNGS MODULUS = <real> E
  POISSONS RATIO = <real> ν
  SHEAR MODULUS  = <real> G
  BULK MODULUS   = <real> K
  LAMBDA         = <real> λ
  TWO MU         = <real> 2μ
  #
  # Orthotropic response
  #
  MODULUS_TTTT = <real> E^0_TTTT
  MODULUS_LLLL = <real> E^0_LLLL
  MODULUS_WWWW = <real> E^0_WWWW
  MODULUS_TTLL = <real> E^0_TTLL
  MODULUS_TTWW = <real> E^0_TTWW
  MODULUS_LLWW = <real> E^0_LLWW
  MODULUS_TLTL = <real> E^0_TLTL
  MODULUS_LWLW = <real> E^0_LWLW
  MODULUS_WTWT = <real> E^0_WTWT
  #
  # Material orientation
  #
  TX = <real> t_x
  TY = <real> t_y
  TZ = <real> t_z
  LX = <real> l_x
  LY = <real> l_y
  LZ = <real> l_z
  #
  # Yield behavior
  #
  YIELD_STRESS = <real> σ_y
  A1           = <real> A_1
  B1           = <real> B_1
  C1           = <real> C_1
  A2           = <real> A_2
  B2           = <real> B_2
  C2           = <real> C_2
  A3           = <real> A_3
  B3           = <real> B_3
  C3           = <real> C_3

  TS  = <real> T_s
```

```
  LS  = <real> L_s
  WS  = <real> W_s
  TLS = <real> TL_s
  LWS = <real> LW_s
  WTS = <real> WT_s

  ESTL = <real>
  ESTW = <real>
  ESLW = <real>
  ESLT = <real>
  ESWT = <real>
  ESWL = <real>

  MODULUS_FUNCTION = <string>
  RATE_FUNCTION    = <string>
  T_FUNCTION       = <string>
  L_FUNCTION       = <string>
  W_FUNCTION       = <string>
  TL_FUNCTION      = <string>
  LW_FUNCTION      = <string>
  WT_FUNCTION      = <string>
  TTP_FUNCTION     = <string>
  LLP_FUNCTION     = <string>
  WWP_FUNCTION     = <string>
  TLTLP_FUNCTION   = <string>
  LWLWP_FUNCTION   = <string>
  WTWTP_FUNCTION   = <string>
  TTLP_FUNCTION    = <string>
  TTWP_FUNCTION    = <string>
END [PARAMETERS FOR MODEL HONEYCOMB]
```

The honeycomb constitutive model is used to model the energy absorbing capabilities of aluminum honeycomb. There are three orthogonal material directions for the model: T, L, and W. The t-direction is generally considered as the "strong" direction, the W-direction is the "weak" direction, and the L-direction has an intermediate strength. This convention, however, does not necessarily need to be followed when defining material inputs.

$$\begin{Bmatrix} \dot{\sigma}_{TT} \\ \dot{\sigma}_{LL} \\ \dot{\sigma}_{WW} \\ \dot{\sigma}_{TL} \\ \dot{\sigma}_{LW} \\ \dot{\sigma}_{WT} \end{Bmatrix} = \begin{bmatrix} E_{TTTT} & E_{TTLL} & E_{TTWW} & 0 & 0 & 0 \\ E_{TTLL} & E_{LLLL} & E_{LLWW} & 0 & 0 & 0 \\ E_{TTWW} & E_{LLWW} & E_{WWWW} & 0 & 0 & 0 \\ 0 & 0 & 0 & E_{TLTL} & 0 & 0 \\ 0 & 0 & 0 & 0 & E_{LWLW} & 0 \\ 0 & 0 & 0 & 0 & 0 & E_{WTWT} \end{bmatrix} \begin{Bmatrix} \dot{d}_{TT} \\ \dot{d}_{LL} \\ \dot{d}_{WW} \\ \dot{d}_{TL} \\ \dot{d}_{LW} \\ \dot{d}_{WT} \end{Bmatrix} \tag{18.104}$$

Output variables available for this model are listed in Table 18.9.

Table 18.9: State Variables for HONEYCOMB Model

Index	Name	Variable Description
1	CRUSH	minimum volume ratio
2	EQDOT	effective strain rate
3	RMULT	rate multiplier
5	ITER	iterations
6	EVOL	volumetric strain

18.15 Viscoplastic Foam

```
BEGIN PARAMETERS FOR MODEL VISCOPLASTIC_FOAM
  #
  # Elastic constants
  #
  YOUNGS MODULUS = <real> E
  POISSONS RATIO = <real> ν
  SHEAR MODULUS  = <real> G
  BULK MODULUS   = <real> K
  LAMBDA         = <real> λ
  TWO MU         = <real> 2μ

  FLOW RATE      = <real> h
  POWER EXPONENT = <real> n
  BETA           = <real> β
  PHI            = <real> φ0

  SHEAR STRENGTH  = <real> A0
  SHEAR HARDENING = <real> A1
  SHEAR EXPONENT  = <real> A2
  HYDRO STRENGTH  = <real> B0
  HYDRO HARDENING = <real> B1
  HYDRO EXPONENT  = <real> B2

  YOUNGS FUNCTION    = <string> hE(θ)
  POISSONS FUNCTION  = <string> hν(θ)
  SS FUNCTION        = <string> hA0(θ)
  SH FUNCTION        = <string> hA1(θ)
  HS FUNCTION        = <string> hB0(θ)
  HH FUNCTION        = <string> hB1(θ)
  RATE FUNCTION      = <string> hh(θ)
  EXPONENT FUNCTION  = <string> hn(θ)
  STIFFNESS FUNCTION = <string> fE(φ)

  #Optional user-specified functions
  SHEAR HARDENING FUNCTION = <string> a(φ) #Do not specify A0, A1, A2
  HYDRO HARDENING FUNCTION = <string> b(φ) #Do not specify B0, B1, B2
  BETA FUNCTION            = <string> β(φ) #Do not specify β
END [PARAMETERS FOR MODEL VISCOPLASTIC_FOAM]
```

The viscoplastic foam model is used to model the rate (and temperature) dependent crushing of foams [15]. It is based on an additive split of the rate of deformation into an elastic and plastic portion

$$D_{ij} = D^{\mathrm{e}}_{ij} + D^{\mathrm{p}}_{ij}. \tag{18.105}$$

The stress in the material is due strictly to the elastic portion of the rate of deformation so that

$$\overset{\circ}{\sigma}_{ij} = \mathbb{C}_{ijkl} D^{\mathrm{e}}_{kl}, \tag{18.106}$$

where $\mathbb{C}_{ijkl}$ are the components of the fourth-order, isotropic elasticity tensor. The stress rate is arbitrary, as long as it is objective. Two objective stress rates are commonly used: the Jaumann rate and the Green-McInnis rate. For problems with fixed principal axes of deformation, these two rates give the same answers. For problems where the principal axes of deformation rotate during deformation, the two rates can give different answers. Generally speaking, there is no reason to pick one objective rate over another.

To describe the rate-dependent response, an over-stress-type yield function is used. Specifically, the rate-independent foam plasticity yield function

$$f = \frac{\bar{\sigma}^2}{a^2} + \frac{p^2}{b^2} - 1 \tag{18.107}$$

is rearranged such that,

$$f = \sigma^* - a, \tag{18.108}$$

where σ^* is the effective stress given by

$$\sigma^* = \sqrt{\bar{\sigma}^2 + \frac{a^2}{b^2} p^2}. \tag{18.109}$$

In (18.109), $\bar{\sigma}$ is the von Mises effective stress ($\bar{\sigma} = \sqrt{\frac{3}{2} s_{ij} s_{ij}}$) and p is the pressure resulting from a stress decomposition of the form,

$$\sigma_{ij} = s_{ij} - p\delta_{ij}. \tag{18.110}$$

Furthermore, a and b are state variables that are functions of the absolute temperature, θ, and maximum solid volume fraction, ϕ, and are defined as[3]

$$a(\theta, \phi) = A_0(\theta) + A_1(\theta)\, \phi^{A_2} \tag{18.111}$$

$$\tag{18.112}$$

$$b(\theta, \phi) = B_0(\theta) + B_1(\theta)\, \phi^{B_2}. \tag{18.113}$$

The temperature dependent material properties in the preceding relations are all defined as, $A_0(\theta) = A_0 h_{A_0}(\theta)$ where A_0 is the reference material parameter and $h_{A_0}(\theta)$ is the relative value as a function

[3] In addition to the given analytical expressions, a and b may be optionally specified as user defined functions of the maximum solid volume fraction. In these cases, however, the temperature dependence is neglected.

of temperature. In addition to the a and b state variables, the Young's modulus and Poisson's ratio are also functions of the absolute temperature. The latter may be written as $\nu(\theta) = \nu h_\nu(\theta)$ while the former is also dependent on the maximum volume fraction of solid material and is given as $E(\theta, \phi) = E h_E(\theta) f_E(\phi)$.

The maximum volume fraction of solid material, ϕ, is given by

$$\phi = \max_{t>0} \tilde{\phi}(t) \tag{18.114}$$

where $\tilde{\phi}(t)$ is the current volume fraction of solid material and is defined as,

$$\tilde{\phi}(t) = \frac{\phi_0}{\exp\left(\varepsilon_v^{\mathrm{p}}\right)} \tag{18.115}$$

with ϕ_0 being the initial solid volume fraction and $\varepsilon_v^{\mathrm{p}}$ is

$$\varepsilon_v^{\mathrm{p}} = \int_0^t D_{kk}^{\mathrm{p}} dt. \tag{18.116}$$

During inelastic deformation ($f > 0$), the corresponding rate of plastic deformation is given in a Perzyna-type form as,

$$D_{ij}^{\mathrm{p}} = \begin{cases} \exp(h(\theta)) \left(\dfrac{\sigma^*}{a} - 1\right)^{n(\theta)} g_{ij} & \text{if} \quad f > 0 \\ 0 & \text{if} \quad f < 0 \end{cases} \tag{18.117}$$

where $h(\theta)$ and $n(\theta)$ are the flow rate and power exponent respectively. The inelastic flow direction, g_{ij}, is given as a linear combination of the associated (with respect to (18.107)), g_{ij}^{a}, and radial, g_{ij}^{r},

$$g_{ij} = (1 - \beta) g_{ij}^{\mathrm{a}} + \beta g_{ij}^{\mathrm{r}}. \tag{18.118}$$

The directions g_{ij}^{a} and g_{ij}^{r} are given by

$$g_{ij}^{\mathrm{a}} = \frac{\frac{\partial f}{\partial \sigma_{ij}}}{|\frac{\partial f}{\partial \sigma_{kl}}|} = \frac{\frac{3}{a^2} s_{ij} - \frac{2}{3b^2} p \delta_{ij}}{|\frac{3}{a^2} s_{ij} - \frac{2}{3b^2} p \delta_{ij}|}, \tag{18.119}$$

$$g_{ij}^{\mathrm{r}} = \frac{\sigma_{ij}}{|\sigma_{kl}|} = \frac{\sigma_{ij}}{\sqrt{\sigma_{kl}\sigma_{kl}}}, \tag{18.120}$$

respectively. In this model, the flow rule weight, β, may be specified as either a constant value or as a function of the maximum solid volume fraction ($\beta = \beta(\phi)$).

In the above command blocks:

- Since the model requires functions to describe the temperature dependence of the elastic modulus and Poisson's ratio, it is recommended that one inputs these properties at some reference temperature. However, any two of the elastic constants can be used for input. Consult the User's Guide chapter on Material Models for more information on elastic constants input.
- The reference value for the flow rate, h, is defined with the `FLOW RATE` command line.
- The reference value of the over-stress exponent, n, is defined with the `POWER EXPONENT` command line.
- The user-defined scalar scaling between associated and radial flow, β, is defined with the `BETA` command line.
- The initial volume fraction of solid material, ϕ_0, is defined with the `PHI` command line.
- The reference value for the shear strength, A_0, is defined with the `SHEAR STRENGTH` command line.
- The reference value for the shear hardening modulus, A_1, is defined with the `SHEAR HARDENING` command line.
- The shear hardening exponent, A_2, is defined with the `SHEAR EXPONENT` command line.
- The reference value for the hydrostatic strength, B_0, is defined with the `HYDRO STRENGTH` command line.
- The reference value for the hydrostatic hardening modulus, B_1, is defined with the `HYDRO HARDENING` command line.
- The hydrostatic hardening exponent, B_2, is defined with the `HYDRO EXPONENT` command line.
- The user-defined and normalized function that gives the elastic modulus as a function of temperature, $h_E(\theta)$, is defined with the `YOUNGS FUNCTION` command line.
- The user-defined and normalized function that gives the Poisson's ratio as a function of temperature, $h_\nu(\theta)$, is defined with the `POISSONS FUNCTION` command line.
- The user-defined and normalized function that gives the shear strength as a function of temperature, $h_{A_0}(\theta)$, is defined with the `SS FUNCTION` command line.
- The user-defined and normalized function that gives the shear hardening modulus as a function of temperature, $h_{A_1}(\theta)$, is defined with the `SH FUNCTION` command line.
- The user-defined and normalized function that gives the hydrostatic strength as a function of temperature, $h_{B_0}(\theta)$, is defined with the `HS FUNCTION` command line.
- The user-defined and normalized function that gives the hydrostatic hardening modulus as a function of temperature, $h_{B_1}(\theta)$, is defined with the `HH FUNCTION` command line.

- The user-defined and normalized function that gives the flow rate as a function of temperature, $h_h(\theta)$, is defined with the `RATE FUNCTION` command line.
- The user-defined and normalized function that gives the over-stress exponent as a function of temperature, $h_n(\theta)$, is defined with the `EXPONENT FUNCTION` command line.
- The user-defined and normalized function that gives the elastic modulus as a function of maximum solid volume fraction, $f_E(\phi)$, is defined with the `STIFFNESS FUNCTION` command line.
- The optional user-defined function that gives the shear strength as a function of the maximum solid volume fraction, $a(\phi)$, is defined with the `SHEAR HARDENING FUNCTION` command line. Note, if this function is defined the `SHEAR STRENGTH`, `SHEAR HARDENING`, and `SHEAR EXPONENT` values should not be specified.
- The optional user-defended function that gives the hydrostatic strength as a function of the maximum solid volume fraction, $b(\phi)$, is defined with the `HYDRO HARDENING FUNCTION` command line. Note, if this function is defined the `HYDRO STRENGTH`, `HYDRO HARDENING`, and `HYDRO EXPONENT` values should not be specified.
- The optional user-defined function that gives the scaling between associated and radial flow as a function of maximum solid volume fraction, $\beta(\phi)$, is defined with the `BETA FUNCTION` command line. Note, if this function is defined the `BETA` value should not be specified.

Output variables available for this model are listed in Table 18.10.

Table 18.10: State Variables for VISCOPLASTIC FOAM Model 18.15

Name	**Description**
`ITER`	number of sub-increments
`EPVOL`	inelastic volumetric strain, $\varepsilon_v^{\mathrm{p}}$
`EDOT`	effective inelastic strain rate, $\dot{\bar{\varepsilon}}^p$
`PHI`	volume fraction of solid material, ϕ
`FA`	shear strength, a
`FB`	hydrostatic strength, b
`STIF`	elastic stiffness as a function of ϕ

18.16 Foam Damage

```
BEGIN PARAMETERS FOR MODEL FOAM_DAMAGE
  #
  # Elastic constants
  #
  YOUNGS MODULUS = <real> E
  POISSONS RATIO = <real> ν
  SHEAR MODULUS  = <real> G
  BULK MODULUS   = <real> K
  LAMBDA         = <real> λ
  TWO MU         = <real> 2μ
  #
  # Yield behavior
  #
  PHI                = <real> φ0
  FLOW RATE          = <real> h
  POWER EXPONENT     = <real> n
  TENSILE STRENGTH   = <real> c
  ADAM               = <real> a_dam
  BDAM               = <real> b_dam
  #
  # Functions
  #
  YOUNGS FUNCTION           = <string> h_E(θ)
  POISSONS FUNCTION         = <string> h_ν(θ)
  RATE FUNCTION             = <string> h_h(θ)
  EXPONENT FUNCTION         = <string> h_n(θ)
  SHEAR HARDENING FUNCTION  = <string> a(φ)
  HYDRO HARDENING FUNCTION  = <string> b(φ)
  BETA FUNCTION             = <string> β(φ)
  YOUNGS PHI FUNCTION       = <string> f_E(φ)
  POISSONS PHI FUNCTION     = <string> f_ν(φ)
  DAMAGE FUNCTION           = <string> w(ε_dam)
END [PARAMETERS FOR FOAM_DAMAGE]
```

The foam damage model was developed at Sandia National Laboratories to model the behavior of rigid polyurethane foams under a variety of loading conditions [16]. For instance, temperature, rate, and tension-compression dependencies are all built into this model. This model, leverages previous efforts and experience with other foam models. Consult the Sierra/SM User Manual chapter on Material Models for additional details. Like those past efforts, this model utilizes an additive decomposition of the strain rates into elastic and inelastic parts,

$$D_{ij} = D^{\mathrm{e}}_{ij} + D^{\mathrm{in}}_{ij}. \tag{18.121}$$

It is also assumed that the elastic response is linear and isotropic such that the stress rate for

isothermal conditions is given by the following equation

$$\overset{\circ}{\sigma}_{ij} = \mathbb{C}_{ijkl} D^{\mathrm{e}}_{kl} = \mathbb{C}_{ijkl} \left(D_{kl} - D^{\mathrm{in}}_{kl} \right), \tag{18.122}$$

with $\mathbb{C}_{ijkl}$ being the fourth-order, isotropic elasticity tensor. The specific stress rate considered is arbitrary as long as it is object. Two common rates satisfying that constraint are the Jaumann and Green-McInnis rates.

The initial yield surface is assumed to be an ellipsoid about the hydrostat and is described by the function

$$f = \frac{\bar{\sigma}^2}{a^2} + \frac{p^2}{b^2} - 1 = 0, \tag{18.123}$$

where a and b are state variables that define the current deviatoric and volumetric strengths, respectively, of the foam. The von Mises effective stress, $\bar{\sigma}$ is a scalar measure of the deviatoric stress given by

$$\bar{\sigma} = \sqrt{\frac{3}{2} s_{ij} s_{ij}}, \tag{18.124}$$

while p is the pressure, or mean stress, and is defined as

$$p = \frac{1}{3} \sigma_{kk}, \tag{18.125}$$

with σ_{ij} and s_{ij} being the components of the Cauchy and deviatoric stress. This latter tensor may be written as,

$$s_{ij} = \sigma_{ij} - p\delta_{ij}, \tag{18.126}$$

where δ_{ij} are the components of the identity tensor - $\delta_{ij} = 1$ if $i = j$, $\delta_{ij} = 0$ if $i \neq j$.

For this model, the yield function (18.123) is re-written as

$$f = \sigma^* - a = 0 \tag{18.127}$$

with the effective stress, σ^*, being a function of the von Mises effective stress, $\bar{\sigma}$, and the pressure, p, as follows

$$\sigma^* = \sqrt{\bar{\sigma}^2 + \frac{a^2}{b^2} p^2}. \tag{18.128}$$

Next, using a Perzyna-type formulation, the following expression for the inelastic strain rate, D_{ij}^{in}, is developed

$$D_{ij}^{\text{in}} = \begin{cases} \dot{\bar{\varepsilon}}^p \, g_{ij} = e^h \left(\dfrac{\sigma^*}{a} - 1 \right)^n g_{ij} & \text{if } \dfrac{\sigma^*}{a} - 1 > 0 \\ 0 & \text{if } \dfrac{\sigma^*}{a} - 1 \leq 0, \end{cases} \tag{18.129}$$

where g_{ij} are the components of a symmetric, second-order tensor that defines the orientation of the inelastic flow. This type of model is sometimes referred to as an over-stress model because the inelastic rate is a function of the over-stress - the distance outside the yield surface. For associated flow, g_{ij} is simply normal to the yield surface and is given by

$$g_{ij}^{\text{a}} = \frac{\dfrac{\partial f}{\partial \sigma_{ij}}}{\left| \dfrac{\partial f}{\partial \sigma_{kl}} \right|} = \frac{\dfrac{3}{a^2} s_{ij} + \dfrac{2}{3b^2} p \, \delta_{ij}}{\left| \dfrac{3}{a^2} s_{kl} + \dfrac{2}{3b^2} p \, \delta_{kl} \right|}. \tag{18.130}$$

When lower density foams are subjected to a simple load path like uniaxial compression, the inelastic flow direction at moderate strains appears nearly uniaxial. In other words, the flow direction is given by the normalized stress tensor as follows

$$g_{ij}^{\text{r}} = \frac{\sigma_{ij}}{|\sigma_{kl}|}. \tag{18.131}$$

This type of flow is called radial flow. The foam damage model has another parameter, β, which allows for the flow direction to be prescribed as a linear combination of associated and radial flow such that,

$$g_{ij} = \frac{(1-\beta) \, g_{ij}^{\text{a}} + \beta \, g_{ij}^{\text{r}}}{\left| (1-\beta) \, g_{kl}^{\text{a}} + \beta \, g_{kl}^{\text{r}} \right|}. \tag{18.132}$$

Rigid polyurethane foams have little ductility when they are subjected to tensile stress. For this loading case, the materials behave more like brittle materials and even for uniaxial compression the foams often show cracking at large strains.

The damage surfaces for the foam damage model are simply three orthogonal planes with the normals given by the positive principal stress axes. The damage surfaces are given by the following equation

$$f_{\text{dam}}^i = \hat{\sigma}^i - c \, (1 - w), \quad ; \quad i = 1, 2, 3 \tag{18.133}$$

where $\hat{\sigma}^i$ is a principal stress, c is the initial tensile strength which is a material parameter, and w is a scalar measure of the damage. As damage occurs, the damage surface will collapse toward the origin and the foam will lose tensile strength. The foam will, however, still have compressive strength.

Damage is taken to be a positive, monotonically increasing function of the damage strain, ε_{dam}, and the damage strain is a function of the maximum principal strain, $\varepsilon_{\max}$, and the plastic volume strain, ε_v^{p}, such that

$$w = w\left(\varepsilon_{\text{dam}}\right) \quad ; \quad \varepsilon_{\text{dam}} = a_{\text{dam}}\varepsilon_{\max} + b_{\text{dam}}\varepsilon_v^{\text{p}}, \tag{18.134}$$

with the material parameters a_{dam} and b_{dam} controlling the rate at which damage is generated in tension and compression, respectively. The model does not allow healing, so the damage never decreases even if the damage strain decreases.

To fully capture temperature, strain rate, and lock-up effects, several material parameters are defined as functions of temperature, θ, and/or some measure of the amount of compaction, e.g. the maximum volume fraction of the solid material obtained during any prior loading, ϕ. For instance,

$$\begin{aligned} E\left(\theta,\phi\right) &= E\, h_E\left(\theta\right)\, f_E\left(\phi\right), \\ \nu\left(\theta,\phi\right) &= \nu\, h_\nu\left(\theta\right)\, f_\nu\left(\phi\right), \end{aligned} \tag{18.135}$$

and the natural logarithm of the reference flow rate, h, and the power law exponent, n are also functions of temperature

$$\begin{aligned} h\left(\theta\right) &= h\, h_h\left(\theta\right) \\ n\left(\theta\right) &= n\, h_n\left(\theta\right). \end{aligned} \tag{18.136}$$

The current deviatoric and volumetric strengths are hardening functions of the maximum volume fraction of the solid material obtained during any prior loading, ϕ, as is the parameter that defines the fraction of associated and radial flow, β. Therefore,

$$\begin{aligned} a = a\left(\phi\right) \quad ; \quad b = b\left(\phi\right) \\ \beta = \beta\left(\phi\right). \end{aligned} \tag{18.137}$$

Through the loading cycle, the maximum volume fraction of solid material is written as,

$$\phi = \max_{t>0} \tilde{\phi}(t) \tag{18.138}$$

where $\tilde{\phi}(t)$ is the current volume faction of solid material defined as

$$\tilde{\phi}(t) = \frac{\phi_0}{\exp\left(\varepsilon_v^{\mathrm{p}}\right)}, \tag{18.139}$$

with ϕ_0 and $\varepsilon_v^{\mathrm{p}}$ being the initial solid volume fraction and plastic volumetric strain, respectively.

The foam damage model, as presented, provides a phenomenological model with enough flexibility to model the observed deformation and failure of rigid polyurethane foams.

- Consult the User's Guide chapter on Material Models for more information on elastic constants input.

Output variables available for this model are listed in Table 18.11. For information about the foam damage model, consult [16].

Table 18.11: State Variables for FOAM DAMAGE Model

Name	**Variable Description**
ITER	number of sub-increments taken in subroutine
EPVOL	plastic volume strain
PHI	maximum volume fraction of solid material
EQPS	equivalent plastic strain
FA	shear strength - a
FB	hydrostatic strength - b
DAMAGE	damage
EMAX	maximum tensile strain
PWORK	plastic work rate

18.17 Thermo EP Power Model

Output variables available for this model are listed in Table 18.12.

Table 18.12: State Variables for THERMO EP POWER Model

Index	Name	Variable Description
1	EQPS	equivalent plastic strain
2	RADIUS	radius of yield surface
3	BACK_STRESS_XX	back stress - xx component
4	BACK_STRESS_YY	back stress - yy component
5	BACK_STRESS_ZZ	back stress - zz component
6	BACK_STRESS_XY	back stress - xy component
7	BACK_STRESS_YZ	back stress - yz component
8	BACK_STRESS_ZX	back stress - zx component

18.18 Thermo EP Power Weld Model

Output variables available for this model are listed in Table 18.13.

Table 18.13: State Variables for THERMO EP POWER WELD Model

Index	Name	Variable Description
	EQPS	equivalent plastic strain
	RADIUS	radius of yield surface
	BACK_STRESS_XX	back stress - xx component
	BACK_STRESS_YY	back stress - yy component
	BACK_STRESS_ZZ	back stress - zz component
	BACK_STRESS_XY	back stress - xy component
	BACK_STRESS_YZ	back stress - yz component
	BACK_STRESS_ZX	back stress - zx component
	WELD_FLAG	

18.19 Universal Polymer Model

```
BEGIN PARAMETERS FOR MODEL UNIVERSAL_POLYMER
  #
  # Elastic constants
  #
  YOUNGS MODULUS = <real> E
  POISSONS RATIO = <real> ν
  SHEAR MODULUS  = <real> G
  BULK MODULUS   = <real> K
  LAMBDA         = <real> λ
  TWO MU         = <real> 2μ
  #
  #
  #
  WWBETA 1 = <real> β_1^w
  WWTAU 1  = <real> τ_1^w
  WWBETA 2 = <real> β_2^w
  WWTAU 2  = <real> τ_2^w
  SPECTRUM START TIME = <real> t_start
  SPECTRUM END TIME   = <real> t_end
  LOG TIME INCREMENT  = <real> dt
  BULK GLASSY 0  = <real> K_0^0
  BULK GLASSY 1  = <real> K_0^1
  BULK GLASSY 2  = <real> K_0^2
  BULK RUBBERY 0 = <real> K_∞^0
  BULK RUBBERY 1 = <real> K_∞^1
  BULK RUBBERY 2 = <real> K_∞^2
  VOLCTE GLASSY 0 = <real> α_0^0
  VOLCTE GLASSY 1 = <real> α_0^1
  VOLCTE GLASSY 2 = <real> α_0^2
  VOLCTE RUBBERY 0 = <real> α_∞^0
  VOLCTE RUBBERY 1 = <real> α_∞^1
  VOLCTE RUBBERY 2 = <real> α_∞^2
  SHEAR GLASSY 0 = <real> G_0^0
  SHEAR GLASSY 1 = <real> G_0^1
  SHEAR GLASSY 2 = <real> G_0^2
  SHEAR RUBBERY 0 = <real> G_∞^0
  SHEAR RUBBERY 1 = <real> G_∞^1
  SHEAR RUBBERY 2 = <real> G_∞^2
  REFERENCE TEMPERATURE   = <real> T_ref
  STRESS FREE TEMPERATURE = <real> T_sf
  WLF C1 = <real> Ĉ_1
  WLF C2 = <real> Ĉ_2
  CLOCK_C1 = <real> C_1
  CLOCK_C2 = <real> C_2
  CLOCK_C3 = <real> C_3
  CLOCK_C4 = <real> C_4
```

```
  CLOCK_C5 = <real> C5
  FILLER VOL FRACTION = <real> Vf
  #
  # In each of the five "PRONY" command lines and in
  # the RELAX TIME command line, the value of i can be from
  # 1 through 30
  #
  RELAX TIME <integer> i = <real> τi
  F1 <integer> i         = <real> f1 i
  F2 <integer> i         = <real> f2 i
END [PARAMETERS FOR MODEL UNIVERSAL_POLYMER]
```

The Universal Polymer model is a phenomenological, nonlinear viscoelastic material model for analyzing stresses and strains in glass-forming materials such as filled and unfilled polymers (e.g., thermoplastics, thermosets) and amorphous inorganic glasses. It represents a simplification of the Potential Energy Clock (PEC) nonlinear viscoelastic model [17, 18] which goes by the name NLVE polymer model in the Sierra codes. The material model was developed to predict the life-cycle behavior of encapsulated components and glass-to-metal seals in design and performance analyses. It predicts a full range of behavior including "yielding" (i.e., accelerations in rates of relaxation generated by deformations), stress relaxation, volume relaxation, creep and physical aging. The model uses a material clock driven by temperature, volume and strain histories (approximating the potential internal energy of NLVE material). The strain measure is obtained from the integration of the rate of deformation tensor. As a special feature, it does allow the user to initiate an analysis from a stress-free temperature, T_{sf}, that is different from the reference temperature, T_{ref}, where the material properties are defined.

The constitutive equation is

$$\begin{aligned}\boldsymbol{\sigma} = &\left[K_g(T) - K_\infty(T)\right]\int_0^t f_1(t^* - s^*)\frac{dI_1}{ds}ds\ \mathbf{I}\\ &-\left[K_g(T)\,\delta_g(T) - K_\infty(T)\,\delta_\infty(T)\right]\int_0^t f_1(t^* - s^*)\frac{dT}{ds}ds\ \mathbf{I}\\ &+2\left[G_g(T) - G_\infty(T)\right]\int_0^t f_2(t^* - s^*)\frac{d\boldsymbol{\varepsilon}_{dev}}{ds}ds\\ &\left[K_\infty(T)\,I_1 - K_\infty(T)\,\delta_\infty(T)\left(T - T_{sf}\right)\right]\mathbf{I} + 2G_\infty(T)\,\boldsymbol{\varepsilon}_{dev}\end{aligned} \tag{18.140}$$

The strain variables in the model are

$$I_1 = \mathrm{tr}\boldsymbol{\varepsilon} = \mathbf{I} : \boldsymbol{\varepsilon} \quad ; \quad \boldsymbol{\varepsilon}_{dev} = \boldsymbol{\varepsilon} - \frac{1}{3}I_1\mathbf{I} \tag{18.141}$$

The glassy bulk modulus is the instantaneous, short time bulk modulus, and it is a function of temperature

$$K_g\left(T\right) = K_{g_{ref}} + \frac{dK_g}{dT}\left(T - T_{ref}\right) = K_{g_{sf}} + \frac{dK_g}{dT}\left(T - T_{sf}\right) \tag{18.142}$$

while the equilibrium bulk modulus is the equilibrium, long time bulk modulus, and is also a function of temperature

$$K_\infty\left(T\right) = K_{\infty_{ref}} + \frac{dK_\infty}{dT}\left(T - T_{ref}\right) = K_{\infty_{sf}} + \frac{dK_\infty}{dT}\left(T - T_{sf}\right) \tag{18.143}$$

The volumetric thermal expansion coefficients have similar forms

$$\begin{aligned} \alpha_g\left(T\right) &= \alpha_{g_{ref}} + \frac{d\alpha_g}{dT}\left(T - T_{ref}\right) = \alpha_{g_{sf}} + \frac{d\alpha_g}{dT}\left(T - T_{sf}\right) \\ \alpha_\infty\left(T\right) &= \alpha_{\infty_{ref}} + \frac{d\alpha_\infty}{dT}\left(T - T_{ref}\right) = \alpha_{\infty_{sf}} + \frac{d\alpha_\infty}{dT}\left(T - T_{sf}\right) \end{aligned} \tag{18.144}$$

while $\delta_g(T)$ and $\delta_\infty(T)$ are the volumetric thermal strains in (18.140)

$$\delta_g(T) = \alpha_{g_{sf}} + \frac{1}{2}\frac{d\alpha_g}{dT}\left(T - T_{sf}\right) \quad ; \quad \delta_\infty(T) = \alpha_{\infty_{sf}} + \frac{1}{2}\frac{d\alpha_\infty}{dT}\left(T - T_{sf}\right) \tag{18.145}$$

The glassy and equilibrium shear moduli are similar, but they also have an I_2 dependence

$$\begin{aligned} G_g\left(T\right) &= G_{g_{ref}} + \frac{dG_g}{dT}\left(T - T_{ref}\right) + \frac{dG_g}{dI_2}I_2 = G_{g_{sf}} + \frac{dG_g}{dT}\left(T - T_{sf}\right) + \frac{dG_g}{dI_2}I_2 \\ G_\infty\left(T\right) &= G_{\infty_{ref}} + \frac{dG_\infty}{dT}\left(T - T_{ref}\right) + \frac{dG_\infty}{dI_2}I_2 = G_{\infty_{sf}} + \frac{dG_\infty}{dT}\left(T - T_{sf}\right) + \frac{dG_\infty}{dI_2}I_2 \end{aligned} \tag{18.146}$$

The relaxation functions in the integrands, f_1 and f_2, have similar forms. They can be represented with stretched exponential functions, while in the code they are evaluated using Prony series expansions

$$f_1(t) = \exp\left(-(t/\tau_1)^{\beta_1}\right) \approx \sum_{i=1}^{N} F_{1\,i} \exp\left(-t/\tau_i\right) \quad ; \quad \sum_{i=1}^{N} F_{1\,i} = 1$$
$$f_2(t) = \exp\left(-(t/\tau_2)^{\beta_2}\right) \approx \sum_{i=1}^{N} F_{2\,i} \exp\left(-t/\tau_i\right) \quad ; \quad \sum_{i=1}^{N} F_{2\,i} = 1 \tag{18.147}$$

The material clock is the fundamental feature of the model. The clock is defined by

$$t - s = \int_s^t \frac{dw}{a(w)} \quad ; \quad \log a = -\hat{C}_1 \left(\frac{N}{\hat{C}_2 + N}\right) \tag{18.148}$$

where

$$N = \left(T - T_{ref}\right) - \int_0^t f_1\left(t^* - s^*\right) \frac{dT}{ds} ds + C_3 \left[I_1(t) - \int_0^t f_1\left(t^* - s^*\right) \frac{dI_1}{ds} ds\right]$$
$$+ C_4 \int_0^t \int_0^t f\left(t^* - s^*, t^* - u^*\right) \frac{d\varepsilon_{dev}}{ds} : \frac{d\varepsilon_{dev}}{du} ds\, du \tag{18.149}$$

If the clock is represented by the WLF equation above T_g, we have

$$\log a = \frac{-C_1\left(T - T_{ref}\right)}{C_2 + \left(T - T_{ref}\right)} \tag{18.150}$$

Equating constants above T_g we obtain

$$\hat{C}_1 = C_1 \quad ; \quad \hat{C}_2 = C_2\left(1 + C_3 \alpha_{\infty_{ref}}\right) \tag{18.151}$$

$$f_v(t) = \exp\left[-\left(\frac{t}{\tau_v}\right)^{\beta_v}\right] \tag{18.152}$$

Output variables available for this model are listed in Table 18.14.

Table 18.14: State Variables for UNIVERSAL POLYMER Model

Name	Variable Description
AEND	
LOGA	potential energy clock

18.20 Other Undocumented Material Models

For a listing of other material models that exist in Sierra/SM See Table 18.15. Support for use of these models is limited.

Table 18.15: Other Material Models Available, but Undocumented

Material Name	Author
CDM EP	Shawn English
UNIVERSAL CURING MODEL	Kevin Long
THERMAL BATTERY SEPARATOR	Kevin Long
JOHNSON COOK DAMAGE	Bill Scherzinger
FROST ASHBY CREEP	Bill Scherzinger
ELASTIC PLASTIC FAIL	Bill Scherzinger
ELASTIC ORTHOTROPIC FAIL	Shawn English
HAIL ICE	Bill Scherzinger
ELASTO_VISCOPLASTIC	Arthur Brown
ELASTIC_UQ_SHELL	Mark Merewether
MLEP_WILKINS_FAIL	Mike Neilsen
UCP_FAIL	Mike Neilsen
SOLDER	
SOLDER_DAMAGE	
COULOMBMIXMODE	Shawn English
EVG	Jake Ostien
SPECTACULAR	Kevin Long
EPHYDROGEN	
HILL_PLASTICITY_DAMAGE	Jake Ostien
CRYSTAL_PLASTIC	David Littlewood

References

[1] S.W. Attaway, R.V. Matallucci, S.W. Key, K.B. Morrill, L.J. Malvar, and J.E. Crawford. Enhancements to Pronto3D to predict structural response to blast. Technical Report SAND2000-1017, Sandia National Laboratories, Albuquerque, NM, 2000. pdf.

[2] ACI318-08: Building code requirements for structural concrete and commentary. Farmington Hills, MI. American Concrete Institute, 2008.

[3] R.M. Brannon, A.F. Fossum, and O.E. Strack. Kayenta: Theory and user's guide. Technical Report SAND2009-2282, Sandia National Laboratories, Albuquerque, NM, 2009.

[4] D. C. Lagoudas, editor. *Shape Memory Alloys: Modeling and Engineering Application*. Springer, New York, NY USA, 2008.

[5] K. Otsuka and X. Ren. Physical metallurgy of Ti-Ni-based shape memory alloys. *Progress in Materials Science*, 50:511–678, 2005.

[6] D. Lagoudas, D. Hartl, Y. Chemisky, L. Machado, and P. Popov. Constitutive model for the numerical analysis of phase transformation in polycrystalline shape memory alloys. *International Journal of Plasticity*, 32-33:155–183, 2012.

[7] D. J. Hartl, D. C. Lagoudas, F. T. Calkins, and J. H. Mabe. Use of a Ni60Ti shape memory alloy for active jet engine chevron application: I. thermomechanical characterization. *Smart Materials and Structures*, 19:015020, 2010.

[8] D. J. Hartl, J. T. Mooney, D. C. Lagoudas, F. T. Calkins, and J. H. Mabe. Use of a Ni60Ti shape memory alloy for active jet engine chevron application: II. experimentally validated numerical analysis. *Smart Materials and Structures*, 19:015021, 2010.

[9] G.R. Johnson and W.H. Cook. A constitutive model and data for metals subjected to large strains, high strain rates and high temperatures. In *Proc. 7th. Int. Symp. on Ballistics*, pages 541–547, The Hague, The Netherlands, 1983.

[10] G.R. Johnson and W.H. Cook. Fracture characteristics of three metals subjected to various strains, strain rates, temperatures and pressures. *Engineering Fracture Mechanics*, 21(1): 31–48, 1985.

[11] A. P. Karafillis and M. C. Boyce. A general anisotropic yield criterion using bounds and a transformation weighting tensor. *Journal of the Mechanics and Physics of Solids*, 41(12): 1859–1886, 1993.

[12] E. A. Olevsky. Theory of sintering: from discrete to continuum. *Materials Science and Engineering*, R23:41–100, 1998.

[13] J. G. Argüello, M. W. Reiterer, and K. G. Ewsuk. Verification, performance, validation, and modifications to the SOVS continuum constitutive model in a nonlinear large-deformation finite element code. *Journal of the American Ceramic Society*, 92(7):1442–1449, 2009.

[14] E. A. Olevsky, V. Tikare, T. J. Garino, and M. V. Braginsky. Simulation of sintering of layered structures. In *Proceedings of PM2000: World Congress on Powder Metallurgy*, Kyoto, Japan, 2002. Japan Society of Powder and Powder Metallurgy.

[15] M. K. Neilsen, W. Y. Lu, B. Olsson, and T. Hinnerichs. A viscoplastic constitutive model for polyurethane foams. In *Proceedings ASME 2006 International Mechanical Engineering Congress and Exposition*, Chicago, IL, 2006. ASME.

[16] M. K. Neilsen, W. Y. Lu, W. M. Scherzinger, T. D. Hinnerichs, and C. S. Lo. Unified creep plasticity damage (UCPD) model for rigid polyurethane foams. Technical Report SAND2015-4352, Sandia National Laboratories, Albuquerque, NM, 2015.

[17] J. M. Caruthers, D. B. Adolf, R. S. Chambers, and P. Shrikhande. A thermodynamically consistent, nonlinear viscoelastic approach for modeling glassy polymers. *Polymer*, 45:4577–4597, 2004.

[18] D. B. Adolf, R. S. Chambers, and M. A. Neidigk. A simplified potential energy clock model for glassy polymers. *Polymer*, 50:4257–4269, 2009.

Chapter 19

Cohesive Material Models

This chapter describes the theory and usage of cohesive models in development. There are typically two different types of cohesive models – *intrinsic* and *extrinsic*. Intrinsic models are used for cohesive surfaces that are known *a priori* and are included in the model from the beginning. These models by definition produce zero traction for zero cohesive separation and have a loading region before failure. Extrinsic models are used when cohesive surfaces are dynamically inserted based on some material criteria. These models typically are initialized to produce an equilibrium traction at zero separation based on the cohesive zone insertion criteria. Section 19.1 describes the intrinsic cohesive zone models in development, whereas Section 19.2 describes the extrinsic models.

19.1 Intrinsic models

19.2 Extrinsic models

19.2.1 Tvergaard-Hutchinson

This model is an extension of the trapezoidal traction-separation model proposed by Tvergaard and Hutchinson [1] generalized to multiple dimensions. The generalization is performed by appropriately scaling the normal and tangential components of the traction and separation into the 1D model depicted in Figure 19.1. In Figure 19.1, λ_c is the normalized final cohesive opening in the effective space, λ_1 is the length of the initial loading branch of the model, λ_2 is the separation length that begins the failure branch of the model, and $\hat{\sigma}$ is the maximum effective traction of the cohesive zone. These parameters have the following restrictions on their values:

$$0 \leq \lambda_1 \leq \lambda_2 \leq \lambda_c = 1, \quad \hat{\sigma} > 0.$$

Finally, as shown in Figure 19.1, for $\lambda > \lambda_1$ unloading may be assumed towards the origin.

Assuming a loading condition ($\lambda > 0,\ \dot{\lambda} > 0$), the slope of the effective traction-separation model is evaluated as follows

$$\hat{t}' = \begin{cases} \hat{\sigma}/\lambda_1, & \lambda \in [0,\ \lambda_1) \\ \hat{\sigma}/\lambda, & \lambda \in [\lambda_1, \lambda_2) \\ \hat{\sigma}(1-\lambda)/(\lambda(1-\lambda_2)), & \lambda \in [\lambda_2, \lambda_c) \\ 0, & \lambda \geq \lambda_c \end{cases}$$

and the effective traction is computed as $\hat{t} = \hat{t}'\lambda$.

The effective traction-separation model is extended to 3D by defining the following additional values:

- The normal failure separation, δ_{cn}

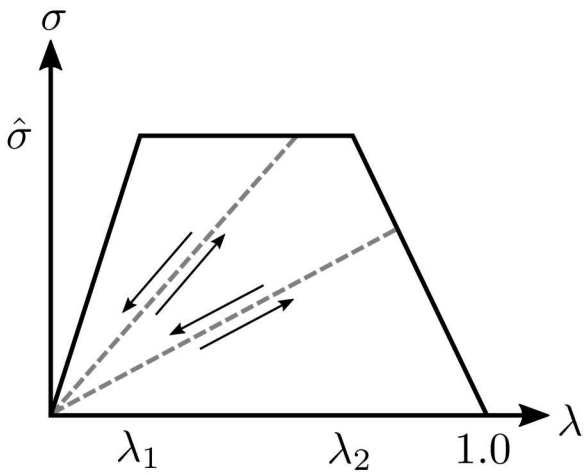

Figure 19.1: The effective traction-separation model following [1].

- The tangential failure separation, δ_{ct}
- The ratio of failure separations, $r = \delta_{cn}/\delta_{ct}$
- The normalized normal separation, $\lambda_n = u_n/\delta_{cn}$
- The normalized tangential separations, $\lambda_t^i = u_t^i/\delta_{ct}$, $i = 1, 2$.
- The effective separation, $\lambda = \sqrt{\lambda_n^2 + (\lambda_t^1)^2 + (\lambda_t^2)^2}$

Then, the traction is computed as

$$\begin{aligned} t_t^1 &= \hat{t}' \lambda_t^1 r, \\ t_t^2 &= \hat{t}' \lambda_t^2 r, \\ t_n &= \hat{t}' \lambda_n. \end{aligned}$$

The model is extended to the extrinsic behavior by computing an effective opening $\tilde{\boldsymbol{\lambda}}$ that recovers the initialization traction. There are two modes of initialization: 1) where the initial effective traction is below the peak traction specified in the input file, and 2) where the initial effective traction exceeds the peak traction in the input file. In the first case, the components of the effective opening ($\tilde{\boldsymbol{\lambda}}$) are computed on the hardening branch of the cohesive model. In the second case, the peak traction is reset to the initial effective traction and the components of the initial effective opening are computed using the condition $|\tilde{\boldsymbol{\lambda}}| = \lambda_1$. Evaluation of the extrinsic effective opening is given by the following:

$$\begin{aligned} \tilde{\sigma} &= \sqrt{(t_n r)^2 + (t_t^1)^2 + (t_t^2)^2}, \\ \hat{\sigma} &= \max(\hat{\sigma}, \tilde{\sigma}), \\ \tilde{\lambda}_t^i &= \frac{t_t^i \lambda_1}{\hat{\sigma} r}, \ i = 1, 2, \\ \tilde{\lambda}_n &= \frac{t_n \lambda_n}{\hat{\sigma}}. \end{aligned}$$

After initialization, the model is evaluated using

$$\lambda = \sqrt{(\lambda_n + \tilde{\lambda}_n)^2 + (\lambda_t^1 + \tilde{\lambda}_t^1)^2 + (\lambda_t^2 + \tilde{\lambda}_t^2)^2}.$$

The model is specified in adagio by the following command block:

```
BEGIN PARAMETERS FOR MODEL TVERGAARD_HUTCHINSON
  INIT TRACTION METHOD = IGNORE|ADD|EXTRINSIC (IGNORE)
  LAMBDA_1 = <real>
  LAMBDA_2 = <real>
  NORMAL LENGTH SCALE = <real>
  TANGENTIAL LENGTH SCALE = <real>
  PEAK TRACTION = <real>
  PENETRATION STIFFNESS MULTIPLIER = <real>
  USE ELASTIC UNLOADING = NO|YES (YES)
END [PARAMETERS FOR MODEL TVERGAARD_HUTCHINSON]
```

The `INIT TRACTION METHOD = EXTRINSIC|ADD` command line relates only to the dynamic insertion of cohesive zone elements through element death or XFEM.

19.2.2 Thouless-Parmigiani

This model is an extension of the Tvergaard-Hutchinson effective traction-separation model described in Section 19.2.1, but the normal and tangential traction components are treated independently. The model is specified in adagio by the following command block:

```
BEGIN PARAMETERS FOR MODEL THOULESS_PARMIGIANI
  INIT TRACTION METHOD = IGNORE|ADD|EXTRINSIC (IGNORE)
  LAMBDA_1_N = <real>
  LAMBDA_1_T = <real>
  LAMBDA_2_N = <real>
  LAMBDA_2_T = <real>
  NORMAL LENGTH SCALE = <real>
  PEAK NORMAL TRACTION = <real>
  TANGENTIAL LENGTH SCALE = <real>
  PEAK TANGENTIAL TRACTION = <real>
  PENETRATION STIFFNESS MULTIPLIER = <real>
  USE ELASTIC UNLOADING = NO|YES (YES)
END [PARAMETERS FOR MODEL THOULESS_PARMIGIANI]
```

References

[1] Viggo Tvergaard and John W. Hutchinson. On the toughness of ductile adhesive joints. *Journal of the Mechanics and Physics of Solids*, 44(5):789–800, 1996.

Chapter 20

Other In-Development Capabilities

This chapter describes other miscellaneous capabilities that are still in development or have limited testing.

20.1 Initial Particle Conversion

```
BEGIN CONVERSION TO PARTICLES AT INITIALIZATION <string>name
  BLOCK   = <string list>block_names
  SECTION = <string>section_name
END
```

The initial particle conversion capability is provided to facilitate the creation of particle meshes for particle based methods—such as smooth particle hydrodynamics (SPH), reproducing kernel particle method (RKPM), or peridynamics—from an initial mesh of solid elements (e.g., hexes).

At the beginning of the analysis the solid element blocks listed in `block_names` are converted to spherical particles of the type defined in the particle section `section_name`. It is important to note that the particle section will thus supersede any section specified in the original solid element block definition (consult [1] section on Element Block Parameters).

Note that elements may also be converted to particles via element death (consult [1] section on Element Death); however, conversion at initialization should offer more robust creation of particle meshes that are (a) compatible with the original mesh boundary conditions and (b) amenable to the chosen particle formulation methodology.

20.2 Shell Contact Lofting Factor

Warning: The shell contact lofting factor only works with Dash contact.

```
BEGIN SHELL SECTION <string>shell_section_name
  # ... see the Elements chapter of [1]
  CONTACT LOFTING FACTOR = <real>contact_lofting_factor
END [SHELL SECTION <string>shell_section_name]
```

The `CONTACT LOFTING FACTOR` line command is available in the `SHELL SECTION` command block to set a lofting factor specifically for use in contact. This contact lofting factor is used in place of the kinematic lofting factor for creation of the shell lofted geometry in contact. If no contact lofting factor is set, the kinematic lofting factor is used for contact.

The contact lofting factor has no effect on the shell element kinematics, and the `LOFTING FACTOR` and `CONTACT LOFTING FACTOR` line commands may be used in combination to independently set the kinematic and contact lofting factors, respectively.

20.3 Reaction Diffusion Solver

An experimental diffusion capability eventually intended for use in phase field fracture. Currently in early development and not recommended for use.

```
BEGIN REACTION DIFFUSION rxndiffname
  BLOCK = <string list>block_names
  INCLUDE ALL BLOCKS
  INITIAL VALUE = <real>value(1.0)
  SOURCE COEFFICIENT = <real>source_coeff(1.0)
  DIFFUSION COEFFICIENT = <real>diff_coeff(0.0)
  REACTION COEFFICIENT = <real<rxn_coeff(1.0)
  SOLVE AT INITIALIZATION = OFF|ON(OFF)
  SOLVE INCREMENT = <integer>solv_incr(1)
  SOLVE EXPLICIT = OFF|ON(OFF)
  GRADIENT CONFIGURATION = MODEL|CURRENT(MODEL)
  BEGIN PRESCRIBED FLUX
    SURFACE = <string>surf_name
    NODE SET = <string>node_set_name
    FUNCTION = <string>func_name
  END
  BEGIN PRESCRIBED FIELD
    SURFACE = <string>surf_name
    NODE SET = <string>node_set_name
    FUNCTION = <string>func_name
  END
END

BEGIN GRADIENT DAMAGE gradDam
  BLOCK = <string>block_names
  INCLUDE ALL BLOCKS
  FORMULATION = LORENTZ|MIEHE|COSINE(LORENTZ)
  INITIAL VALUE = <real>value(1.0)
  SOURCE COEFFICIENT = <real>source_coeff(1.0)
  DIFFUSION COEFFICIENT = <real>diff_coeff(0.0)
  REACTION COEFFICIENT = <real<rxn_coeff(1.0)
  SOLVE AT INITIALIZATION = OFF|ON(OFF)
  SOLVE INCREMENT = <integer>solv_incr(1)
  SOLVE EXPLICIT = OFF|ON(OFF)
  SUBCYCLES = <int>num_sub(1)
  GRADIENT CONFIGURATION = MODEL|CURRENT(MODEL)
  BEGIN PRESCRIBED FIELD
    SURFACE = <string>surf_name
    NODE SET = <string>node_set_name
    FUNCTION = <string>func_name
  END
END
```

20.4 Phase Field Fracture Material

An experimental fracture capability. Currently in early development and not recommended for use.

```
BEGIN MATERIAL <name>
  BEGIN PARAMETERS FOR MODEL PHASE_FIELD_LINEAR_ELASTIC
  END
END

BEGIN PFFRAC phasefieldfracname
  FRACTURE LENGTH SCALE = <real>reaction_value
  CONDITIONING COEFFICIENT = <real>diffusion_value
  FRACTURE ENERGY = <real>forcing_value
END
```

20.5 Discrete Element Method (DEM)

The discrete element method is a particle based element formulation. This method is in early development, experimental, and currently not recommended for use.

```
BEGIN DEM OPTIONS
 ....
END
BEGIN DEM SECTION
 ....
END
```

References

[1] Sierra/SolidMechanics Team. Sierra/SolidMechanics 4.46 User's Guide. Technical Report SAND2017-9759, Sandia National Laboratories, Albuquerque, NM, 2017.

Index

Distribution

1	0899	Technical Library, 9536 (1 electronic)


Sandia National Laboratories